RSC Advances

REVIEW

View Article Online
View Journal | View Issue

Check for updates

Cite this: *RSC Adv.*, 2025, **15**, 39705

A bibliometric review of triazine hybrids: synthesis, reactions, and applications spanning the last quarter-century (2000–2025)

Hajar A. Ali,[a] Mohamed A. Ismail[a] and Eslam A. Ghaith *[ab]

This comprehensive review delves into the intricate world of triazines, including their structures and the chemical diversity of their isomers. Additionally, this report encompasses a wide range of synthetic approaches, describing numerous reactions for attaining triazines, such as Bamberger, Bischler, inverse-electron-demand Diels–Alder, and Diels–Alder reactions. Moreover, this review describes the progress made in the chemistry of triazines, which is organized based on their reaction types, spotlighting the recent development. Accordingly, triazines stand out as a transformative strategy in the progress of synthetic chemistry due to their diverse applications in medicine, pharmacy, industry, and agriculture. Besides, triazine hybrids are important pharmacophores in the development of medications due to their captivating biological efficacy and biocompatibility. Consequently, this review presents a vast number of marketed drugs containing a triazine template while delineating their molecular mechanisms of action in disrupting disease pathways. Moreover, triazine cores are highlighted as flexible platforms for constructing and fine-tuning metal complexes and catalytic ligands in the period from 2000 to mid-2025. We anticipate that this review will be valuable to researchers focusing on the structural design and advancement of triazines.

Received 9th August 2025
Accepted 23rd September 2025

DOI: 10.1039/d5ra05849j

rsc.li/rsc-advances

Open Access Article. Published on 21 Oktober 2025. Downloaded on 9/06/2026 1:40:11 PG.
This article is licensed under a Creative Commons Attribution-NonCommercial 3.0 Unported Licence.

1. Introduction

Nitrogen-containing heterocyclic skeletons and their derivatives have historically been invaluable as a source of therapeutic agents.[1] Among the myriad nitrogenous heterocyclic scaffolds in organic chemistry, triazine hybrids hold a prominent position owing to their diverse structural significance and biological activities.[2] These compounds are a six-membered subclass of heterocycles and are composed of three nitrogenous atoms within their ring structure,[3] existing in three distinct *regio*-isomer arrangements: 1,2,3-triazine (*ν*-triazine), 1,2,4-triazine (*α*-triazine), and 1,3,5-triazine (*s*-triazine).[4] Among these isomers, *s*-triazine is the most extensively investigated due to its biological significance. Triazine undergoes nucleophilic substitution reactions, rather than electrophilic reactions, as its isomers have electron-withdrawing nitrogenous atoms and their resonance energies are lower than that of the benzene ring.[5] Notably, the 1,2,4-triazine motif is encountered in a multitude of natural products such as reumycin, fervenulin, and toxoflavin (Table 1).[6] Additionally, triazine derivatives are among the most privileged structural hybrids and constitute the core unit of many pharmaceuticals,[7] bioactive compounds, and materials[8] owing to their photophysical properties.[9] Remarkably, numerous triazine-containing drugs have been approved by the FDA[10] for the treatment of a wide range of clinical conditions, including cycloguanil,[11] decitabine,[12] altretamine,[13,14] almitrine,[15–17] bimiralisib,[18] lamotrigine[19,20] and triazavirin[21–23] (Table 2).

Tunable stimulus-responsive fluorescent and colorimetric probes based on triazine molecules have become hallmark tools in molecular biology because they give dynamic information with regard to the quantity of molecules and the localization of ions without requiring genetic engineering of the sample. Additionally, these probes for ions and molecules have attracted considerable attention owing to their suitability for bioimaging, industrial, environmental, and analytical applications as well as for the detection of hazardous compounds[24–26] with the clarity and vast sensitivity of absorption and fluorescence techniques. In the realm of organic light-emitting diodes (OLEDs) and nonlinear optics (NLOs), styryl *s*-triazine derivatives have been harvested as fluorophore materials.[27] This is due to the existence of a donor–π system–acceptor (push–pull) structural motif within these compounds (Fig. 1).[28] Moreover, triazine scaffolds are used as reactive azo dyes, and also as carriers for the preparation of immobilized enzymes and cation exchangers.[29,30]

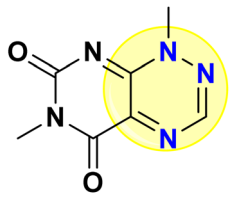
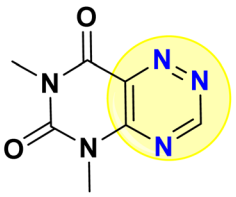
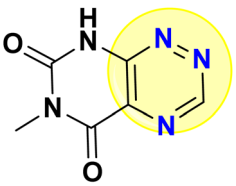
In light of the ever-increasing importance of triazines, they are pivotal in advancing high-performance and stable solar cells, including photosensitizer solar cells, organic solar cells

[a]*Chemistry Department, Faculty of Science, Mansoura University, El-Gomhoria Street, Mansoura 35516, Egypt. E-mail: abdelghaffar@mans.edu.eg; Tel: +201024410784*
[b]*Chemistry Department, Faculty of Science, New Mansoura University, New Mansoura City, Egypt*

© 2025 The Author(s). Published by the Royal Society of Chemistry

Open Access Article. Published on 21 Oktober 2025. Downloaded on 9/06/2026 1:40:11 PG. This article is licensed under a Creative Commons Attribution-NonCommercial 3.0 Unported Licence.

Table 1 Experimental skeletons for naturally occurring 1,2,4-triazines and their isolation, therapeutic target, IC_{50}, and mechanism of action

Natural triazine compounds	Isolation	Therapeutic target	MIC value	Mechanism
 (Toxoflavin)	Produced by *Burkholderia gladioli* HDXY-02 from *Lycoris aurea*	[Antifungal]		Toxoflavin has inhibitory activities against tested azole-resistant isolates using azole target 14-*a* sterol demethylase cyp51A and non-cyp51A gene mutations[6b]
		M. oryzae	128 μg mL^{-1}	
		R. solani	128 μg mL^{-1}	
		F. graminearum	256 μg mL^{-1}	
		A. fumigatus	64 μg mL^{-1}	
		A. nidulans	128 μg mL^{-1}	
		C. albicans	64 μg mL^{-1}	
		C. neoformans	128 μg mL^{-1}	
 (Fervenulin)	Isolated from a nematicidal actinomycete, *Streptomyces* sp. CMU-MH021, on *Meloidogyne incognita*	Nematicidal activity	30 μg mL^{-1}	Fervenulin demonstrates inhibitory effects on egg hatching and increases mortality of second-stage juveniles of root-knot nematodes, through disrupting cellular processes or metabolic pathways essential for egg viability and juvenile survival[6c]
 (Reumycin)	Isolated from the culture broth of *Streptomyces* sp. TPMA0082	[Antibacterial]		Reumycin inhibits the binding of the autoinducer to the LasR receptor in the las system, thereby suppressing the production of *P. aeruginosa* virulence factors, embedding pyocyanin, elastase, rhamnolipids, motility, and biofilms, without affecting bacterial growth[6d]
		S. aureus ATCC 25923	128 μg mL^{-1}	
		E. coli ATCC 25922	256 μg mL^{-1}	
		P. aeruginosa ATCC 27853	>256 μg mL^{-1}	
		P. aeruginosa PAO1	>256 μg mL^{-1}	

(OSCs), and perovskite solar cells (PSCs), due to their unique optoelectronic features, such as efficient charge transport, strong light-harvesting ability, and good thermal/chemical stability (Fig. 2).[31–35] Some examples of photosensitizer triazines used in solar cells are illustrated in Fig. 2.

2. Synthesis

Numerous synthetic approaches have been reported in the literature for the preparation of triazine scaffolds. They can be divided into three types according to their structure, *i.e.*, 1,2,3-, 1,2,4-, and 1,3,5-triazines.

2.1 Synthesis of *unsymmetric*-1,2,3-triazines

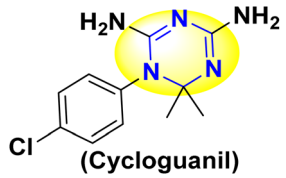
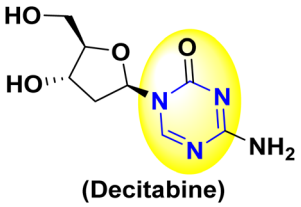
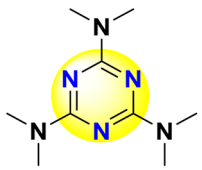
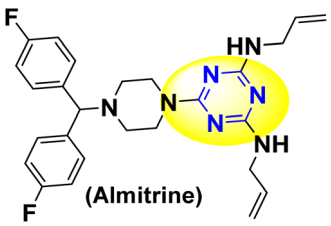
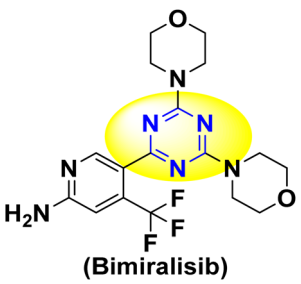
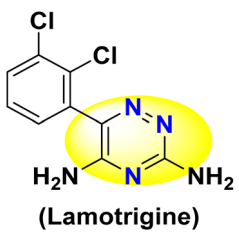
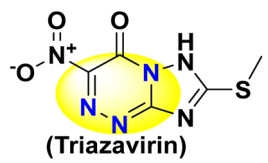
1,2,3-Triazines, often referred to as *vic*-triazines or *v*-triazines, exhibit lower stability in comparison to 1,2,4- and 1,3,5-triazine isomers.[4,5] Additionally, *v*-triazines are classified as biologically active scaffolds with effective antifungal, anticancer, antibacterial, anti-inflammatory, analgesic, antiviral, and anti-proliferative activities.[36–38]

2.1.1 From azide scaffolds. An efficient route for accessing 1,2,3-triazine derivatives **2** is *via* the base-catalyzed reaction of diazido-alkenoates **1** with cesium carbonate (Cs_2CO_3) in dimethyl formamide (DMF) or with basic potassium bicarbonate ($KHCO_3$) in dimethyl sulfoxide (DMSO), as shown in Scheme 1. The elegant synthetic route toward compound **2** is initiated with the abstraction of the benzylic hydrogen of alkenoates **1** to afford intermediate **2A**, which is then subjected to electrocyclic ring annulation to form intermediate **2B**. Finally, the elimination of the azide group from **2B** yields triazines **2** (Scheme 1).[39] Method A offers higher yields (up to 88%) for certain substrates but requires longer reaction times (up to 20 h), while, method B proceeds under milder and more practical conditions, with shorter reaction times (1–8 h), though the yields are slightly lower in some cases (32–85%). Substituents such as 4-F, 4-Me, 4-MeO, and Ph require longer reaction times (up to 20 h in Method A) compared to Method B (3–8 h). Additionally, some electron-withdrawing groups such as 4-F_3C, 3-Cl, 3-Br, 4-NO_2 and 4-CN show higher yields in method A (58–82%) than in method B (32–81%). Conversely, bulky substituents such as Ar = Ph, R = (O*t*-Bu) give a slightly higher yield in

© 2025 The Author(s). Published by the Royal Society of Chemistry

Open Access Article. Published on 21 Oktober 2025. Downloaded on 9/06/2026 1:40:11 PG. This article is licensed under a Creative Commons Attribution-NonCommercial 3.0 Unported Licence.

Table 2 The approved triazine drugs and their therapeutic names and targets

Biologically active triazine compounds & generic name	Therapeutic target	MIC value	Mechanism	Trade name
 (Cycloguanil)	Antibacterial[11] *S. aureus* ATCC 11632 *E. coli* ATCC 25922 *P. aeruginosa* PAQ1	MIC90 >128 μg mL^{-1} >128 μg mL^{-1} >128 μg mL^{-1}	Cycloguanil acts as an inhibitor of dihydrofolate reductase (DHFR) and also disrupts bacterial membrane integrity	Lamictal
 (Decitabine)	Myelodysplastic syndromes[12]	Dosing 15–20 mg per m^2 per day	It inhibits cell proliferation by irreversibly blocking DNA synthesis at high doses as well as blocks hypermethylation and consequently re-expression of tumor suppressor genes at low doses[12]	Dacogen
 (Altretamine)	Antineoplastic agent[13] Anticancer[14]	Dosing 260 mg per m^2 per day orally for 14 days[13]	Altretamine is classified by methanethiol (MeSH) as an alkylating antineoplastic agent. This structure damages tumor cells *via* the synthesis of the weakly alkylating agent formaldehyde, a product of cytochrome 450 mediated *N*-demethylation[14]	
 (Almitrine)	COVID-19 in *Trypanosoma cruzi*[15–17] *L. amazonensis* *T. cruzi*	 2.2 μM 1.6 μM	Almitrine improves respiration in patients with chronic obstructive pulmonary disease by raising the arterial oxygen tension while Vectarion decreasing the arterial carbon dioxide tension[15]	Duxil Vectarion
 (Bimiralisib)	Treat lymphoma[18]	Dosing 60 mg	Bimiralisib has pan class phosphoinositide 3-kinases (PI3K) inhibitory activity to inhibited α, β, γ and & isoforms[18]	—
 (Lamotrigine)	Antiepileptic[19,20]	Effective dose 100 to 450 mg per day	Lamotrigine inhibits the release of glutamate evoked by 4-aminopyridine (4AP) in a concentration-dependent manner. This inhibitory effect is connected with a reduction in the depolarization-evoked increase in the cytoplasmic free Ca^{2+} concentration ($[Ca^{2+}]C$)[19]	Lamictal
 (Triazavirin)	Antiviral *S. aureus* SARS-COV-2 COVID-19 (ref. 21–23)	50 and 100 mg per kg per day	Triazavirin is a guanosine nucleotide analog which inhibits RNA synthesis[21–23]	Triazavirin

© 2025 The Author(s). Published by the Royal Society of Chemistry

Open Access Article. Published on 21 Oktober 2025. Downloaded on 9/06/2026 1:40:11 PG.
This article is licensed under a Creative Commons Attribution-NonCommercial 3.0 Unported Licence.

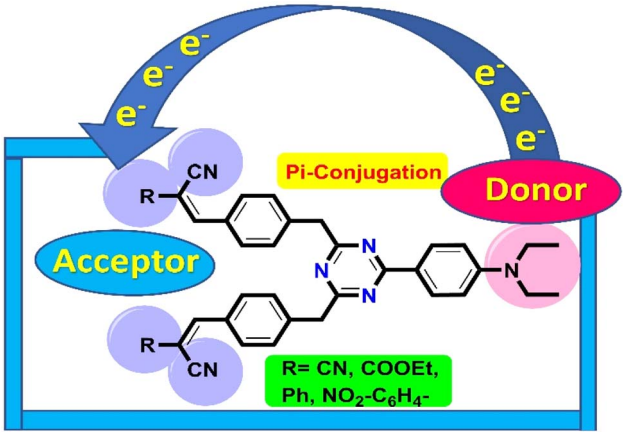


Fig. 1 Styryl *s*-triazines as fluorophore materials.

method A (77%) compared to method B (72%). In the case of heteroaromatics such as pyridine, method B achieves a better yield (85%) than method A (71%). Method A allows better regioisomeric control owing to its higher temperature and longer time, possibly favoring thermodynamic equilibration. In contrast, method B, leads to reduced selectivity in certain cases owing to its kinetically controlled conditions.

2.1.2 From acyclic chains. Triazine-*N*-oxide derivatives represent fascinating heterocyclic motifs that have proved to be effective synthetic frameworks, in addition to their biological applications, high energy content, and fluorescent aspects.[40] Nitrosyl addition of *tert*-butyl nitrite (*t*-BuONO) to ethyl-diazobutenoate derivatives **3** in the presence of a mixture of dichloromethane (DCM) and hexafluoro-*iso*-propanol (HFIP), followed by cyclization, afforded triazine-*N*-oxide **2** in high yields up to 99% (Scheme 2).[40]

The proposed mechanism for the formation of triazine-*N*-oxides has been illustrated as shown in Scheme 3, where the terminal olefinic carbon of compound **3** nucleophilically attacks *t*-BuONO to form intermediate **3A.** Subsequently, the *t*-BuO^- group is extruded from **3A** with the aid of HFIP to yield intermediate **3B.** Then, this intermediate undergoes intramolecular [5 + 1] cycloaddition reaction, followed by nucleophilic attack of the nitrosyl nitrogen to the terminal nitrogen of the diazonium ion to furnish intermediate **3C**, which finally undergoes deprotonation with the aid of the *t*-BuO^- ion to afford **2** (Scheme 3).[40]

2.1.3 From pyrrole derivatives. Alternatively, Migawa and colleagues employed RANEY® nickel for the desulfurization reaction of amino-(methylthio)pyrrole-dicarboxamide **4** to give aminopyrrole-dicarboxamide **5.** Then, in the diazotization step, *t*-BuONO was dropwise added to **5** at 0 °C to give hydroxy-pyrrolo-triazine-carboxamide **6** (Scheme 4).[41]

2.1.4 From isonitrile derivatives. The reaction depicted in Scheme 5 involves the synthesis of 4-alkoxybenzotriazines **8a–p** *via* the treatment of tosylmethyl isocyanide Tos(MIC) **7** with alcohols in the presence of sodium hydride (NaH) in tetrahydrofuran (THF). Mechanistically, the reaction starts with the α-deprotonation of Tos(MIC) **7** by strong bases such as potassium tertiary butoxide (*t*-BuOK) and NaH to yield the TosMIC anion intermediate **8A.** Then, this anion is subjected to nucleophilic attack on the electrophilic azide. Additionally, this anion undergoes a 6-*endo-trig* cyclization, wherein the nucleophilic N1 atom attacks the isocyanide carbon to give cyclized

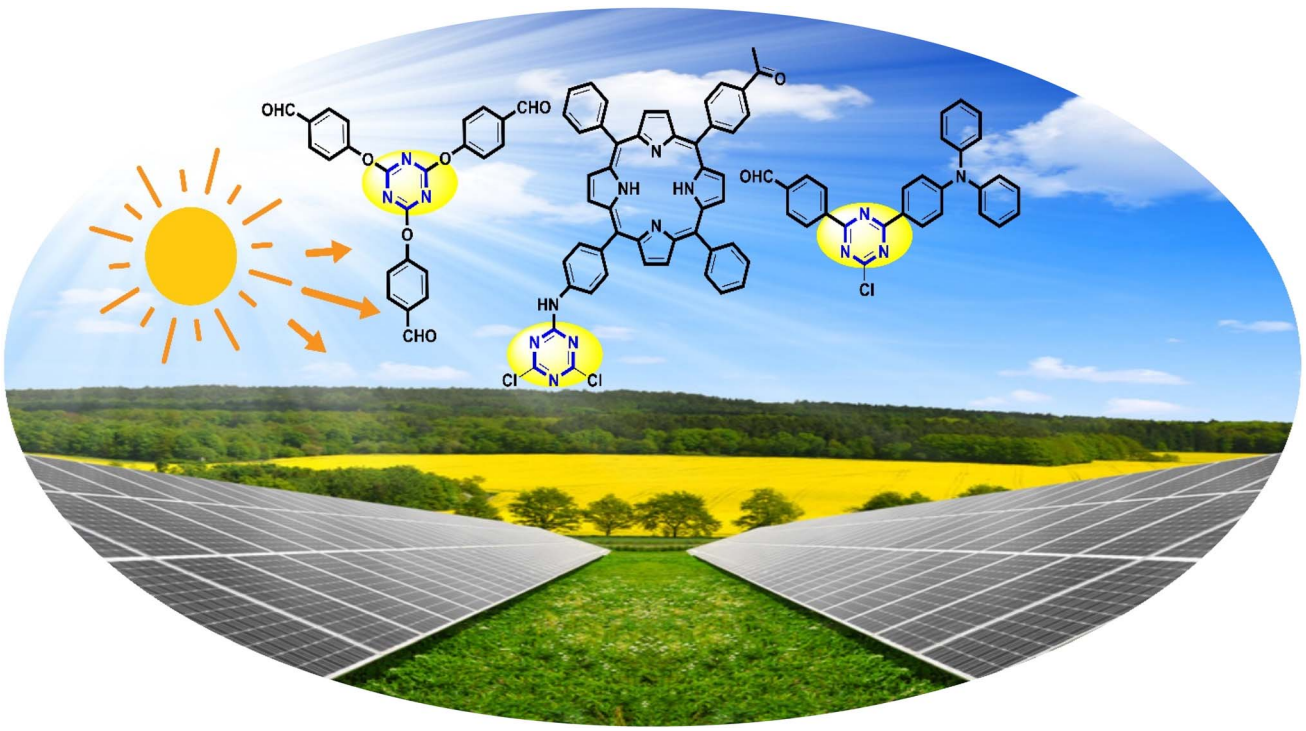
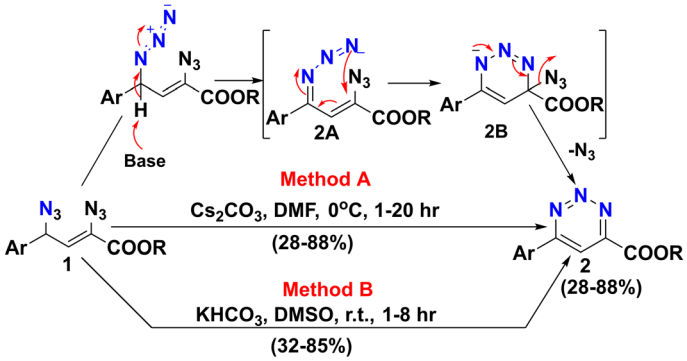


Fig. 2 Examples of triazine-based photosensitizers applied in solar energy.

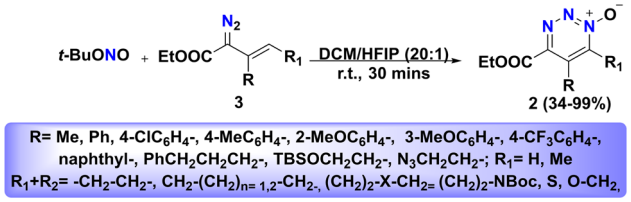
© 2025 The Author(s). Published by the Royal Society of Chemistry

Open Access Article. Published on 21 Oktober 2025. Downloaded on 9/06/2026 1:40:11 PG.
This article is licensed under a Creative Commons Attribution-NonCommercial 3.0 Unported Licence.



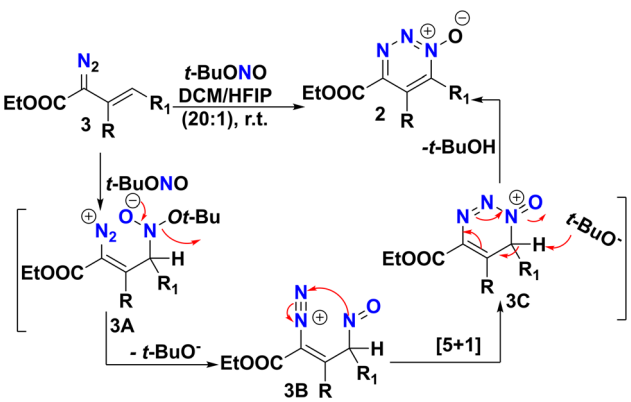
Ar	R	Time (hr) A	Time (hr) B	Method A (Yield%)	Method B (Yield%)	Ar	R	Time (hr) A	Time (hr) B	Method A (Yield%)	Method B (Yield%)
Ph-	OBn	6	4	83	71	4-$MeOC_6H_4$-	Me	20	8	65	75
Ph-	O-*t*-Bu	20	8	77	72	4-$F_3CC_6H_4$-	Me	2	1	82	80
4-FC_6H_4-	Me	20	3	76	85	4-$NO_2C_6H_4$-	Me	1	1	59	32
2-ClC_6H_4-	Me	8	7	28	42	4-CNC_6H_4-	Me	1	1	58	48
3-ClC_6H_4-	Me	8	3	82	81	naphthyl-	Me	5	5	88	80
3-BrC_6H_4-	Me	2	2	81	74	thienyl	Me	2	2	88	55
4-MeC_6H_4-	Me	20	8	76	69	pyr	Me	3	1	71	85

Scheme 1 Base-catalyzed synthesis of *v*-triazines.



Scheme 2 Synthesis pathway for triazine-*N*-oxide.

intermediate **8B** *via* a transition state **8C**. Subsequently, the exergonic process eliminates the tosyl group from intermediate **8B** to produce the aromatic benzotriazine intermediate **8D**. Afterward, this intermediate is susceptible to nucleophilic attack by another molecule of an alkoxide ion to give intermediate **8E**, corresponding with the elimination of the cyanide

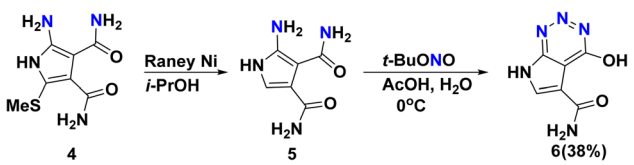


Scheme 3 Plausible mechanism for establishing triazine-*N*-oxide.

(CN) group to furnish 4-alkoxybenzotriazine **8**. Benzotriazines represent a salient class of nitrogenous heterocyclic scaffolds known for their diverse pharmacological properties, given that they show a broad spectrum of biological activities, including antidepressant through interaction with 5-HT1A receptors, as well as anesthetic, antifungal, and antihypertensive actions (Scheme 5).[42]

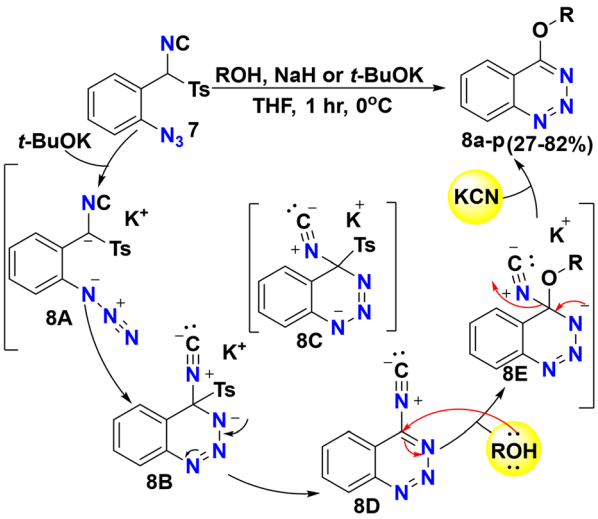
2.1.5 From imidazolidine derivatives. Fused *v*-triazines **10** were synthesized *via* diazotization reaction, starting with dissolving imidazolidines **9** in trifluoroacetic acid (TFA) to furnish substituted amino-oxazoles intermediate **10A**, which was subsequently stirred with sodium nitrite ($NaNO_2$) for 20 min at 15 °C, and then basified with NaOH solution to yield fused triazines **10** (Scheme 6).[43]

2.1.6 From pyridine derivatives. In 2013, the reaction of dichloro-nitropyridine **11** with *N*-methyl-2-pyrrolidone (NMP) and cuprous cyanide (CuCN) generated cyano-chloro-nitropyridine **12**, which, under treatment with sodium hyposulfite ($Na_2S_2O_3$) and tetrabutylammonium bromide (TBAB) in a combined DCM and H_2O system, reduced the nitro group to amino-pyridine **13**. Consequently, the coupling reaction of compound **13** with aniline derivatives **14** in the presence of $NaNO_2$ furnished substituted chloro-(phenyltriazenyl)



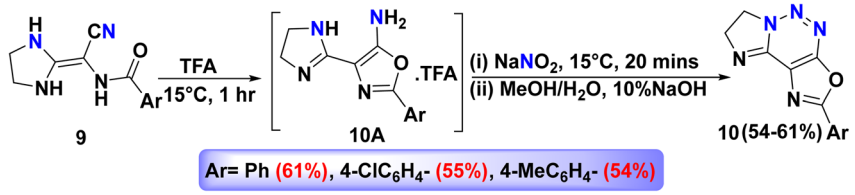
Scheme 4 Formation of fused triazine **6** through diazotization reaction.

Open Access Article. Published on 21 Oktober 2025. Downloaded on 9/06/2026 1:40:11 PG.
This article is licensed under a Creative Commons Attribution-NonCommercial 3.0 Unported Licence.

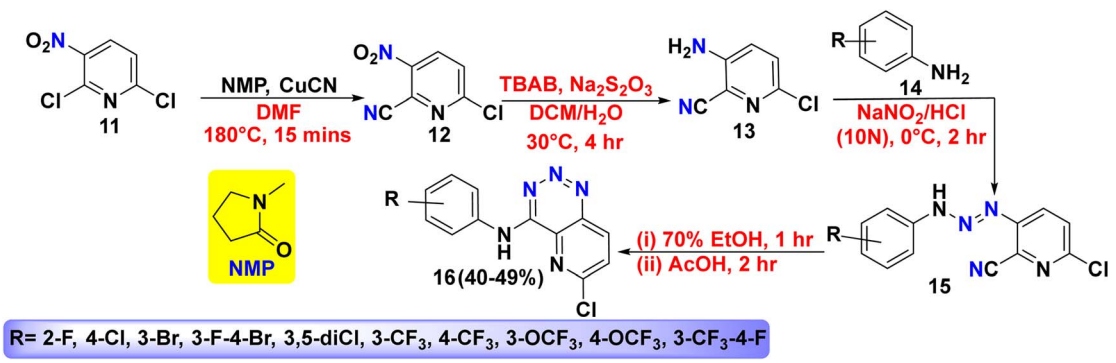


no	R	Yield		R	Yield
a	Me	60	i	but-3-yn-	69
b	*n*-Bu-	74	j	pent-3-yn	51
c	isopropyl	82	k	Bn	85
d	*t*-Bu	40	l	4-(allyl)-8-chloro-	70
e	*sec*-butyl	80	m	4-(allyl)-5-bromo-	72
f	-CH(CF$_3$)$_2$	71	n	pyridin-2-ylmethyl-	73
g	allyl-	88	o	4-(allyl)-7-(trifluoromethyl)	77
h	propyn-	62	p	4-((2-isopropyl-5-methylcyclohexyl) oxy)	27

Scheme 5 Mechanistic route for the synthesis of alkyl benzotriazines.



Scheme 6 Formation of fused triazines.



Scheme 7 Synthetic strategy for the constitution of fused pyrido-triazines.

picolinonitrile **15**, followed by ring annulation and rearrangement with acetic acid (AcOH) to give fused pyrido-triazine derivatives **16** (Scheme 7), which were evaluated as a VEGFR-2 inhibitor.[44]

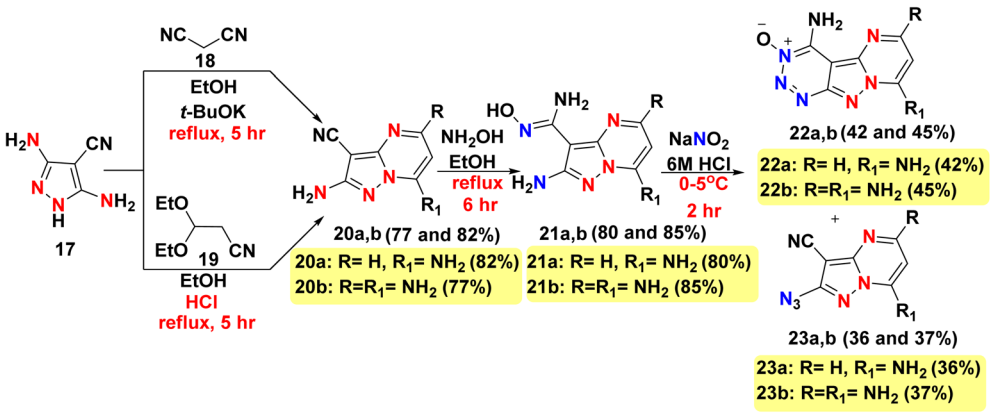
2.1.7 From pyrazole derivatives. Pyrazolo[1,5-*a*]pyrimidine-3-carbonitrile derivatives **20a** and **b** were synthesized through the reaction of diamino-4-cyano-pyrazole **17** with malononitrile (**18**) or 3,3-diethoxypropionitrile (**19**). Afterward, treatment of compounds **20a** and **b** with hydroxylamine (NH_2OH) furnished hydroxypyrazolo[1,5-*a*]pyrimidine-3-carboximidamide **21a** and **b**. In contrast, diazotization reaction of **21a** and **b** with $NaNO_2$ under acidic conditions afforded aminopyrimido-pyrazolo[3,4-*d*][1,2,3]triazine-3-oxide **22a,b** and azidopyrazolo[1,5-*a*] pyrimidine-3-carbonitrile **23a** and **b** (Scheme 8).[45]

2.2 Synthesis of *unsym*-1,2,4-triazines

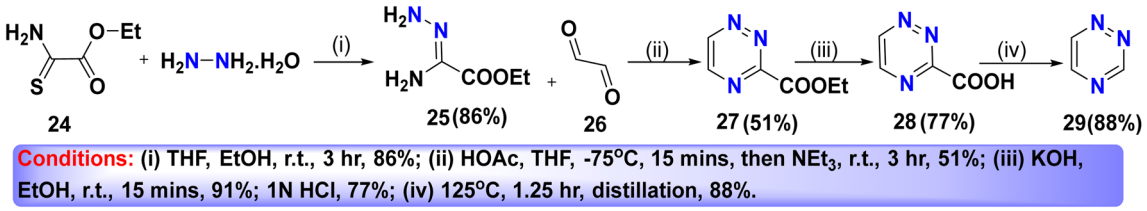
1,2,4-Triazines are well-recognized pharmacophores, which demonstrate a wide array of biological activities, in particular, anti-inflammatory, antihistaminergic, anti-HIV, antiviral, anti-cancer, antifungal, cardiotonic, anti-protozoal, neuroleptic, analgesic, antihypertensive, tuberculostatic, antimalarial, anti-microbial, cyclin-dependent kinase inhibitors, antiparasitic, and estrogen receptor modulators.[46] For instance, lamotrigine, containing a 1,2,4-triazine core, has been used as an

© 2025 The Author(s). Published by the Royal Society of Chemistry

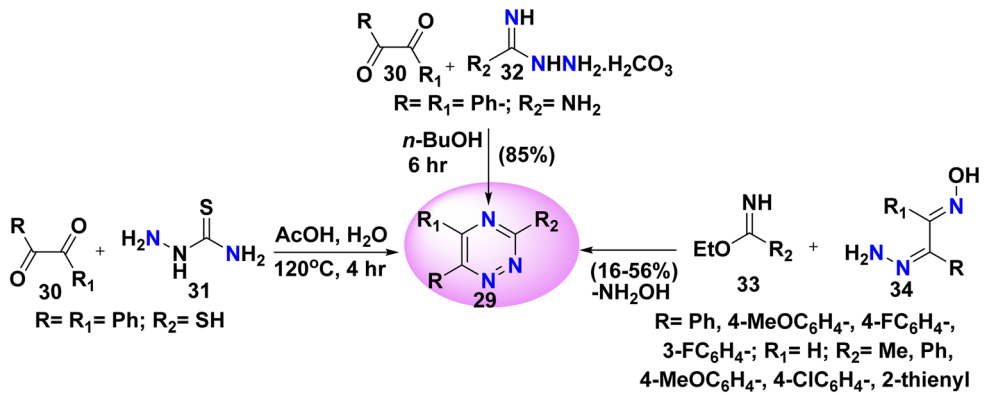
Open Access Article. Published on 21 Oktober 2025. Downloaded on 9/06/2026 1:40:11 PG.
This article is licensed under a Creative Commons Attribution-NonCommercial 3.0 Unported Licence.



Scheme 8 Formation of pyrimido-pyrazolo-triazines and fused azido-pyrazolo-pyrimidine derivatives.



Scheme 9 Preparation of parent 1,2,4-triazine.



Scheme 10 Synthesis of 1,2,4 triazine scaffolds.

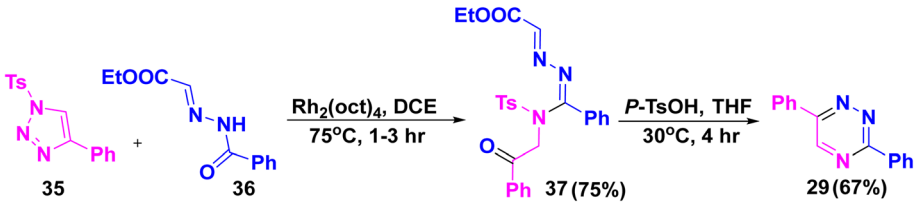
antiepileptic drug, implying that it is involved in the blockade of sodium channels.[47]

2.2.1 Condensation of hydrazine derivatives with carbonyl compounds. The multistep synthesis of 1,2,4-triazine (**29**) was reported by Palmer and coworkers. Initially, the starting ethyl amino(hydrazono)acetate **25** was prepared by reacting ethyl amino(thioxo)acetate (**24**) with hydrazine hydrate. The resulting hydrazone **25** was then condensed with glyoxal (**26**) to yield ethyl-triazine-carboxylate **27**, which was subsequently subjected to saponification reaction, followed by hydrolysis into its corresponding carboxylic acid **28**. Finally, decarboxylation of carboxylic derivative **28** afforded triazine **29** (Scheme 9).[48]

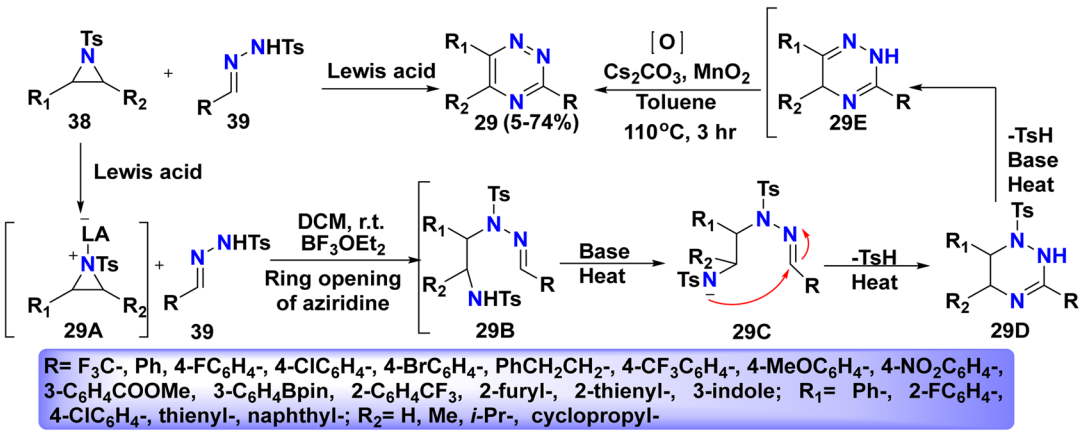
There are many reliable methods for accessing triazine derivatives *via* condensation reaction. Among them, the condensation reaction involving a mixture of benzil (**30**) with thiosemicarbazide (**31**) in a mixture of acetic acid and water at 120 °C for 4 h afforded diphenyl-triazine-thione **29**.[49] Analogously, aminoguanidine bicarbonate **32** was reacted with benzil (**30**) in *n*-BuOH to furnish amino triazine derivatives **29**.[50] Alternatively, substituted 1,2,4-triazines **29** were obtained *via* condensing a mixture of ethyl imidate derivatives **33** and hydrazineylideneacetaldehyde oxime **34** (Scheme 10).[51]

2.2.2 From triazoles. Meng *et al.*[52] showcased the utilization of a rhodium catalyst to prepare diphenyl triazine **29**. The one-pot reaction of phenyl-tosyl-triazole **35** with ethyl(benzoylhydrazineylidene)acetate **36** in dichloroethane (DCE) gave ethyl-((((4-methyl-*N*-(oxo-phenylethyl)phenyl) sulfonamido)(phenyl)methylene)hydrazineylidene)acetate **37**, which underwent hydrolysis using *p*-toluene sulfonic acid (*p*-TsOH) to furnish disubstituted-triazine **29** (Scheme 11).[52]

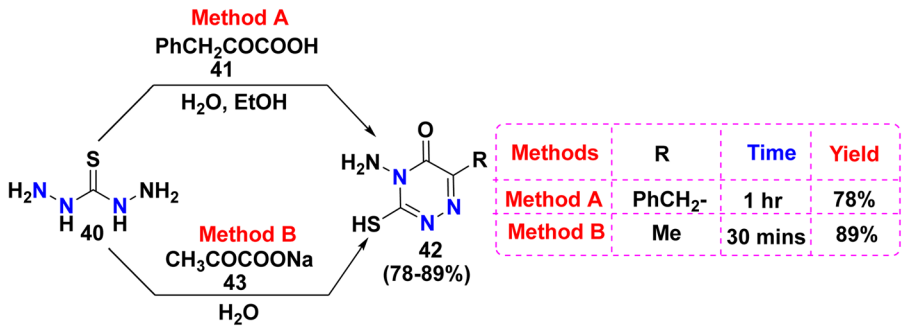
Open Access Article. Published on 21 Oktober 2025. Downloaded on 9/06/2026 1:40:11 PG.
This article is licensed under a Creative Commons Attribution-NonCommercial 3.0 Unported Licence.



Scheme 11 Rhodium-catalyzed synthesis of triazine.



Scheme 12 Tentative mechanism for the synthesis of 1,2,4-triazines.



Scheme 13 Synthesis of amino-mercapto-triazinone.

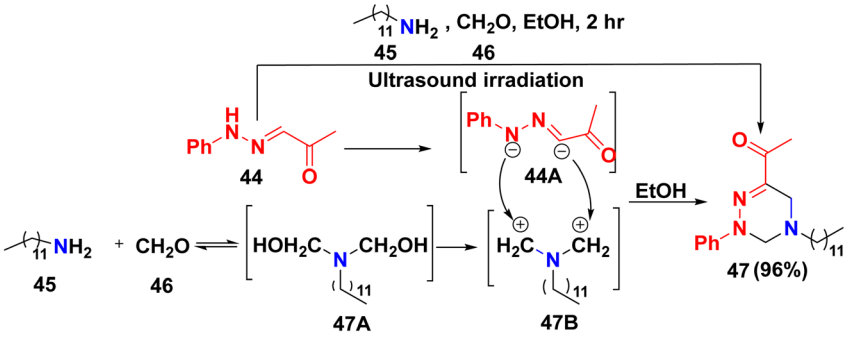
2.2.3 From aziridines. The one-pot reaction of aziridines **38** with *N*-tosyl hydrazone **39** in the presence of Lewis acid gave triazine scaffold **29**. The tentative mechanism for triazine formation was hypothesized as shown in Scheme 12. Firstly, the Lewis acid activates the aziridine ring to give intermediate **29A**, while hydrazone **39** works as a nucleophile, which influences the ring opening of **29A** *via* C–N bond cleavage to form intermediate **29B**. Subsequently, an acidic proton of the NHTs moiety is removed to afford intermediate **29C**, which is then subjected to heat activation, leading to ring annulation with the elimination of the tosyl moiety to furnish intermediate **29D**. Afterward, the other tosyl group in intermediate **29D** is eliminated to generate dihydrotriazine **29E**. Ultimately, triazine derivatives **29** are produced by oxidizing the dihydrotriazine with MnO_2 (Scheme 12).[53]

2.2.4 From thiocarbohydrazide. Hamama *et al.*[54] observed that an equimolar amount of thiocarbohydrazide (**40**) and phenylpyruvic acid (**41**) in ethanol and water under reflux for 1 h produced amino-benzyl-mercapto-triazine-one **42** in 78% yield. Soon after, amino-methyl-mercapto triazinone **42** was synthesized by refluxing a mixture of thiocarbohydrazide (**40**) with sodium pyruvate (**43**) for 30 min in water (Scheme 13).[55] Method B (R = Me) yields 89% in just 30 min, compared to method A (R = $PhCH_2$–), which gives 78% yield after 1 h. The smaller methyl group in method B likely reduces the steric hindrance, promoting faster and more efficient cyclization compared to the bulkier benzyl group in method A, which may slow the reaction and lower the yield.

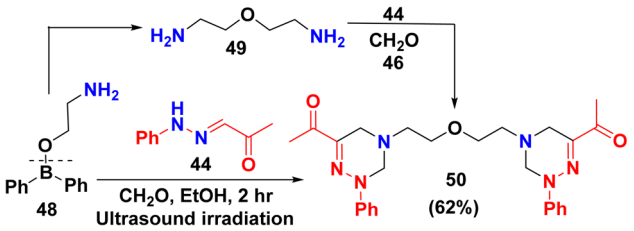
2.2.5 Double Mannich reaction for triazine synthesis. Recently, Ali *et al.*[56] reported the formation of (dodecyl-phenyl-triazinyl)ethanone **47** through a catalyst-free multicomponent

© 2025 The Author(s). Published by the Royal Society of Chemistry

Open Access Article. Published on 21 Oktober 2025. Downloaded on 9/06/2026 1:40:11 PG.
This article is licensed under a Creative Commons Attribution-NonCommercial 3.0 Unported Licence.



Scheme 14 Domino one-pot synthesis of (dodecyl-phenyl-triazin-yl)ethanone 47.



Scheme 15 Preparation of ((oxybis(ethane-diyl))bis(phenyl-triazine-diyl))bis(ethanone) 50.

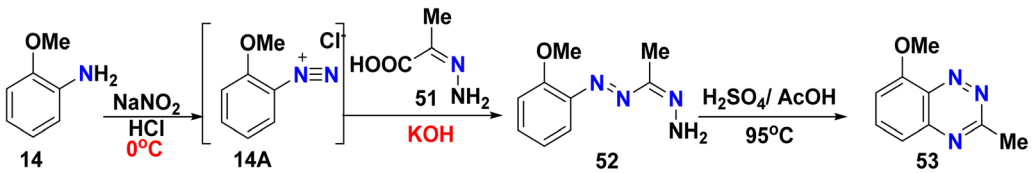
Mannich reaction. This reaction involved (phenylhydrazineylidene)propan-2-one **44**, dodecyl amine (**45**), and formalin (CH_2O) (**46**) in ethanol, facilitated by ultrasound irradiation. The plausible mechanism for the formation of **47** may proceed as depicted in Scheme 14. At the onset, the condensation of dodecyl amine **45** and two molecules of formalin **46** generates methylol intermediate **47A**. Subsequently, removal of two hydroxyl groups from this intermediate gave carbonium ion **47B**, $RN(CH_2^+)_2$. Concurrently, the elimination of two acidic protons from compound **44** produces carbanion intermediate **44A**. Ultimately, the nucleophilic carbanion of intermediate **44A** reacts with electrophilic carbonium ion **47B**, leading to (dodecyl-phenyl-tetrahydro-triazin-yl) ethanone **47**.

Analogously, the bis-double Mannich reaction of aminoethyl diphenylborinate **48**, compound **44**, and CH_2O **46** afforded ((oxybis(ethane-diyl))bis(2-phenyl-1,2,4-triazine-diyl)) bis(ethanone) **50**. Its mechanism begins with the cleavage of aminoethyl diphenylborinate **48**, followed by dimerization to produce 2,2′-oxybis(ethanamine) (**49**). Subsequently, the bis-double Mannich product **50** is formed *via* aminomethylation of oxybis(ethanamine) **49** with compounds **44** and **46** (Scheme 15).[56]

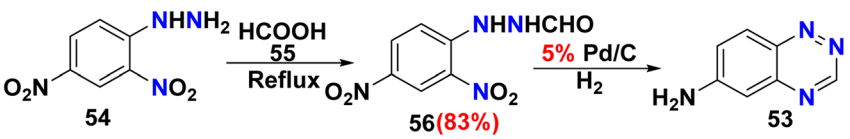
2.2.6 Difunctionalized triazine synthesis. Furthermore, disubstituted benzotriazine **53** was synthesized through a multistep reaction, starting with the diazotization of substituted aniline **14** with $NaNO_2$ in the presence of hydrogen chloride (HCl) to furnish diazonium salt **14A**, and then the resultant product was coupled with hydrazone of pyruvic acid **51** to afford hydrazone compound **52**, which, under the influence of sulfuric acid (H_2SO_4) and AcOH, underwent ring annulation to afford fused triazine **53** (Scheme 16).[57]

Formylation of dinitrophenyl hydrazine **54** with formic acid (HCOOH) (**55**) gave (dinitrophenyl)formohydrazide **56**, which underwent reduction with a palladium/carbon catalyst (Pd/C) to yield aminobenzotriazine **53** (Scheme 17).[58]

Cheng *et al.*[59] reported the synthesis of substituted toxoflavin[60] beginning with the reaction of substituted aminouracil **57** with molecular oxygen to form substrate radical **62A** and superoxide. Then, these reactive species combine to form

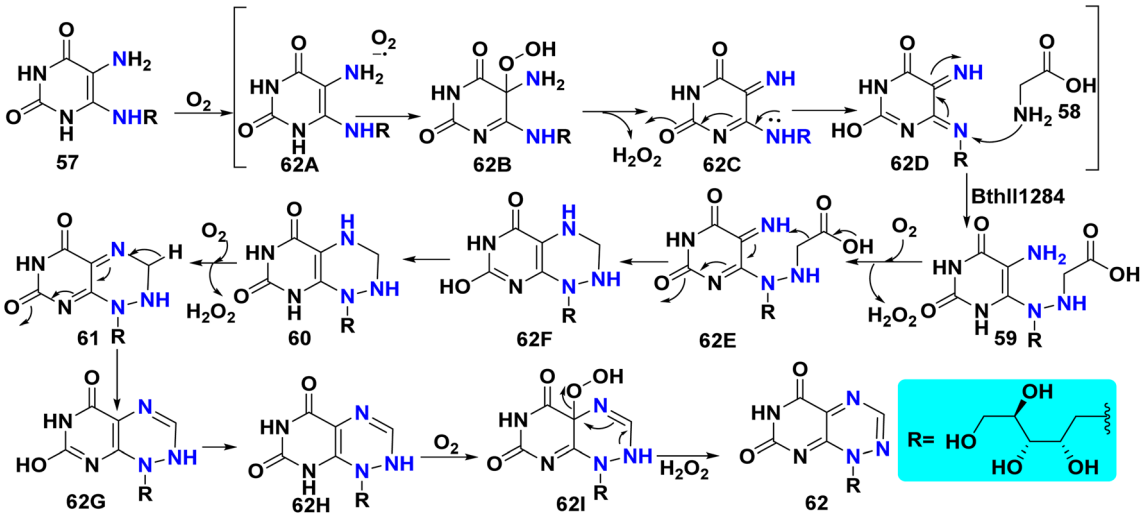


Scheme 16 Bamberger reaction for triazine synthesis.

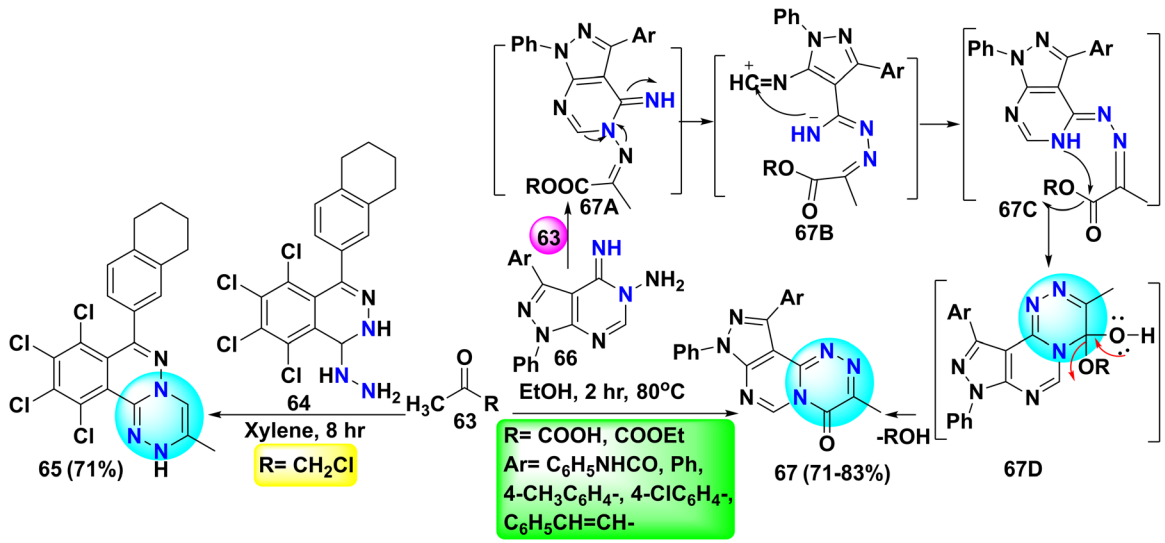


Scheme 17 Bischler reaction for the formation of fused triazine.

Open Access Article. Published on 21 Oktober 2025. Downloaded on 9/06/2026 1:40:11 PG.
This article is licensed under a Creative Commons Attribution-NonCommercial 3.0 Unported Licence.



Scheme 18 Enzyme-catalyzed formation of toxoflavin.



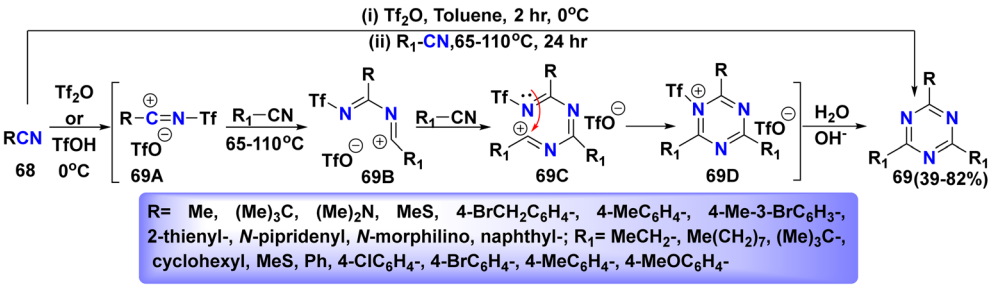
Scheme 19 Synthesis of polycyclic 1,2,4-triazine scaffolds.

hydroperoxide intermediate **62B**. Afterward, hydrogen peroxide is eliminated, and the initial two-electron oxidation is completed, affording iminouracil intermediate **62C**. Subsequently, this intermediate undergoes tautomerization to form imine intermediate **62D** at the C6 position. Next, BthII1284 catalyzed the formation of compound **59**, in which a new N–N bond is generated through the nucleophilic attack of the amino group of glycine **58** into intermediate **62D**. At this stage, the structure reverts to the oxidizable aminouracil form compound **59**, followed by a second two-electron oxidation, producing intermediate **62E**. Alternatively, the remaining steps occur spontaneously, starting with decarboxylation, initiating the generation of a C–N bond *via* intermediates **62F** to give compound **60**. Afterward, the third two electron oxidation occurs to produce compound **61**. The conjugated system of scaffold **61** provides H^- at the acidic C9 position and subject to deprotonation, enabling the reverse tautomerization to the amino uracil from **62G** to **62H**. Ultimately, the fourth two-electron oxidation finishes the synthesis of 1,2,4-triazine, producing scaffold **62** passing through intermediate **62I** (Scheme 18).

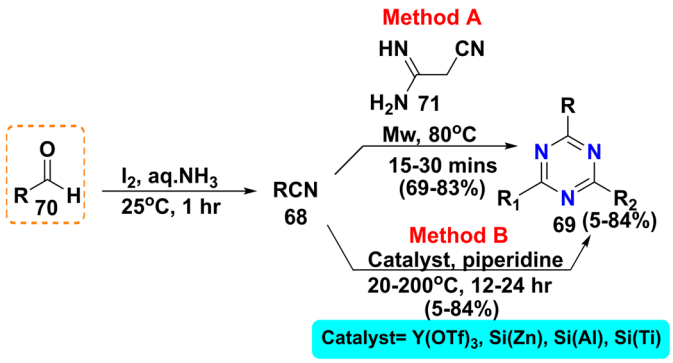
Phthalazine-triazine **65** can be achieved *via* the reaction of hydrazineyl dihydrophthalazine **64** with chloropropanone (**63**) in xylene.[61] In contrast, Helmy *et al.*[62] successfully synthesized biologically active pyrazolo-pyrimido-triazine-one derivatives **67** *via* the formation of intermediate **67A**, which is generated by the reaction of pyruvic acid or ethyl pyruvate **63** with imino-amino derivatives **66**. Afterward, intermediate **67A** undergoes *in situ* Dimroth rearrangement *via* ring opening to form intermediate **67B**, which then undergoes intramolecular cyclization to produce intermediate **67C**. Subsequently, nucleophilic addition of an NH group of pyrimidine to carbonyl (C=O) occurs,

© 2025 The Author(s). Published by the Royal Society of Chemistry

Open Access Article. Published on 21 Oktober 2025. Downloaded on 9/06/2026 1:40:11 PG.
This article is licensed under a Creative Commons Attribution-NonCommercial 3.0 Unported Licence.



Scheme 20 Triazine hybrid formation from the reaction of Tf_2O with RCN.



Method A			Method B													
R	R_1= R_2	Yield	R= R_1= R_2	Si(Al)				Si(Zn)				Si(Ti)				$Y(OTf)_3$			
				% Yield	hr Time	°C Temp		% Yield	hr Time	°C Temp		% Yield	hr Time	°C Temp		% Yield	hr Time	°C Temp	
Ph	NH_2	71	*N*-morphilino	22	24	200		60	24	200		38	24	20		84	24	200	
4-$MeOC_6H_4$-	NH_2	69	*N*-piperidinyl	72	24	20		75	24	200		63	24	200		31	24	200	
4-$NO_2C_6H_4$-	NH_2	76	Ph	–	—	—		13	24	200		—	—	—		55	24	20	
2-Furyl	NH_2	77	4-$F_3CC_6H_4$-	6	24	200		35	24	200		5	24	200		42	12	200	
2-Thienyl-	NH_2	83	Ph-N(N)-CN	0	24	200		30	24	200		8	24	200		30	24	200	

Scheme 21 Construction of 1,3,5-triazine derivatives **69**.

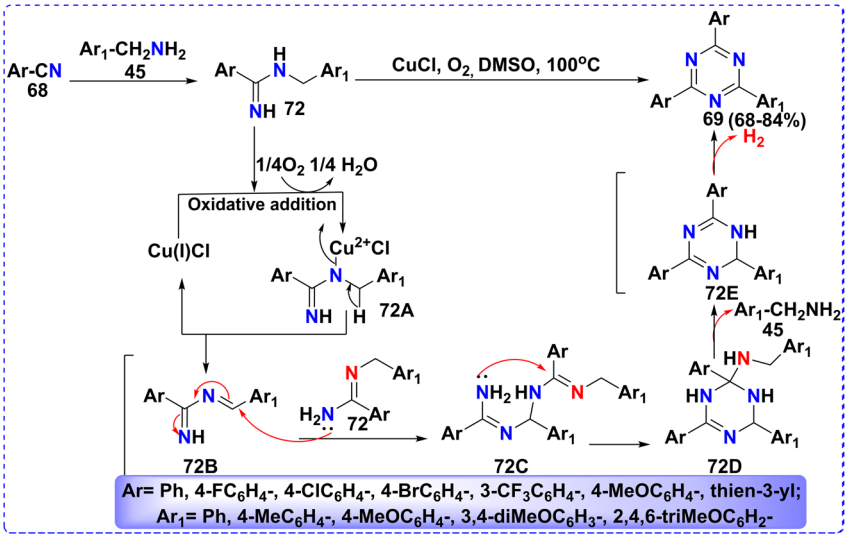
leading to the formation of a triazine ring in cycloadduct **67D**. Finally, elimination of a water or ethanol molecule from cycloadduct **67D** yields compound **67** (Scheme 19).[62]

2.3 Synthesis of *symmetrical*-1,3,5-triazines

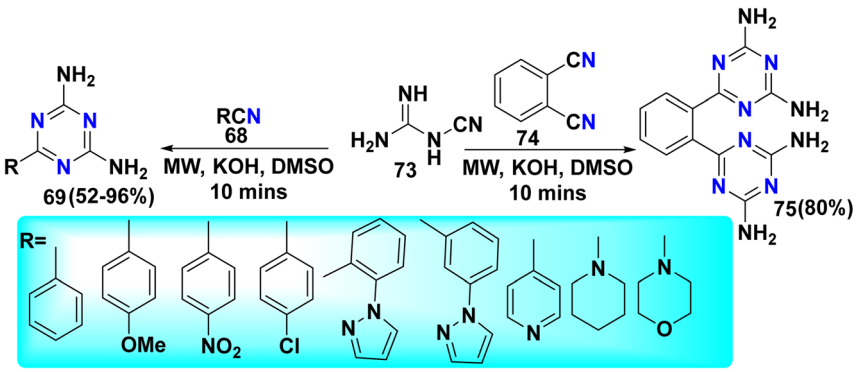
2.3.1 From carbonitriles. The one-pot reaction of nitrile scaffold **68** with triflic anhydride (Tf_2O) or triflic acid (TfOH) at low temperature, followed by adding a certain amount of different nitrile hybrids, and then refluxing the following in toluene at a temperature up to 110 °C, furnished trisubstituted triazine **69** (Scheme 20).[63] Alternatively, Herrera and coworkers[63] suggested that the anticipated mechanism for the synthesis of trisubstituted triazine **69** initiates with reacting nitrile scaffold **68** with Tf_2O, which leads to triflate nitrilium intermediate **69A**. Afterward, another nucleophilic nitrile molecule **68** attacks the carbonium center of imino intermediate **69A** to form intermediate **69B**. Subsequently, an additional nitrile molecule **68** is nucleophilically attacked by intermediate **69B** from its cationic carbon to give intermediate **69C**, which is then cyclized to give triflate triazine intermediate **69D**. Ultimately, intermediate **69D** undergoes basic hydrolysis to afford **69** (Scheme 20).[63]

Under microwave irradiation, the reaction of aldehydes **70** with iodine in aqueous ammonia afforded nitriles **68**, which underwent [2 + 3] cycloaddition with cyanoacetimidamide **71**, yielding triazine derivatives **69**.[64] Whereby, cyclotrimerization reaction of three nitrile molecules **68** in the presence of Lewis-acid catalyst such as $Y(OTf)_3$ or silica-supported Lewis acid [Si(Ti), Si(Zn), Si(Al)] and piperidine gave trisubstituted-triazines **69** (Scheme 21).[65] Method A demonstrates superior performance with yields of 69–83%, high selectivity, and operational simplicity, requiring only moderate heating and short microwave irradiation. Method B offers greater flexibility through various solid catalysts (Si(Al), Si(Zn), Si(Ti), $Y(OTf)_3$), but optimal yields (up to 84%) are substrate- and catalyst-dependent, with some cases as low as 5% and much longer reaction times (up to 24 h). Electron-rich heteroaromatics (furyl,

Open Access Article. Published on 21 Oktober 2025. Downloaded on 9/06/2026 1:40:11 PG.
This article is licensed under a Creative Commons Attribution-NonCommercial 3.0 Unported Licence.



Scheme 22 Copper-catalyzed mechanism for the synthesis of triaryl-triazines.



Scheme 23 Reaction of nitrile hybrids with cyanoguanidine.

thienyl) generate better yields under method A, while electron-withdrawing groups (*e.g.*, 4-$NO_2C_6H_4$) give slightly reduce yields. In condition B, bulky or heterocyclic groups (piperidinyl and morpholino) lead to inconsistent yields influenced by catalyst type and substrate electronics.

The copper-catalyzed synthesis of 2,4,6-triaryl-triazines **69** was attained from the nucleophilic addition of amine derivatives **45** to arylnitrile **68** to give benzylbenzamidines **72**, which underwent cyclization reaction using the readily accessible CuCl catalyst and O_2 atmosphere into triazines **69**. Debnath *et al.*[66] proposed the mechanistic pathway for the formation of triazine **69**, starting with the oxidative addition of **72** using atmospheric O_2 and Cu catalyst to furnish intermediate **72A**, which then undergoes demetalation to form azadiene **72B**. Subsequently, another molecule of compound **72** is nucleophilically added from its unshared electrons to the electrophilic carbon center of intermediate **72B** to form **72C**, which then undergoes intramolecular annulation and nucleophilic addition to form **72D**. Then, benzyl amine **45** is split to give dihydrotriazine **72E**. Ultimately, aromatization of **72E** gives triazine **69** (Scheme 22).

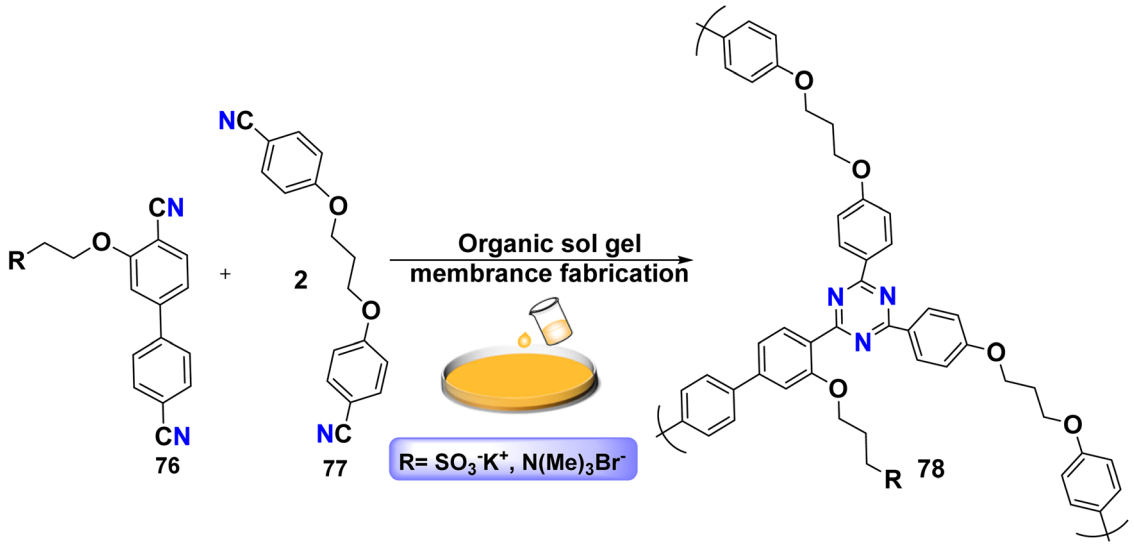
Diamino-*s*-triazines have been utilized as flavoenzymes as well as antitumor agents. Under microwave irradiation, treatment of nitrile scaffolds **68** with cyanoguanidine (**73**) for 10 min in DMSO afforded 2,4-diamino-1,3,5-triazine **69**. Similarly, under these conditions, the reaction of phthalonitrile (**74**) with cyanoguanidine (**73**) led to the synthesis of bis-triazines **75** (Scheme 23).[67]

The superacid-catalyzed organic sol–gel reaction of various aryl nitrile monomers, such as potassium ((dicyano-[biphenyl]-3-yl)oxy)ethane-sulfonate **76** or dicyano-biphenyl-oxy-trimethylethan-aminium bromide with (propane-diyl*bis*(oxy)) dibenzonitrile monomer **77**, was used to construct covalent triazine framework (CTF) membrane **78**. Due to ultrahigh ion diffusivity of CFT with low permeability, they are used in flow battery technology (Scheme 24).[68]

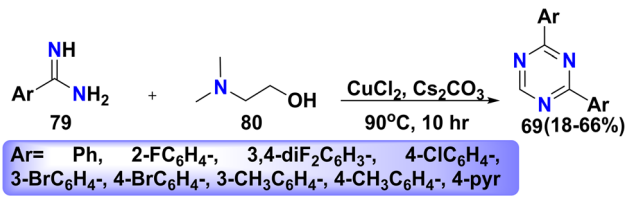
2.3.2 From amidines. Disubstituted 1,3,5-triazines show a broad spectrum of biological activities, including antimalarial, anti-inflammatory, antitumor, and antibacterial properties. Furthermore, the copper-catalyzed synthesis of 2,4-disubstituted triazine derivatives **69** was achieved *via* the reaction of arylamidines **79** with carbon synthon *N*,*N*-

© 2025 The Author(s). Published by the Royal Society of Chemistry

Open Access Article. Published on 21 Oktober 2025. Downloaded on 9/06/2026 1:40:11 PG.
This article is licensed under a Creative Commons Attribution-NonCommercial 3.0 Unported Licence.



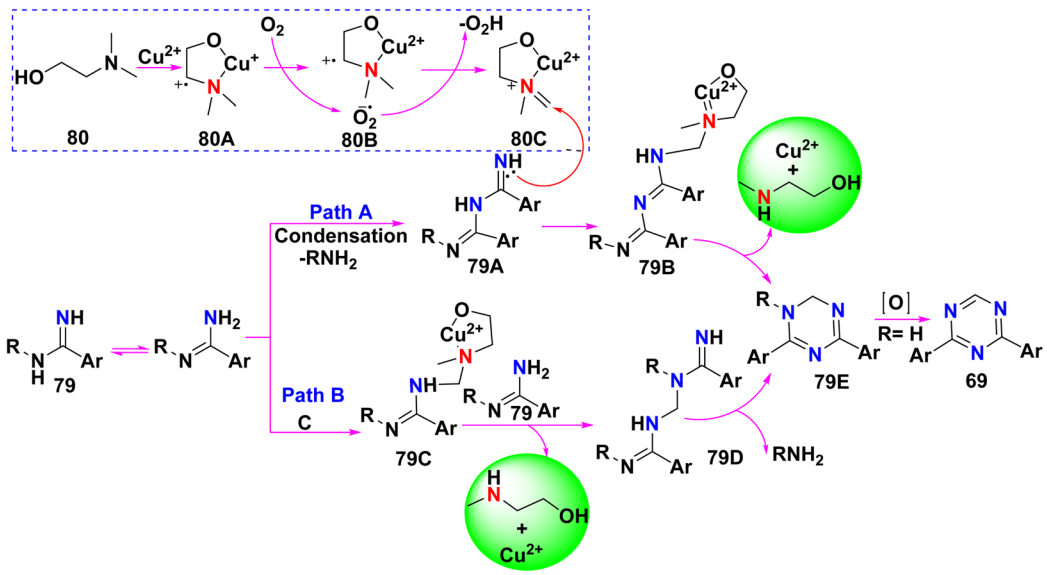
Scheme 24 Synthesis of the CTF membrane.



Scheme 25 Preparation of diaryl-triazines 69.

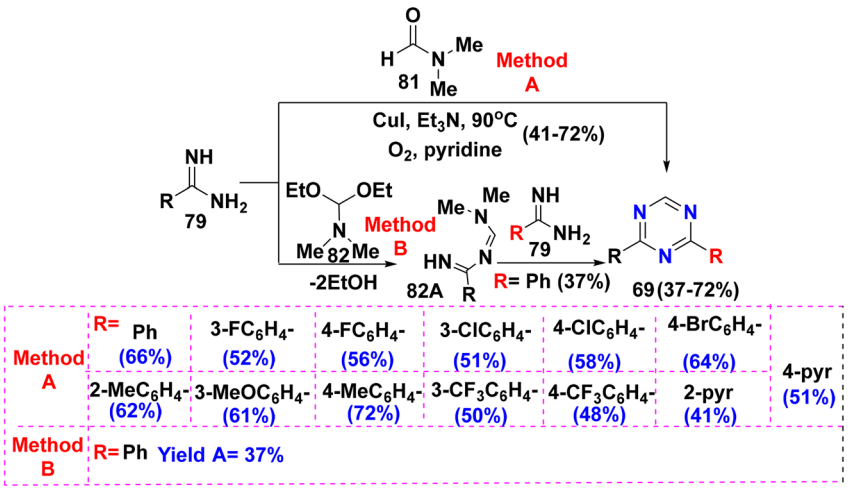
dimethylethanolamine (DMEA) **80** in the presence of copper chloride ($CuCl_2$) and Cs_2CO_3 (Scheme 25).[69]

Yan *et al.*[69] suggested the intricate mechanism for the synthesis of 2,4-disubstituted triazine **69** *via* two synthetic routes. The first step involves the coordination of DMEA with Cu^{2+} to generate intermediate **80A**, which then undergoes a Fenton-like reaction to produce radical cation **80B**. Next, reactive iminium ion intermediate **80C** is afforded when removing one proton from intermediate **80B**. Alternatively, the deamination reaction between two amidine scaffolds **79** proceeds through intermediate **79A**, which couples with **80C** to afford intermediate **79B** (path A). Simultaneously, intermediate **79B** undergoes annulation by eliminating *N*-methyl-ethanolamine to form product **79E**, and regenerates copper salt (Cu^{2+}) for the subsequent cycle. Ultimately, oxidation of intermediate **79E** in air furnishes scaffold **69**. Alternatively, the other conceivable route involves coupling intermediate **80C**with compound **79** to provide intermediate **79C**. Then, another amidine molecule **79** nucleophilically attacks intermediate **79C** to synthesize intermediate **79D**, followed by an annulation

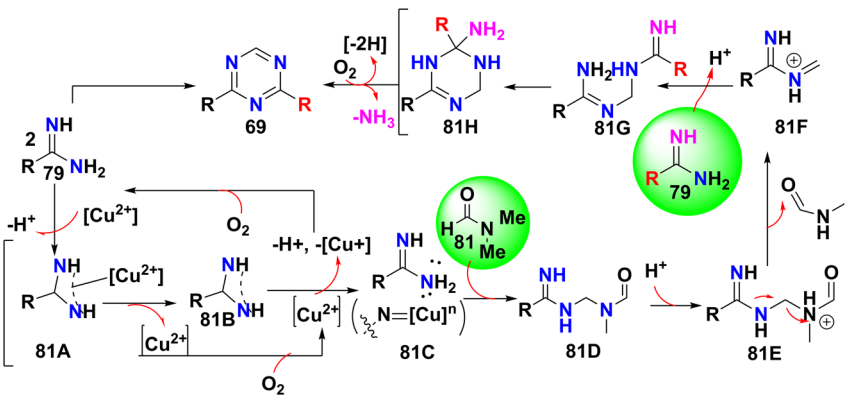


Scheme 26 Mechanistic pathways for the synthesis of disubstituted triazines.

Open Access Article. Published on 21 Oktober 2025. Downloaded on 9/06/2026 1:40:11 PG.
This article is licensed under a Creative Commons Attribution-NonCommercial 3.0 Unported Licence.



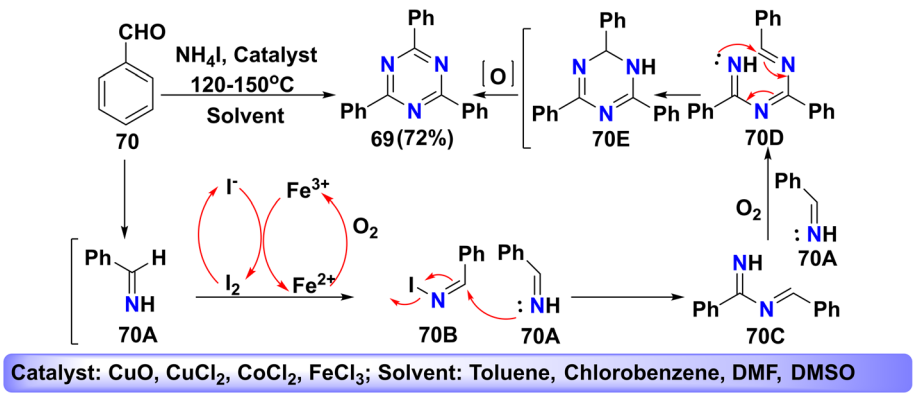
Scheme 27 Two synthetic pathways of disubstituted triazines 69.



Scheme 28 Copper-catalyzed mechanism for triazine formation.

process to give **79E**, which is oxidized to triazines (path B) (Scheme 26).

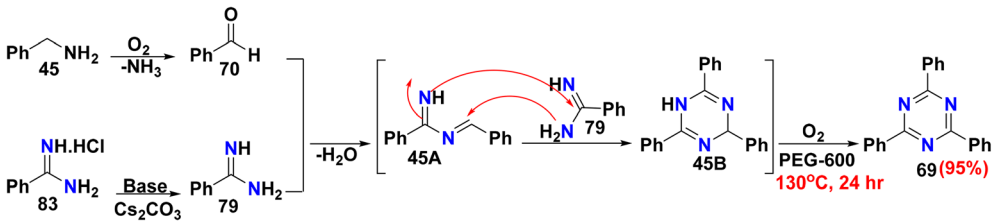
In 2014, Xu *et al.*[70] demonstrated the formation of 2,4-disubstituted-triazines **69** *via* the aerobic copper-catalyzed annulation of amidines **79** with DMF **81** as a carbon source in a basic medium. Alternatively, the cyclization reaction of phenylamidine **79** with diethoxy-dimethylmethanamine **82**, which serves as a formylating agent, afforded [(dimethylamino) methylene]benzamidine **82A**. Subsequently, intermediate **82A** combines with another amidine molecule **79** to yield diphenyltriazine **69** in 37% yield (Scheme 27). Method A provides an efficient route for the direct synthesis of 2,4-disubstituted-1,3,5-triazines from readily accessible feedstocks. Moreover, amidines with electron-donating groups (*e.g.*, –Me and –OMe)



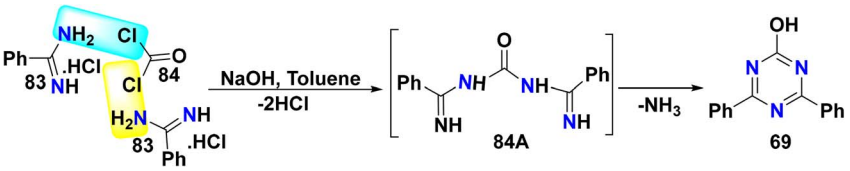
Scheme 29 Formation of triphenyl-triazine.

© 2025 The Author(s). Published by the Royal Society of Chemistry

Open Access Article. Published on 21 Oktober 2025. Downloaded on 9/06/2026 1:40:11 PG.
This article is licensed under a Creative Commons Attribution-NonCommercial 3.0 Unported Licence.



Scheme 30 Plausible mechanism of the formation of triphenyltriazine.



Scheme 31 Mechanistic pathway for the formation of diphenyl-triazinol.

consistently yield higher product amounts than those bearing electron-withdrawing groups (*e.g.*, –F and $–CF_3$). Conversely, method B is limited by its harsh reaction conditions such as elevated temperatures, lower yields, and narrow substrate scope restricted to symmetrical 2,4-diaryl-1,3,5-triazines. Additionally, the necessity for prefunctionalization complicates its workup and negatively impacts its environmental sustainability.

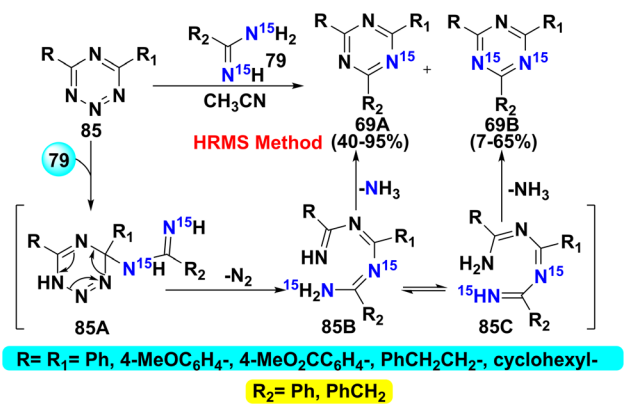
The mechanistic steps for the construction of triazine **69** are outlined in Scheme 28. Initially, the sequential dual single electron oxidation of amidine **79** to copper nitrene intermediate complex **81C** occurs, passing through intermediates **81A** and **81B**, followed by direct insertion into the C(sp^3)–H bond of DMF **81** to yield intermediate **81D**. Alternatively, protonating intermediate **81D** helps the cleavage of the polar C–N bond of the diaminomethyl moiety of **81E**, resulting in the production of iminium cation **81F** by removing the methylformamide molecule. Next, intermediate **81G** is produced by the electrophilic addition of **81F** to amidine **79**, followed by tautomerization. Then, aminal **81H** is generated by the intramolecular nucleophilic addition of an amino group to the imino center of **81G**. Ultimately, product **69** is obtained through the thermodynamically favorable deamination of **81H** and O_2-promoted dehydrogenative aromatization reactions (Scheme 28).[70]

Treatment of benzaldehyde (**70**) with ammonium iodide (NH_4I) in the presence of a transition state catalyst afforded triphenyl triazine **69**. The proposed mechanism for the synthesis of triazine **69** is illustrated in Scheme 29. The initial step involves the reaction of aldehydes **70** with NH_4I under ambient conditions to furnish imines **70A**. Afterward, an iron(III) ion (Fe^{3+}) oxidizes iodide ion (I^-) to form iodine (I_2), which subsequently oxidizes imine intermediate **70A** to yield *N*-iodoaldimine intermediate **70B**. Then, other molecules of intermediate **70A** condense with intermediate **70B** to afford intermediate **70C**. Following this, under aerobic conditions, intermediate **70A** is added to **70C** to furnish intermediate **70D**, which autocycles, resulting in the formation of intermediate **70E**. Finally, this intermediate undergoes an oxidation reaction to produce **69** (Scheme 29).[71]

Tiwari and coworkers[72] reported the synthesis of triazines **69** *via* an *in situ* oxidative cleavage process that converts benzylamine (**45**) into benzaldehyde (**70**). Alternatively, benzamidine salt **83** is neutralized with Cs_2CO_3 to afford the free base benzamidine **79**. Meanwhile, benzamidine **79** is reacted with freshly prepared benzaldehyde **70** to furnish intermediate **45A**. Another benzamidine molecule **79** is added to intermediate **45A** to give triphenyl-dihydrotriazine **45B**, which undergoes a dehydrogenative aromatization process in the presence of molecular oxygen as a green oxidant with PEG-600 to **69** (Scheme 30).[72]

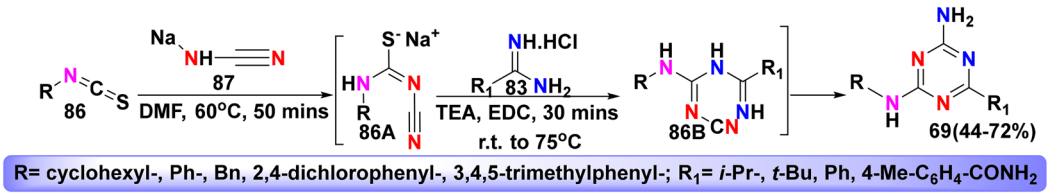
In the same context, diphenyl-triazinol **69** was achieved by reacting two molecules of arylamidine hydrochloride **83** with phosgene gas ($COCl_2$) (**84**), affording intermediate bis-imidylurea **84A**, which underwent ring closure upon heating above its melting point to form hydroxy-triazine **69** with the removal of an ammonia molecule (Scheme 31).[73]

Treatment of electron-deficient tetrazine **85** with electron-rich amidine **79** in the presence of acetonitrile (CH_3CN)

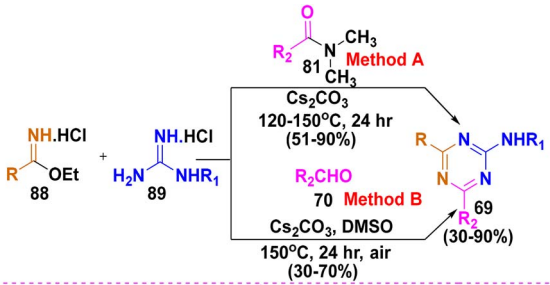


Scheme 32 Concerted and stepwise addition/cyclization Diels–Alder mechanism for triazine formation.

Open Access Article. Published on 21 Oktober 2025. Downloaded on 9/06/2026 1:40:11 PG.
This article is licensed under a Creative Commons Attribution-NonCommercial 3.0 Unported Licence.



Scheme 33 Synthetic route for the formation of triazine scaffolds **69**.



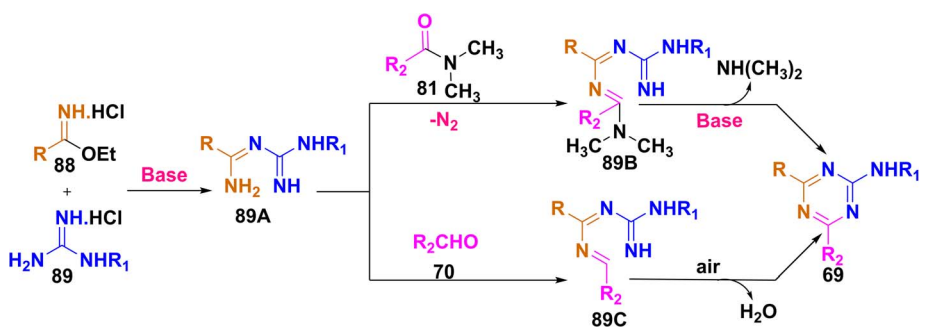
Method A				Method B			
R	R_1	R_2	Yield	R	R_1	R_2	Yield
Ph	H	H	90	Ph	H	Ph	68%
4-$CH_3C_6H_4$-	H	H	88	4-$CH_3C_6H_4$-	H	4-$CH_3C_6H_4$-	65%
3-$CH_3C_6H_4$-	H	H	75	Ph	*n*-C_6H_{13}-	Ph	49%
4-ClC_6H_4-	H	H	71	Ph	H	4-ClC_6H_4-	58%
4-BrC_6H_4-	H	H	73	Ph	H	4-$MeOC_6H_4$-	54%
4-$CF_3C_6H_4$-	H	H	72	4-$CH_3C_6H_4$-	H	4-ClC_6H_4-	57%
4-$CH_3OC_6H_4$-	H	H	85	4-$CF_3C_6H_4$-	H	Ph	70%
3-$CH_3C_6H_4$-	*n*-C_6H_{13}-	H	54	4-$CF_3C_6H_4$-	H	4-$CH_3C_6H_4$-	64%
4-ClC_6H_4-	*n*-C_6H_{13}-	H	68	4-$CF_3C_6H_4$-	H	3-MeC_6H_4-	52%
4-$CF_3C_6H_4$-	*n*-C_6H_{13}-	H	62	4-$CH_3C_6H_4$-	H	Pentyl	33%
Ph	*n*-C_6H_{13}-	Me	51	4-$CF_3C_6H_4$-	H	Pentyl	30%

Scheme 34 Formation of triazines from guanidine salts and aryl imidate.

furnished singly and doubly ^{15}N-triazines **69**.[74] Whereby, substituted triazines **69A** and **69B** may be rationalized *via* an addition/N_2 elimination/cyclization mechanism, starting with adding amidines **79** to electron-deficient tetrazine **85** to afford intermediate **85A**, followed by losing N_2 gas to give intermediate **85B**. Finally, deamination reaction followed by cyclization occurs to afford single ^{15}N-triazine **69A**. Alternatively, if intermediate **85B** is tautomerized to intermediate **85C**, double ^{15}N-triazine **69B** is synthesized (Scheme 32).[74]

The synthetic pathway for the preparation of triazine scaffolds **69**, as depicted in Scheme 33, commences with the reaction of isothiocyanate derivatives **86** with sodium hydrogen cyanamide (NaHNCN) (**87**) in DMF, yielding *N*-cyanothiourea sodium salts **86A**. This transformation involves the nucleophilic attack of the cyanamide anion **87** on the electrophilic carbon center of isothiocyanate **86** to give *N*-cyanothiourea intermediate **86A**. Subsequently, *N*-cyanothiourea sodium salt **86A** undergoes a reaction with amidine hydrochloride salts **83** at room temperature in the presence of triethylamine (TEA) and a coupling reagent (1-ethyl-3-(3-dimethylaminopropyl) carbodiimide) (EDC). During this step, the amidine **83** nucleophile attacks the electrophilic carbon of intermediate **86A**, producing unstable intermediate **86B**. Finally, this intermediate undergoes intramolecular cyclization to afford the corresponding 2,4-diamino-1,3,5-triazine derivatives **69** (Scheme 33).[75]

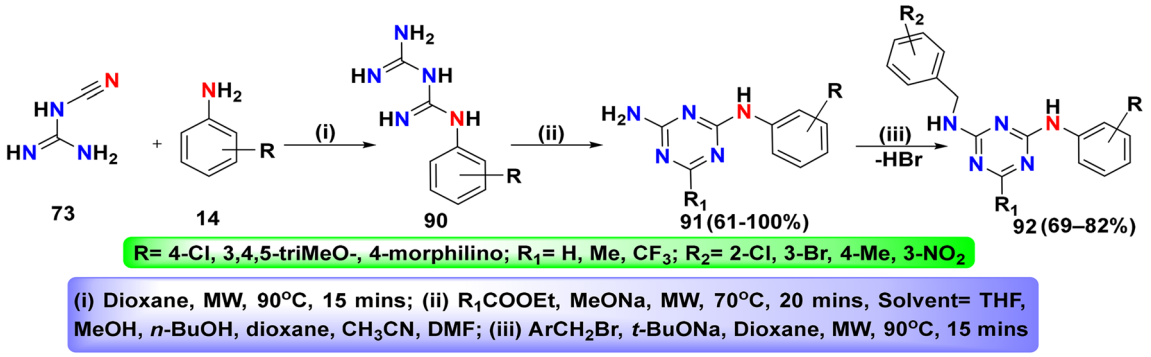
2.3.3 From guanidine. A simple and efficient base-mediated method has been developed for the synthesis of unsymmetrical 1,3,5-triazin-2-amines. The reaction of arylimidate salt **88** and guanidine hydrochloride derivatives **89** in the presence of amide derivatives such as DMF or *N*,*N*-dimethylacetamide (DMA) or *N*,*N*-dimethylpropionamide afforded 2-amine-triazines **69**. Similarly, the multicomponent reaction (MCR) of **88** and **89** with aldehyde derivatives **70** in the presence of DMSO under base-mediated Cs_2CO_3 furnished **69** (Scheme 34).[76] Method A provides higher yields across most substrates, with yields ranging from 51% to 90%, while method B affords a broader yield (30–70%) depending on the substrate combination. For instance, the unsubstituted compound (R = Ph, R_1 = R_2 = H in method A) achieves the highest yield (90%)



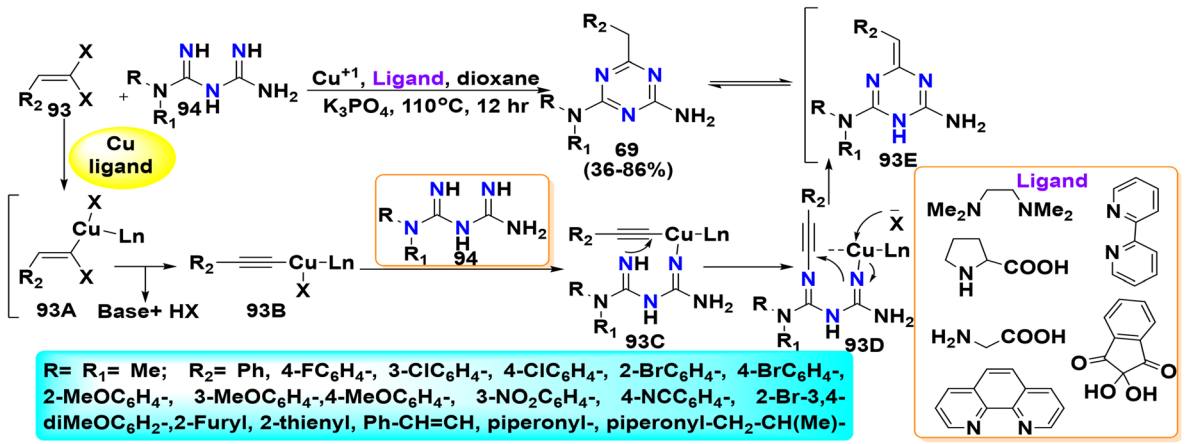
Scheme 35 Mechanism pathway for triazine formation from guanidine salts.

© 2025 The Author(s). Published by the Royal Society of Chemistry

Open Access Article. Published on 21 Oktober 2025. Downloaded on 9/06/2026 1:40:11 PG.
This article is licensed under a Creative Commons Attribution-NonCommercial 3.0 Unported Licence.



Scheme 36 Formation of biologically active substituted-triazine-4,6-diamines.



Scheme 37 Possible mechanism for the copper-catalyzed synthesis of triazines.

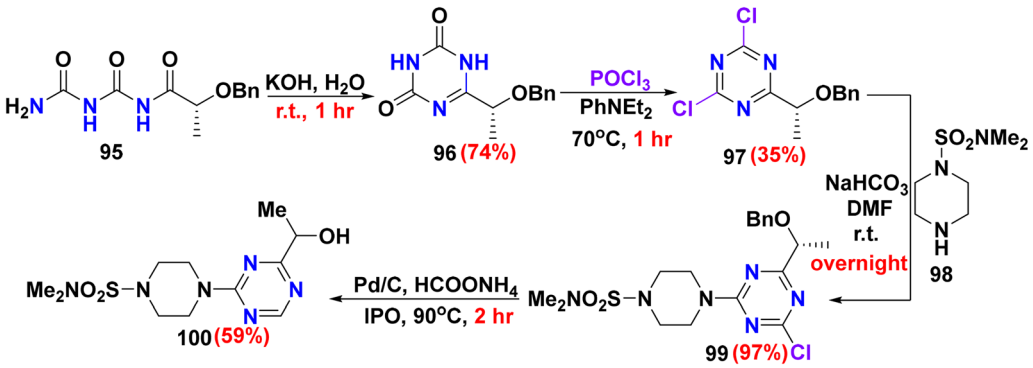
compared to 68% (R = Ph, R_1 = H, R_2 = Ph) in method B. Method A worked well for *meta*- and *para*-substituted (3-$CH_3C_6H_4$– and 4-$CH_3C_6H_4$–), and various electron-withdrawing groups (EWGs; Cl, Br, and CF_3) and electron-donating groups (EDGs, Me, and OMe). Alternatively, in method B, aromatic aldehydes were tolerated under base-mediated conditions, while aliphatic aldehydes could form the corresponding products.

The possible mechanism for the preparation of 2-amine-triazine derivatives **69** can be rationalized *via* three steps, beginning with the nucleophilic attack of guanidine **89** to imidate **88** in the presence of Cs_2CO_3 provide intermediate **89A**; next, its amino group attacks the acyl group of the amide moiety to afford intermediate **89B**; ultimately, this intermediate undergoes intramolecular cyclization, corresponding with eliminating a dimethyl amine moiety to yield compound **69**. Alternatively, under base-mediated and oxidized conditions, the amino group of intermediate **89A** attacks aldehydes **70**, furnishing intermediate **89C**, followed by intramolecular oxidative dehydration/cyclization of **89C**, yielding compound **69** (Scheme 35).[76]

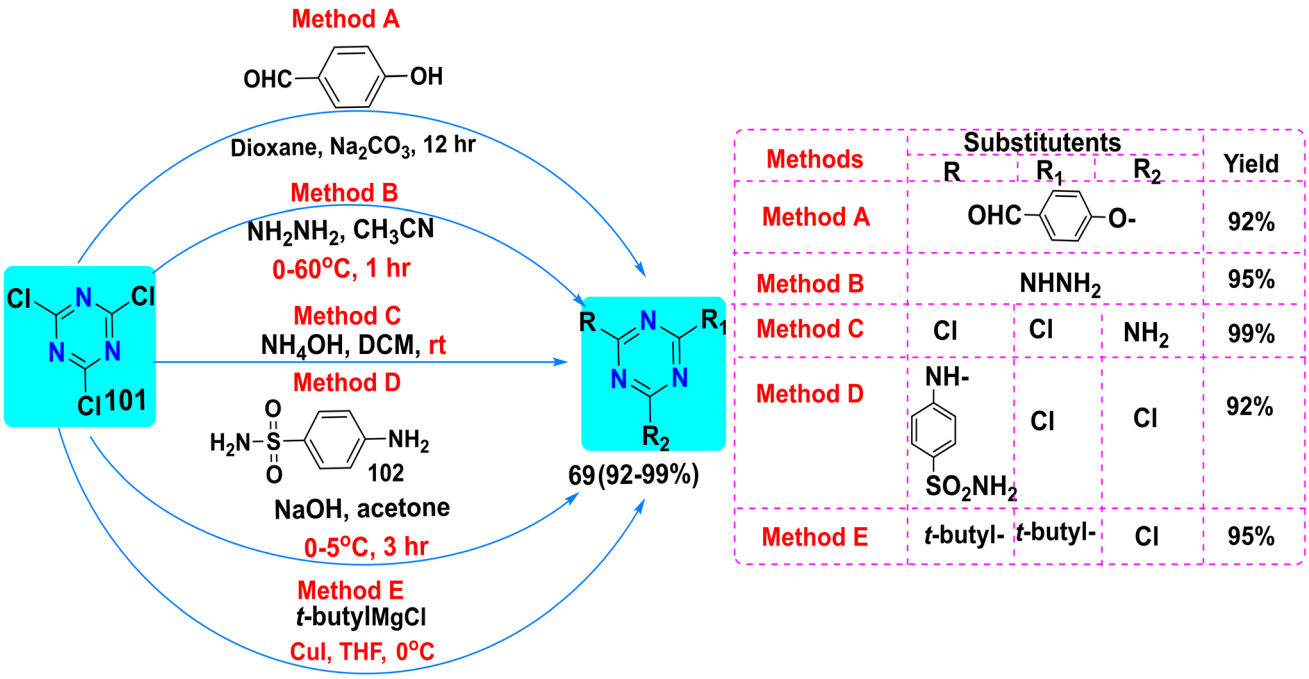
Diamino-1,3,5-triazine derivatives **92** have a wide range of chemotherapeutic activities, including antimicrobial, anti-tumor, herbicidal, antimalarial, anti-angiogenesis, antiviral, depressant for reticuloendothelial hyperfunction, and cyclin-dependent kinase inhibition. Under microwave irradiation, trisubstituted-triazines **92** were synthesized in three steps, starting with the nucleophilic addition of aniline derivatives **14** to cyanoguanidine **73**, which afforded phenyl biguanide derivatives **90**. Then, compound **90** was reacted with ester derivatives in the presence of THF and sodium methoxide (MeONa) to furnish 2-amino-(phenyl)-amino-alky-triazines **91** in up to quantitative yield. Ultimately, compound **92** was obtained *via* treatment of substituted-benzyl bromide with amino triazine derivatives **91**, which led to the elimination of the HBr molecule under the influence of basic sodium-*tert*-butoxide (*t*-BuONa) (Scheme 36).[77]

2.3.4 From biguanidines. A transition metal promoted the formation of disubstituted-amino-triazines **69** *via* the reaction of dihaloalkene **93** with biguanides **94** in the presence of a readily available Cu catalyst and potassium phosphate (K_3PO_4).[78] Scheme 37 depicts the probable mechanism for the formation of triazines **69**, where the first step involves the insertion of a catalytic amount of [Cu–ligand] between the C–X bond of compound **93** to afford intermediate **93A**. Then, the dehydrohalogenation process under the influence of base furnished alkyne complex **93B**. Next, biguanide derivatives **94** nucleophilically attack Cu^+ of **93B** to form intermediate **93C**. As

Open Access Article. Published on 21 Oktober 2025. Downloaded on 9/06/2026 1:40:11 PG.
This article is licensed under a Creative Commons Attribution-NonCommercial 3.0 Unported Licence.



Scheme 38 Synthetic strategy to generate triazine-sulfonamide.



Scheme 39 Synthesis of triazines from cyanuric chloride.

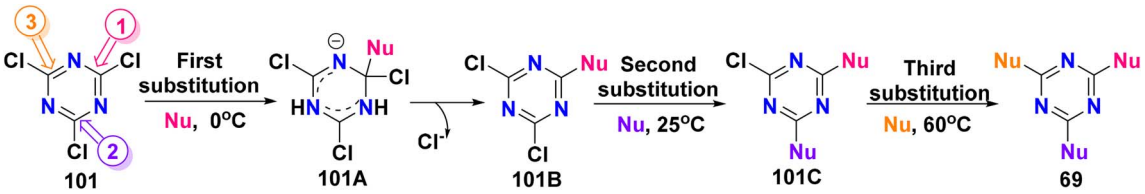
a result, intermediate **93C** undergoes intramolecular nucleophilic attack *via* its N atom to generate intermediate **93D.** Next, dihydro-triazin-intermediate **93E** is formed *via* demetalization with the help of a halogen ion, and then intramolecular nucleophilic attack from the other N atom. Finally, intermediate **93E** undergoes tautomerization to form aromatic product **69** (Scheme 37).[78]

(Hydroxyethyl)-triazin-2-yl-dimethylpiperazine-sulfonamide **100** was obtained through four steps. Firstly, triazine-dione scaffold **96** was synthesized *via* intramolecular cyclization reaction of benzyloxy-*N*-ureidocarbonyl-propionamide **95** in a basic medium. Secondly, chlorination of compound **96** with phosphorous oxychloride ($POCl_3$) furnished dichloro-triazine derivatives **97.** Thirdly, compound **97** was coupled with piperazine derivative **98,** to afford binary piperazine-triazine derivative **99**, which finally underwent dechlorination and debenzylation to yield compound **100** under the influence of a palladium catalyst (Scheme 38).[79]

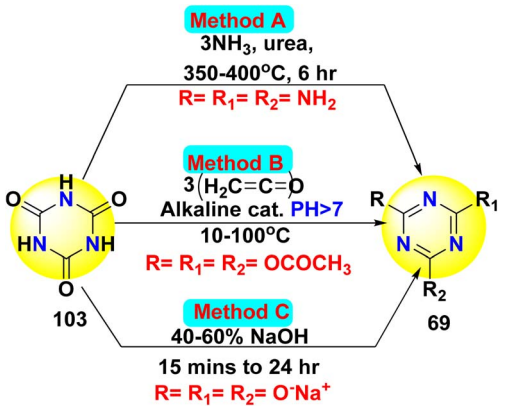
2.3.5 From cyanuric chloride. The first successful attempt to prepare 1,3,5-triazine involved the use of the readily available and cost-efficient raw material cyanuric chloride (**101**) as a chlorinated analog of *s*-triazine[80] *via* nucleophilic displacement of the three leaving group chlorine atoms. One of the most significant advantages of this methodology is the ability to control the nucleophilic substitution, whereas the reactivity of chlorine atoms decreases as the substitution in the ring increases.[31b] Due to the presence of three electrophilic active sites in cyanuric chloride, it is more susceptible to nucleophilic attack with several reagents containing C^-, O^-, S^-, and N^- atoms with basic behavior, less sterically hindered, and a perfect platform to synthesize novel drug candidates with excellent biological and physicochemical properties.[80b] 1,3,5-Triazines have been demonstrated to be potentially potent

© 2025 The Author(s). Published by the Royal Society of Chemistry

Open Access Article. Published on 21 Oktober 2025. Downloaded on 9/06/2026 1:40:11 PG.
This article is licensed under a Creative Commons Attribution-NonCommercial 3.0 Unported Licence.



Scheme 40 Suggested mechanism for the preparation of trisubstituted triazines.

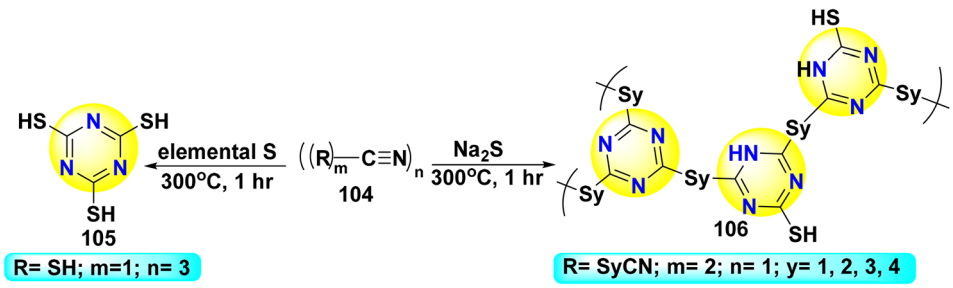


Scheme 41 Formation of triazines 69 from cyanuric acid.

against malaria, viruses, cancer, and microbes. Whereby, treatment of 4-hydroxybenzaldehyde with cyanuric chloride (**101**) in the presence of dioxane and basic sodium carbonate (Na_2CO_3) afforded (triazine-2,4,6-triyl)*tris*(oxy)tribenzaldehyde **69**.[81] Alternatively, the reaction of **101** with hydrazine hydrate (NH_2NH_2) in the presence of CH_3CN gave trihydrazineyl-triazine **69**.[82] Further, Viira *et al.*[83] reported the synthesis of amino-dichloro-triazine derivatives **69** by stirring a mixture of **101** with NH_4OH in DCM. In the same context, stirring a mixture of **101** with primary aromatic amine such as aminobenzenesulfonamide **102** in the presence of NaOH at 0–5 °C furnished ((dichloro-triazin-2-yl)amino)benzenesulfonamide **69**.[84] Under nitrogenous atmospheric conditions, a combination of Grignard reagent such as *tert*-butyl magnesium chloride (*t*-butylMgCl) and copper(I) iodide (CuI) was added to **101** to yield di-*t*-butyl-chloro-triazine **69** (Scheme 39).[85] A comparative evaluation of the five synthetic methods reveals that method C consistently delivers the highest yield (99%) due to the strong nucleophilicity and regioselectivity of ammonium hydroxide, enabling the efficient displacement of multiple chlorines. Methods B and E also offer high efficiencies, each affording 95% yield. Method E enables selective dialkylation, demonstrating tolerance toward steric bulk at the R and R_1 positions. Methods A and D, while effective (yields 92%), lead to the introduction of more complex or multifunctional groups (aromatic aldehyde for A and sulfonamide-substituted aniline for D), confirming the flexibility of these methods for diverse structural modifications.

The plausible mechanism for the synthesis of trisubstituted *s*-triazine **69** from cyanuric chloride starts with the nucleophilic aromatic substitution on (C-1) of compound **101** at 0 °C to afford intermediate **101A**, which readily removes an HCl molecule to form monosubstituted triazine **101B**, and then the second substitution is achieved on (C-2) at ambient temperature to furnish disubstituted triazine **101C**. The last substitution can be performed at 60 °C on (C-3) to yield trisubstituted triazine **69** and the three chlorine atoms leave as three molecules of HCl, which are neutralized with a base (Scheme 40).[31b,86]

Treatment of cyanuric acid (**103**) with ammonia under the influence of pressure and 350–400 °C afforded melamine **69**.[87] Melamine is a durable thermosetting plastic utilized in high-pressure decorative laminates,[88] insulation,[89] and fire-retardant additives,[90] as well as in the impregnation of décor paper,[91] and fertilizer for crops.[92] Also, melamine derivatives treat African trypanosomiasis.[93] Alternatively, the reaction of ketene with **103** gave triazine-triyl triacetate **69**. Conversely, replacing three hydrogens of cyanuric acid (**103**) when it is in the form of enol with an alkali earth metal such as NaOH furnished triazine salts **69** (Scheme 41).[87] The harsh thermal conditions in method A may promote efficient substitution; however, decomposition may occur, leading to decreasing selectivity. In contrast, the lower temperature in method B allow better control and enhance the selectivity. Alternatively, in method C, the base-promoted conditions enable efficient



Scheme 42 Synthesis of triazine-thiol derivatives.

Open Access Article. Published on 21 Oktober 2025. Downloaded on 9/06/2026 1:40:11 PG.
This article is licensed under a Creative Commons Attribution-NonCommercial 3.0 Unported Licence.

nucleophilic substitution and permit faster reaction times, but is limited in substrate scope and regioselectivity depending on the nature of the substituents. Electron-withdrawing groups (*e.g.*, $OCOCH_3$) tend to react better in method B, while electron-donating groups may require harsher conditions as in method A.

Alternatively, triazine-trithiol **105** was obtained through the trimerization reaction of thiocyanic acid (HSCN) (**104**) in the presence of elemental sulfur at 300 °C. Similarly, polymerization of thiocyanogen (NC–S_2–CN) afforded a polymerized chain of triazine-thiol **106** (Scheme 42).[94]

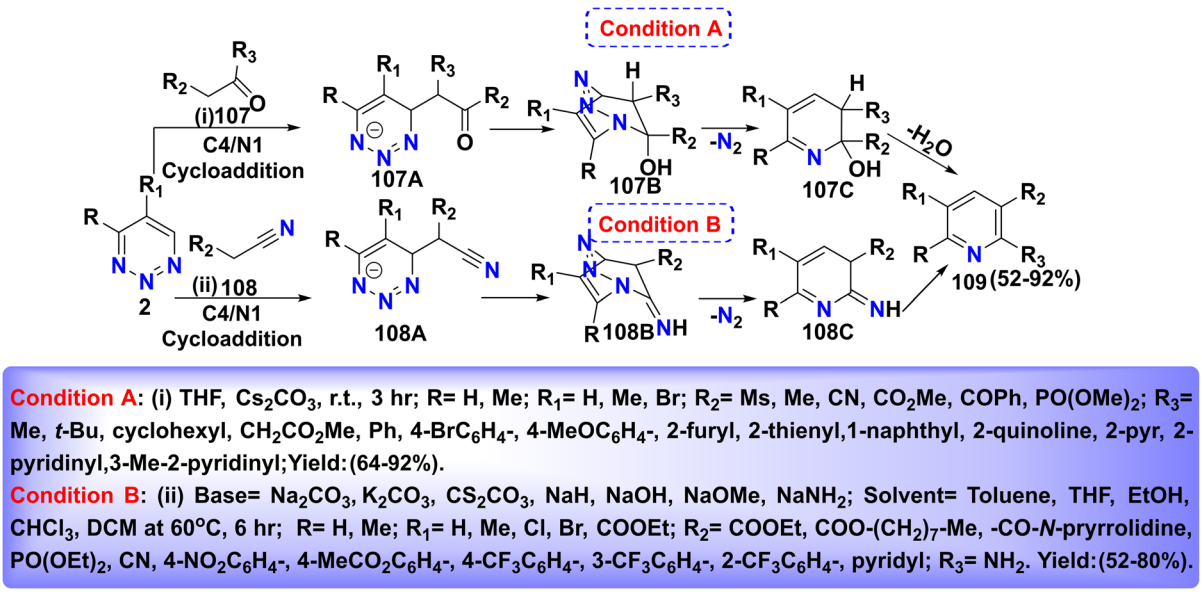
3. Reactions

3.1 Reactions of 1,2,3 triazines

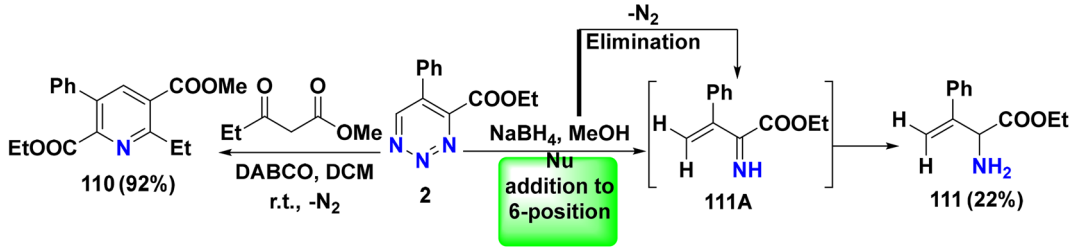
3.1.1 Addition/N_2 elimination/cyclization reaction. Pyridine scaffolds are an important class of compounds that are ubiquitous in numerous pharmaceuticals and natural products. Whereby, pyridine hybrids are prepared through the addition/N_2 elimination/cyclization cascade reaction of triazine **2** with ketones **107** or acetonitrile derivatives **108** in the presence of Cs_2CO_3. Scheme 43 gives insight into the reaction mechanism, which under the influence of nucleophilic addition reaction between electron-rich alpha-ketones **107** or acetonitriles **108** with electron-deficient triazine **2** from its C-4 atom affords tetrahedral intermediate **107A** or **108A**, followed by intramolecular nucleophilic addition of nitrogenous anion to the carbonyl or cyano-groups to furnish intermediate **107B** and **108B**, respectively. Following this, an elimination step occurs where N_2 gas is expelled, affording intermediate **107C** or **108C**. Ultimately, intermediate **107C** undergoes dehydration to furnish pyridine scaffold **109**, while the C=N double bond of intermediate **108C** undergoes isomerization reaction to form aminopyridine hybrid **109** (Scheme 43).[95]

The classic inverse-electron-demand Diels–Alder (IEDDA) of ethyl-5-phenyl-triazine-4-carboxylate **2** with β-ketoester such as methyl-3-oxopentanoate **110** in the presence of basic 1,4-diazabicyclo[2.2.2]octane (DABCO) yielded ethyl-5-methyl-6-ethyl-3-phenylpyridine-dicarboxylate **109**. In contrast, the reaction of compound **2** with sodium borohydride ($NaBH_4$) in methanol at 0 °C leads to nucleophilic addition at the 6-position of the triazine ring, followed by extrusion of nitrogen gas to afford imine intermediate **111A**, which undergoes reduction to furnish ethyl-amino-phenylbutanoate **111** (Scheme 44).[96]

3.1.2 Reaction with carbon dioxide. Triazine **2** has been readily converted into triazine carboxylic acid **112** by using



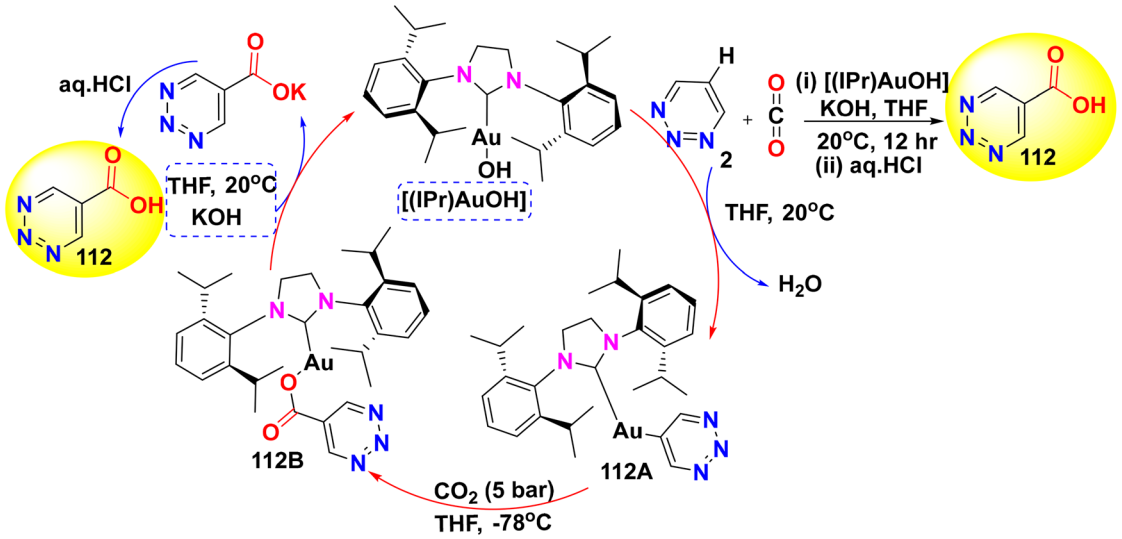
Scheme 43 Reaction of triazine with alpha-ketone and acetonitrile derivatives.



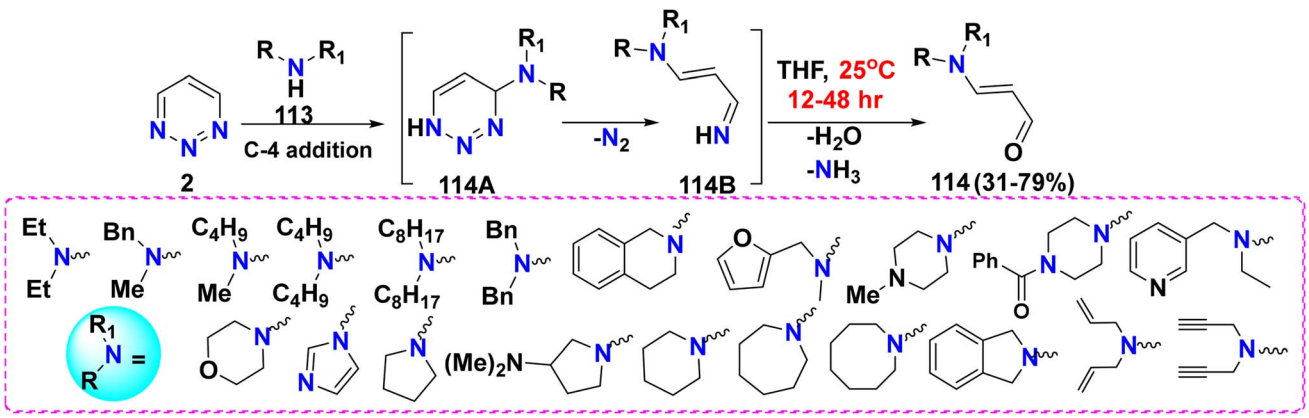
Scheme 44 IEDDA reaction for the synthesis of pyridines and the reduction of triazine.

© 2025 The Author(s). Published by the Royal Society of Chemistry

Open Access Article. Published on 21 Oktober 2025. Downloaded on 9/06/2026 1:40:11 PG.
This article is licensed under a Creative Commons Attribution-NonCommercial 3.0 Unported Licence.



Scheme 45 Proposed mechanism for the formation of triazine carboxylic acid.



Scheme 46 Reaction of triazine with various amines.

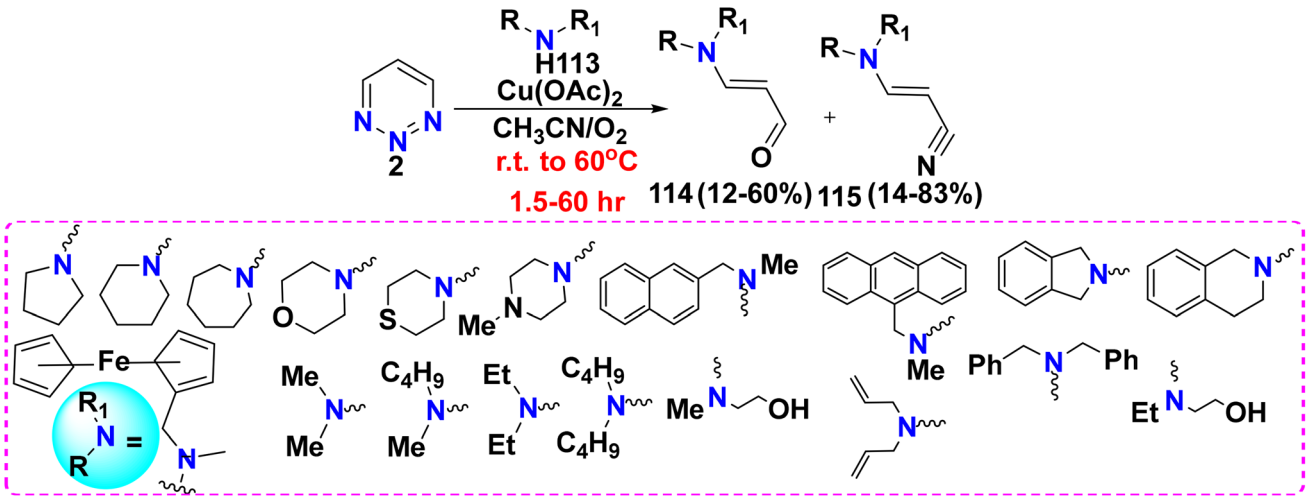
carbon dioxide (CO_2) and a catalytic amount of *N*-heterocyclic carbene bearing a gold hydroxide complex [(IPr)AuOH] under basic conditions. Moreover, to ascertain an approach for this methodology, the plausible mechanism of triazine and CO_2 is shown in Scheme 45, involving protonolysis of [(IPr)AuOH] by triazine **2** to furnish gold(I) triazine intermediate **112A**. After that, **112A** is saturated with CO_2 at −78 °C, followed by the nucleophilic addition of the triazine ligand to the electron-deficient carbon center of CO_2, resulting in carboxylate complex **112B**. Afterward, **112B** undergoes metathesis using KOH, which led to the regeneration of [(IPr)AuOH], and precipitation of potassium triazine-carboxylate. Finally, neutralization of potassium triazine carboxylate furnishes **112** (Scheme 45).[97]

3.1.3 Reaction with amines. Scheme 46 illustrates a significant synthetic methodology for the preparation of β-enaminals **114**, starting with the cycloaddition reaction of nucleophilic secondary amine **113** to the C-4 atom of electrophilic triazine **2** to afford intermediate **114A**, which quickly liberates N_2 gas to form imine intermediate **114B**. Then, intermediate **114B** is hydrolyzed using THF, and subsequently undergoes deamination to produce β-enaminal **114** (Scheme 46).[98,99]

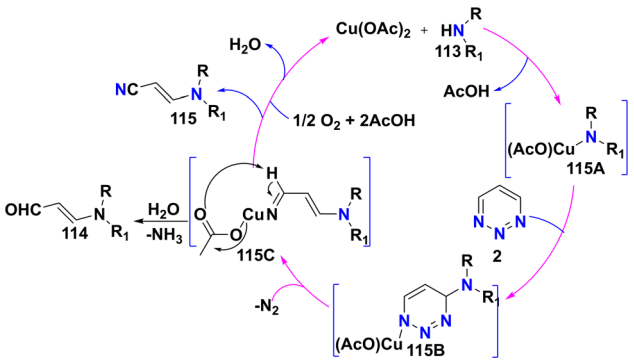
Structurally diverse nitrile-containing molecules are integral to numerous natural products and medicinal drugs. Small organic nitriles serve as versatile pharmaceutical synthons owing to their capacity to be transformed into amines, aldehydes, carboxylic acids, amides, and nitrogen-containing heterocycles. Additionally, Yang *et al.*[98] described the use of a green copper-catalyzed aerobic oxidation methodology to form a mixture of *β*-enaminal **114** and amino acrylonitrile **115** through the reaction of amines **113** with triazine **2** in the presence of copper(II) acetate ($Cu(OAc)_2$) and an oxygenated atmosphere (Scheme 47).

As depicted in Scheme 48, Yang *et al.*[98] described the proposed mechanism for the synthesis of β-aminoenal **114** and nitrile scaffolds **115**, starting with the coordination of amine **113** with a Cu catalyst to form intermediate **115A**, followed by amino cupration of triazine ring **2** to form amine adduct **115B**,

Open Access Article. Published on 21 Oktober 2025. Downloaded on 9/06/2026 1:40:11 PG.
This article is licensed under a Creative Commons Attribution-NonCommercial 3.0 Unported Licence.



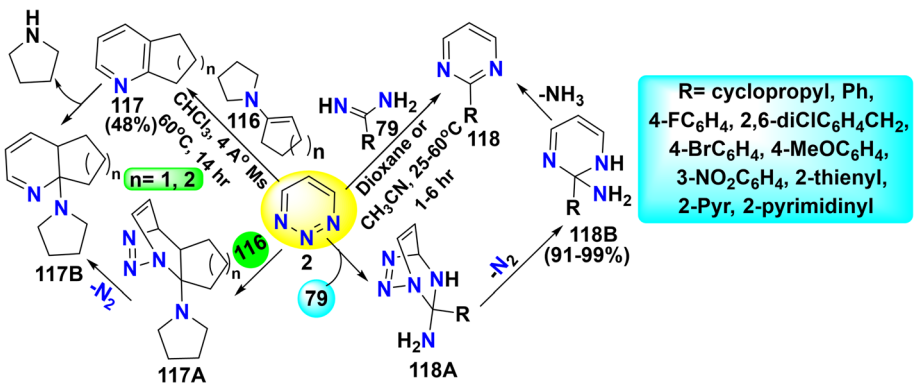
Scheme 47 Treatment of triazine with secondary amines.



Scheme 48 Mechanistic pathway towards the preparation of β-enaminals.

which is *in situ* liberates N_2 gas to produce β-amino-α,β-unsaturated Cu–imine complex **115C**. Afterward, the basic anion acetate of the $Cu(OAc)_2$ catalyst facilitates the dehydrogenative oxidation process and β-elimination of intermediate **115C**, resulting in the formation of nitrile scaffold **115**, while hydrolysis of **115C** occurs under the impact of H_2O produces *β*-aminoenals **114** (Scheme 48).

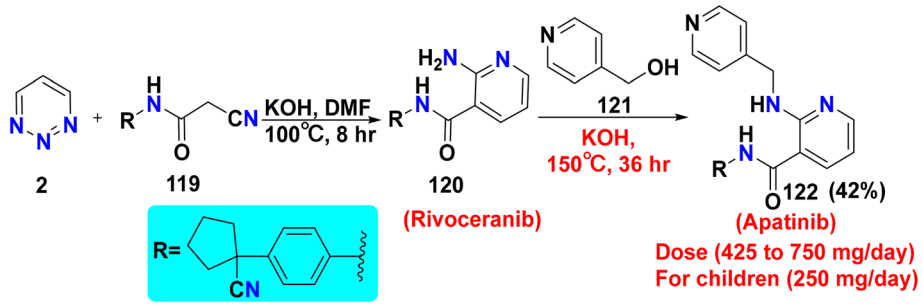
3.1.4 Reaction with enamines & amidines. IEDDA has been employed in the total synthesis of natural compounds with highly functionalized heterocyclic aromatic systems.[100] Accordingly, the [4 + 2] cycloaddition reaction of electron-deficient triazine **2** as C=N diene with electron-rich enamine derivatives **116** or amidine **79** as dienophile through IEDDA produced cyclopenta[*b*]pyridine **117** and pyrimidine derivatives **118**, respectively. To explore the synthetic pathways for their synthesis, enamine double bond **116** attacks triazine **2** from its C4–N1 atoms through a concerted [4 + 2] cycloaddition, leading to intermediate **117A**, followed by expelling N_2 gas to furnish intermediate **117B**. Ultimately, this intermediate undergoes further transformation, resulting in the loss of the pyrrolidine molecule and producing fused pyridine **117**. Similarly, the synthesis of pyrimidine derivative **118** commences with the nucleophilic attack of amidine **79** on triazine **2**, leading to the formation of tetrazine intermediate **118A**. The subsequent elimination of N_2 gas facilitates the conversion to intermediate **118B**, which ultimately undergoes deamination to yield pyrimidine scaffolds **118**, as illustrated in Scheme 49.[101]



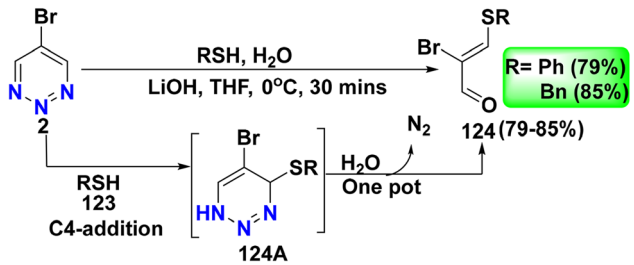
Scheme 49 Treatment of triazine with enamines and amidines.

© 2025 The Author(s). Published by the Royal Society of Chemistry

Open Access Article. Published on 21 Oktober 2025. Downloaded on 9/06/2026 1:40:11 PG.
This article is licensed under a Creative Commons Attribution-NonCommercial 3.0 Unported Licence.



Scheme 50 Synthesis of the Apatinib drug.

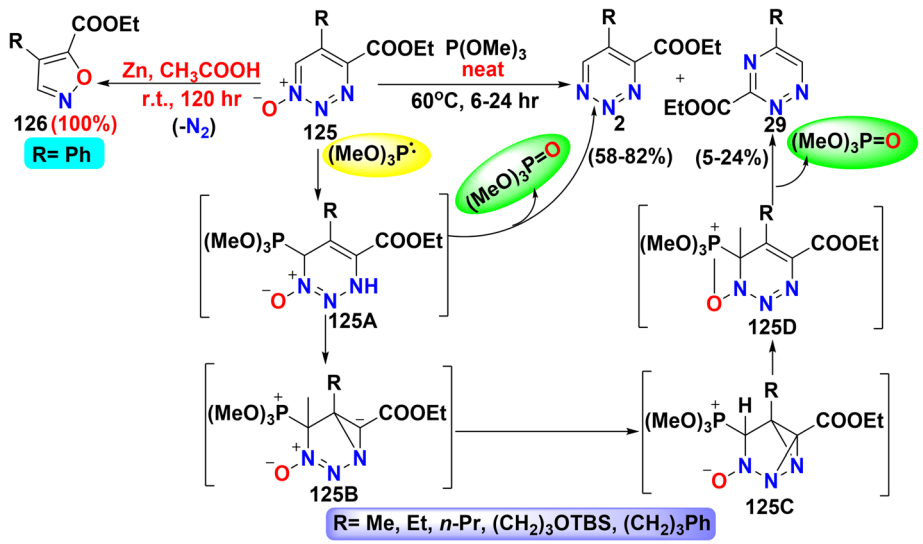


Scheme 51 Synthesis of β-thioenals.

3.1.5 Reaction with cyanoacetamide derivatives. Apatinib drug **122** was synthesized *via* a two-step sequential process, starting with the cycloaddition reaction of triazine **2** to (cyanocyclopentyl)phenyl-cyanoacetamide **119** in the presence of basic KOH in DMF to afford Rivoceranib drug **120**.[102] Following this, coupling scaffold **120** with pyridin-4-ylmethanol (**121**) furnished Apatinib **122**, a potent anticancer and anti-angiogenic agent with a demonstrated therapeutic efficiency against bone and soft tissue sarcoma sickness (Scheme 50). Also, Apatinib and Rivoceranib drugs are used to treat tumors by inhibiting tumor angiogenesis *via* targeting key signaling pathways. The typical initial dose for Apatinib ranges from 425 to 750 mg per day, except for children, where the initial dosage is 250 mg per day.[103–105]

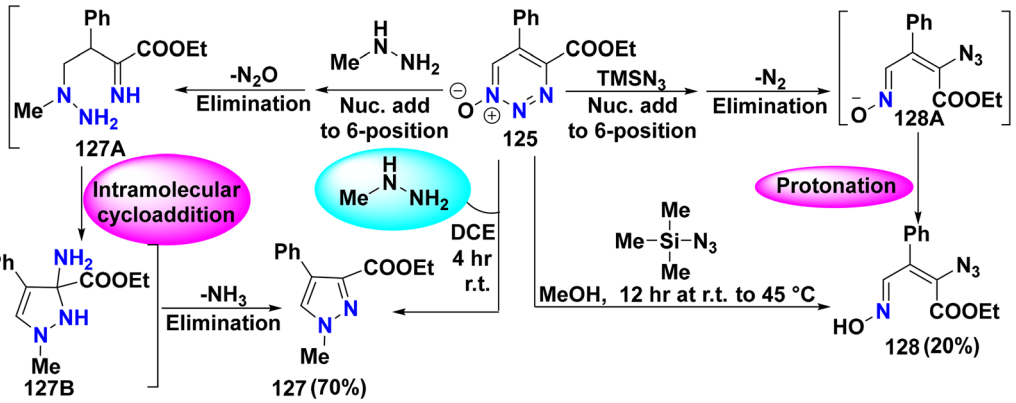
3.1.6 Reaction with thiols. α-Substituted β-thioenals **124** were synthesized by stirring a mixture of triazine **2** and thiol derivatives **123** in an ice bath. The proposed mechanism for the synthesis of compound **124** involves nucleophilic addition of thiol **123** to the C-4 position of triazine **2** to afford tetrahedral intermediate **124A**, followed by adding a water molecule, which is readily accomplished with denitrogenative ring opening to furnish β-thioenals **124**, showing remarkable biological activities (Scheme 51).[106]

3.1.7 Miscellaneous reactions. The thermal decomposition of 1-oxide-aryl-1,2,3-triazine-4-carboxylates **125** with Zn as a deoxygenation agent yielded isoxazoles **126** with the extrusion of dinitrogen, in quantitative yields. Conversely, deoxygenation of 1,2,3-triazine-1-oxides **125** using trimethyl phosphite ($P(OMe)_3$) leads to the formation of both 1,2,3- and 1,2,4-triazine derivatives **2** and **29**. This process is initiated by nucleophilic addition of trimethyl phosphite to the 6-position of the triazine-1-oxides **125** to afford intermediate **125A**. Subsequent Dimroth-type rearrangement proceeds *via* either a stepwise or concerted mechanism from **125A** to **125D**,

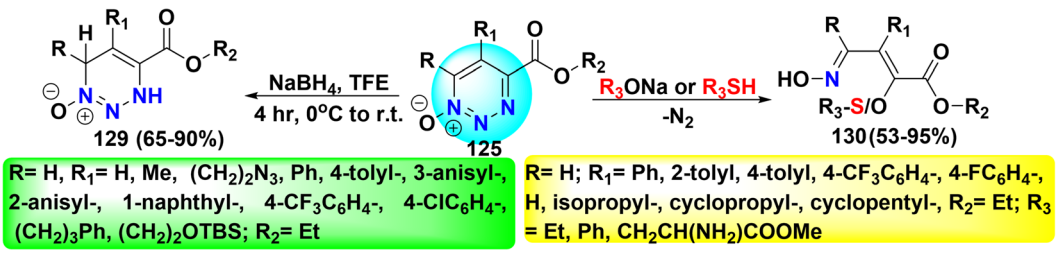


Scheme 52 Deoxygenation of 1,2,3-triazine-1-oxides **2**.

Open Access Article. Published on 21 Oktober 2025. Downloaded on 9/06/2026 1:40:11 PG.
This article is licensed under a Creative Commons Attribution-NonCommercial 3.0 Unported Licence.



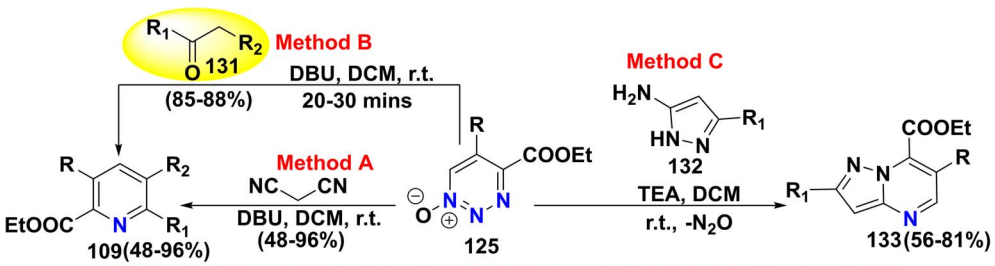
Scheme 53 Reaction of triazine-1-oxides **125** with nucleophiles.



Scheme 54 Selective nucleophilic addition of triazine *N*-oxides.

facilitating the structural reorganization necessary for the formation of the 1,2,4-triazine framework **29**. Conversely, 1,2,3-triazine derivatives **2** are obtained from the deoxygenation and elimination of trimethyl phosphate from intermediate **125A** (Scheme 52).[107]

Treatment of triazine-*N*-oxide **125** with methylhydrazine ($MeNHNH_2$) in DCE results in nucleophilic addition at the C-6



Method A				Method C		
R	R_1	R_2	Yield	R	R_1	Yield
Ph	NH_2	CN	94%	Ph	Ph	66
2-$MeOC_6H_4$-	NH_2	CN	96%	Ph	Me	81
4-MeC_6H_4-	NH_2	CN	92%	Ph	H	78
4-FC_6H_4-	NH_2	CN	84%	Ph	4-MeC_6H_4-	70
4-$CF_3C_6H_4$-	NH_2	CN	81%	Ph	4-MeC_6H_4-	64
2-naphthyl-	NH_2	CN	91%	Ph	2-Furyl-	56
cyc-C_3H_5-	NH_2	CN	84%	2-$MeOC_6H_4$-	4-MeC_6H_4-	69
cyc-C_5H_9-	NH_2	CN	48%	4-FC_6H_4-	4-ClC_6H_4-	80
Method B				4-$CF_3C_6H_4$-	4-MeC_6H_4-	73
R	R_1	R_2	Yield	2-naphthyl-	4-MeC_6H_4-	72
Ph	CH_2COOMe	CH_2COOMe	88%			
Ph	Me	SO_2Me	85%			

Scheme 55 Formation of pyridine and pyrazolo pyrimidine derivatives from triazine-1-oxides.

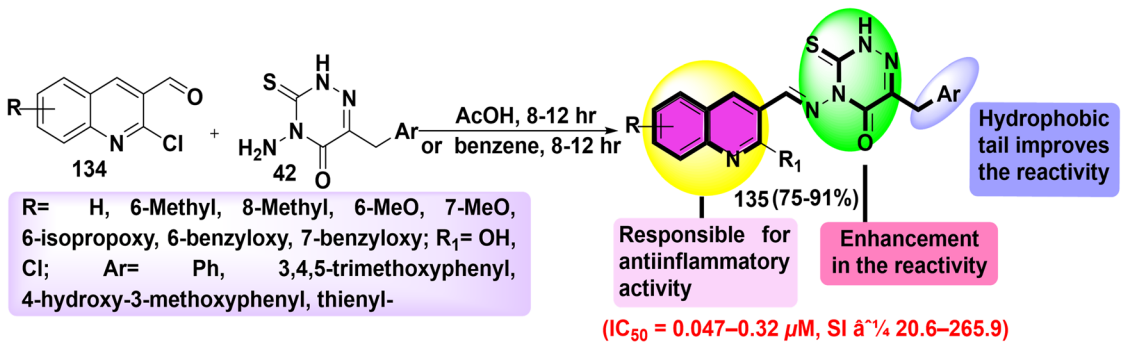
© 2025 The Author(s). Published by the Royal Society of Chemistry

Open Access Article. Published on 21 Oktober 2025. Downloaded on 9/06/2026 1:40:11 PG. This article is licensed under a Creative Commons Attribution-NonCommercial 3.0 Unported Licence.

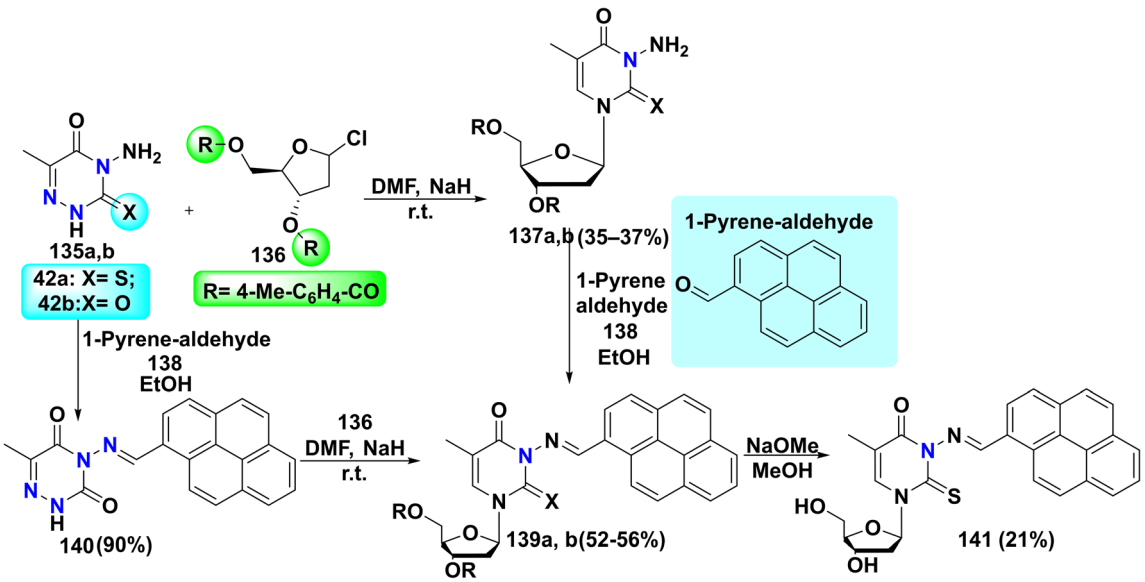
position of the triazine ring, followed by extrusion of nitrous oxide (N_2O) to afford ethyl 4-hydrazineyl-2-imino-3-phenylbutanoate intermediate **127A**. Afterward, this intermediate undergoes intramolecular cycloaddition to give intermediate **127B**, followed by the elimination of ammonia to afford pyrazole derivative **127**. In contrast, treatment of triazine-*N*-oxide **125** with trimethylsilyl azide ($TMSN_3$) in MeOH, the site selectivity of nucleophilic addition is reversed. The azide anion adds to the C-4 position of the triazine ring, leading to the elimination of nitrogen gas to form intermediate **128A**, which is subsequently protonated to furnish enoxime product **128** (Scheme 53).[96]

Dihydro-triazine-4-carboxylate-1-oxides **129** were obtained *via* the reduction of triazine-4-carboxylate-1-oxides **125** with $NaBH_4$ in trifluoroethanol (TFE). Alternatively, treatment of triazine *N*-oxides **125** with sodium ethoxide (EtONa) or thiols (RSH) in EtOH at room temperature resulted in selective *o*-nucleophilic addition at the 4-position, followed by nitrogen extrusion, furnishing the corresponding enoximes **130** (Scheme 54).[96]

In the presence of DBU (1,8-diazabicyclo[5.4.0]undec-7-ene) as a base and using DCM as the solvent at room temperature, 1,2,3-triazine-1-oxides **125** reacted efficiently with malononitrile to afford a variety of substituted pyridines **109**. Similarly, under identical reaction conditions, the treatment of triazine-1-oxides **125** with 1-(methylsulfonyl)propan-2-one **131** led to methylsulfonyl-substituted pyridines **109**. Furthermore, the reaction of triazine-1-oxides **125** with aminopyrazoles **132** in the presence of TEA in DCM furnished pyrazolo[1,5-*a*]pyrimidine derivatives **133**, accompanied by the release of N_2O (Scheme 55).[108] Method A generally provides higher yields (up to 96%), when $R_1 = NH_2$ and $R_2 = CN$. Method B shows slightly lower



Scheme 56 Formation of triazine-clubbed quinoline hybrids and their structure–activity relationship (SAR).



Virus	Sample 1mg/mL				
	137a	137b	139a	140	141
Coxsackie B	Weak	Moderate	-ve	Weak	Moderate
HAV-10	Moderate	Moderate	Weak	Moderate	Strong

Scheme 57 Synthetic strategy for the formation of various 1,2,4-triazine nucleosides.

Open Access Article. Published on 21 Oktober 2025. Downloaded on 9/06/2026 1:40:11 PG.
This article is licensed under a Creative Commons Attribution-NonCommercial 3.0 Unported Licence.

yields (85–88%) when bulkier or more electron-withdrawing ester groups are used as R_1 and R_2. Electron-donating groups on the aryl ring (*e.g.*, 2-$MeOC_6H_4$ and 4-MeC_6H_4) enhance the yield (92–96%), possibly due to the increased nucleophilicity of the amine. In contrast, electron-withdrawing groups (*e.g.*, 4-$CF_3C_6H_4$ and 4-FC_6H_4) lead to a moderate decrease in yield (81–84%). Bulky or cyclic groups such as cyclo-C_5H_9 show significantly lower yields (48%), suggesting that steric hindrance reduces the reactivity.

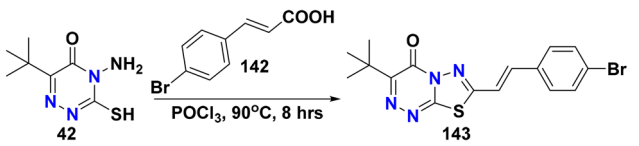
3.2 Reactions of 1,2,4 triazines

3.2.1 Condensation reaction. The condensation reaction of triazine **42** with chloro-quinoline-carbaldehyde derivative **134** in refluxing AcOH or benzene afforded (((hydroxy or chloro quinolin-3-yl)methylene)amino)-thioxo-dihydro-triazin-one derivatives **135** (Scheme 56). Triazine-appended quinoline scaffolds demonstrated excellent potency as dual COX-2/15-LOX inhibitors as well as inhibitors of ROS, NO, IL-6, and TNF-α inflammatory mediators (Scheme 56). Lipopolysaccharides (LPS), key components of the outer membrane of Gram-negative bacteria, activate RAW 264.7 macrophages, inducing COX-2 expression and upregulating inducible nitric oxide synthase (iNOS). This leads to increased nitric oxide (NO) production, which helps maintain the COX-2 levels. Moreover, activated macrophages produce reactive oxygen species (ROS), further amplifying inflammation by promoting pro-inflammatory cytokine release.[109]

The synthesis of deoxy-di-*o*-(4-methylbenzoyl)-β-D-*erythro*-pentofuranosyl derivatives **137** was attained through the reaction of amino-methyl-thioxo-triazin-5-one **42a** or amino-methyl-triazin-3,5-dione **42b** with deoxy-di(4-methylbenzoyl)-*erythro*-pentofuranosyl chloride **136** in the presence of NaH in DMF at room temperature. Then, condensation of scaffold **137** with pyrenealdehyde (**138**) afforded methyl-[(pyren-ylmethylene)amino]-[deoxy-di-*o*-(4-methylbenzoyl)-*erythro*-pentofuranosyl]triazine-dione derivatives **139**. Otherwise, under similar conditions, methyl-((pyrenylmethylene)amino)-triazine-dione **140** was retrieved by preliminary condensing **42a** and **42b** with **138**, which was subsequently coupled with compound **136** to give nucleoside base **139**. Ultimately, hydrolysis of compound **139a** with NaOMe in MeOH gave methyl-[(pyren-ylmethylene) amino]-(deoxy-β-D-*erythro*-pentofuranosyl)-thioxo-triazine-5-one **141** (Scheme 57), which demonstrated antiviral activity against the Hepatitis A virus (HAV-10) and Coxsackie B virus. These compounds work by inhibiting the inosine monophosphate dehydrogenase (IMPDH) enzyme existing in the purine nucleotide biosynthetic pathway.[110]

In contrast, the condensation reaction of amino-*tert*-butyl-sulfanyl-triazin-one **42** with bromo cinnamic acid **142** in the presence of $POCl_3$ produced [bromophenyl-ethenyl]-*tert*-butyl-[1,3,4]thiadiazolo[2,3-*c*][1,2,4]triazin-one **143** (Scheme 58). Docking simulations showed that compound **143** robustly binds to the receptor Mpro with a binding affinity of -8.2 kcal mol^{-1}, which supports its inhibition activity against COVID-19.[111] Additionally, Lohith *et al.*[111] reported the elucidation of the structure of skeleton **143** through its single crystal X-ray diffraction (Fig. 3).

Bis-triazine ligands depict one of the most efficient soft nitrogenous-donor ligands for separating trivalent actinides from trivalent lanthanides, a vital process for the reprocessing of spent nuclear fuel. Bis-heterocyclic amide derivatives **146a** and **b** were produced through the base hydrolysis of triazine ethyl ester **144**, followed by amide coupling with a cyclic diamine, such as piperazine (**145**), using a coupling agent, such as hexafluorophosphate azabenzotriazole tetramethyl uronium (HATU) in DMF. Alternatively, under microwave irradiation, the direct condensation of compound **144** with piperazine (**145**) in



Scheme 58 Synthetic route toward [bromophenyl-ethenyl]-*tert*-butyl-thiadiazolo-triazin-one **143**.

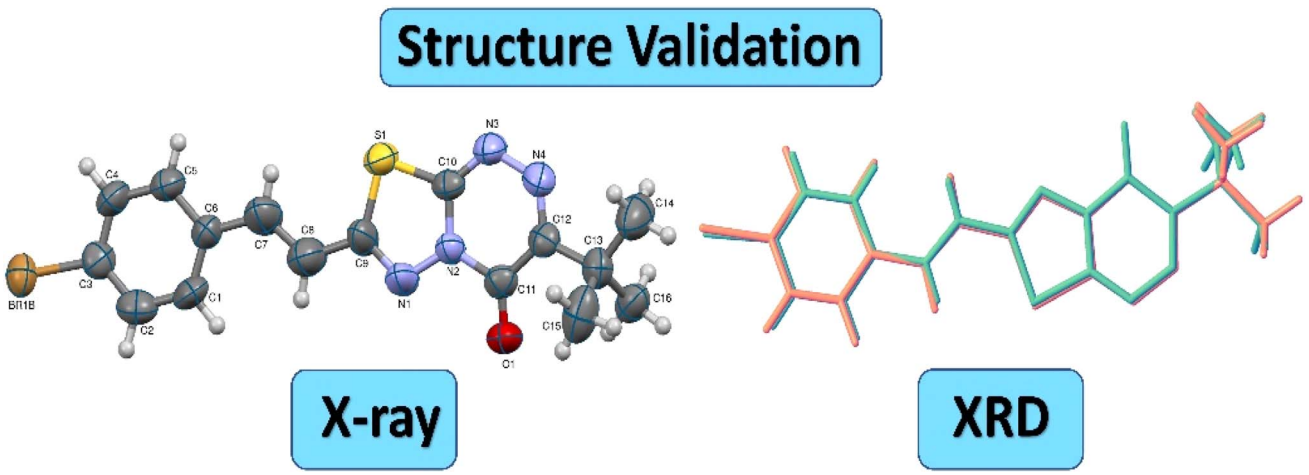
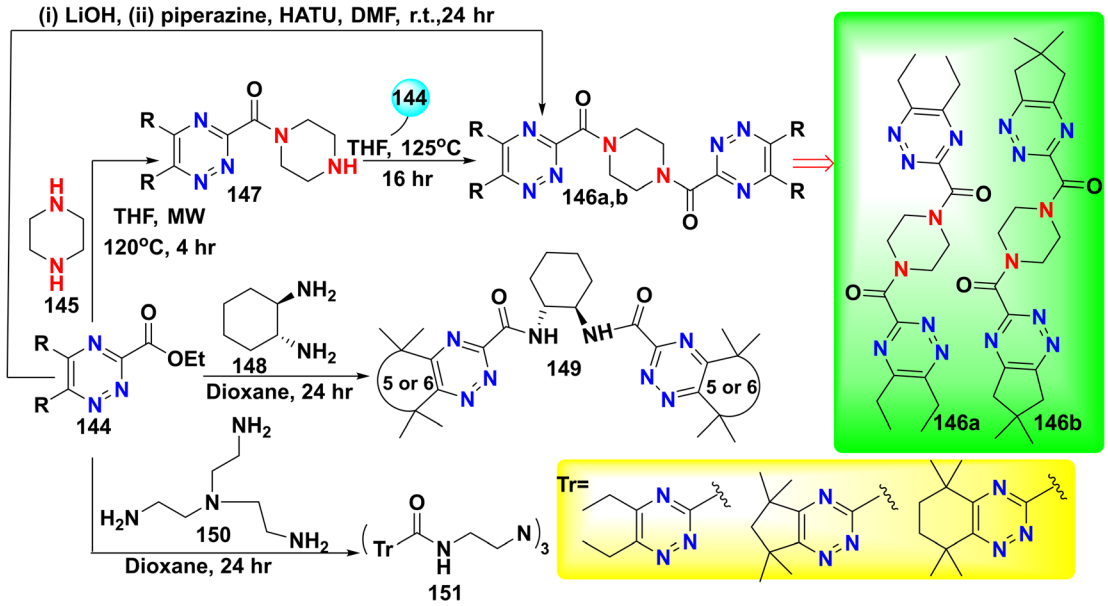


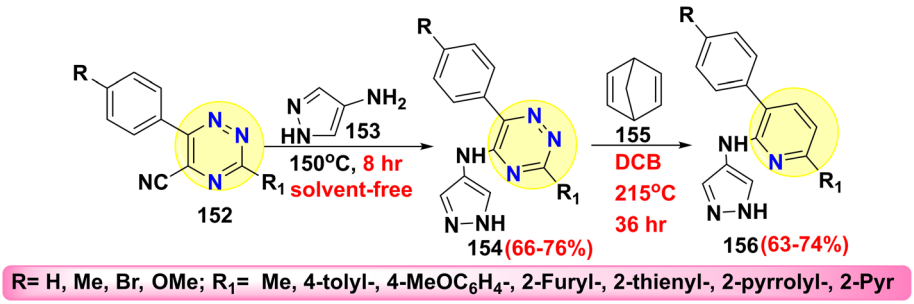
Fig. 3 Structure validation of compound **143** with X-ray and XRD analysis.[111]

© 2025 The Author(s). Published by the Royal Society of Chemistry

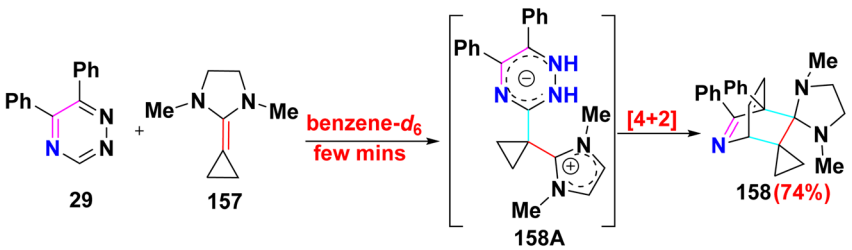
Open Access Article. Published on 21 Oktober 2025. Downloaded on 9/06/2026 1:40:11 PG.
This article is licensed under a Creative Commons Attribution-NonCommercial 3.0 Unported Licence.



Scheme 59 Synthesis of triazine ligands.



Scheme 60 Construction of pyrazole-clubbed pyridines.

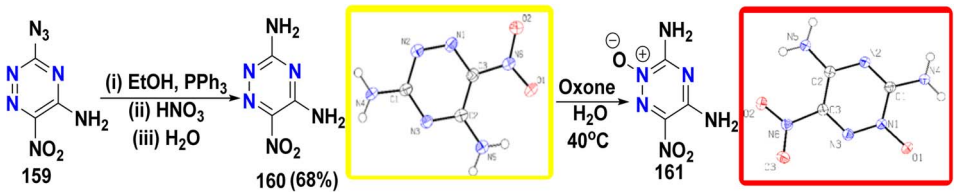


Scheme 61 Mechanistic pathway for cycloadduct triazine **158** formation.

THF afforded piperazinyl(triazin-yl)methanone **147**, which reacted with another molecule of compound **144** to give bis-triazine amide **146a** and **b**. Whereby, tetradentate-triazine-carboxamide derivatives **149** were produced *via* the condensation of compound **144** with cyclohexane-diamine **148**. Alternatively, amidation of compound **144** with *tris*(2-aminoethyl) amine (**150**) in dioxane led to three bidentate-triazine-carboxamide **151** (Scheme 59).[112]

3.2.2 SN ipso/aza-Diels–Alder reactions. The *ipso*-substitution reaction of cyano-triazine derivatives **152** with amino pyrazole **153** was implemented under neat conditions at 150 °C to afford pyrazol-triazin-amine derivative **154**. Afterward, aza-Diels–Alder reaction of compound **154** with bicyclo[2.2.1] heptadiene (**155**) in 1,2-dichlorobenzene (DCB) at 215 °C furnished pyrazole-clubbed pyridine derivatives **156** (Scheme 60). These compounds exhibited important inhibitory activity against JAK1, SYK, and FAK1 kinases, as well as cytotoxic effects on different cancer cells, including A-172, Hs578T, and HepG2 cells (Scheme 60).[113]

Open Access Article. Published on 21 Oktober 2025. Downloaded on 9/06/2026 1:40:11 PG.
This article is licensed under a Creative Commons Attribution-NonCommercial 3.0 Unported Licence.



Scheme 62 Synthesis of both nitro-triazine-diamine and diamino-nitro-triazine-oxide and their confirmed structure by X-ray analysis.[115]

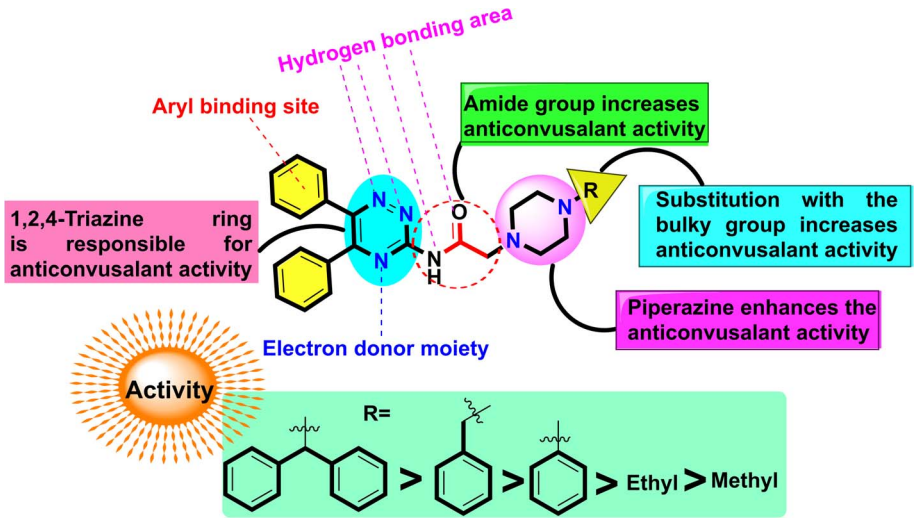
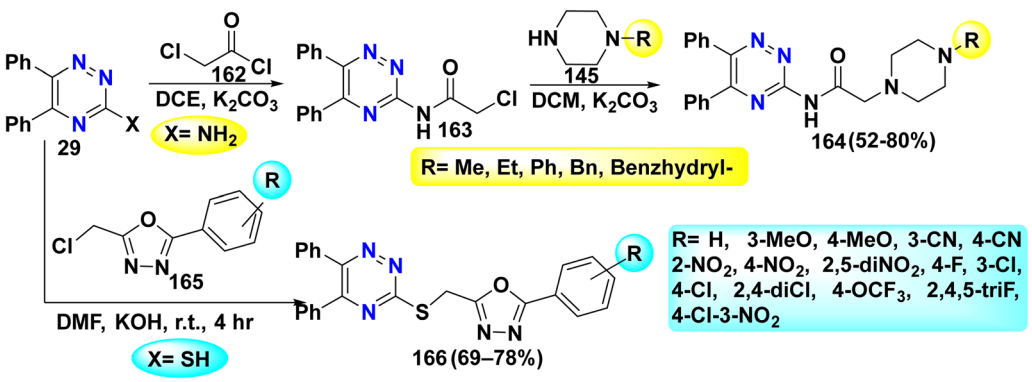


Fig. 4 SAR studies and bonding interactions[116] for piperazine-appended 1,2,4-triazine derivatives **164**.

The hetero-Diels–Alder (HDA) reaction of diphenyl-triazine **29** with cyclopropylidene-dimethyl imidazoline **157** yielded cycloadduct product **158** through a stepwise mechanism, starting with the concerted cycloaddition of **29** to **157** to form zwitterionic intermediate **158A.** After that, this intermediate is intramolecularly cyclized, rearranged, and expelled N_2 gas to furnish dimethyl-diphenyl-azadispiro[cyclopropane-bicyclo [2.2.2]octane-imidazolidine]-diene **158** (Scheme 61).[114]

3.2.3 Reduction & oxidation reaction. The reduction of amino-azido-nitro-triazine **159** to nitro-triazine-diamine **160** was carried out *via* a modified Staudinger reaction, utilizing a reducing agent triphenylphosphine (PPh_3). In contrast, diamino-nitro-triazine-oxide **161** was produced by oxidizing nitro-triazine-diamine **160** in water with the incremental addition of potassium peroxymonosulfate (Oxone®, $2KHSO_5 \cdot KHSO_4 \cdot K_2SO_4$) (Scheme 62). These compounds can be used as potentially insensitive energetic materials.[115]

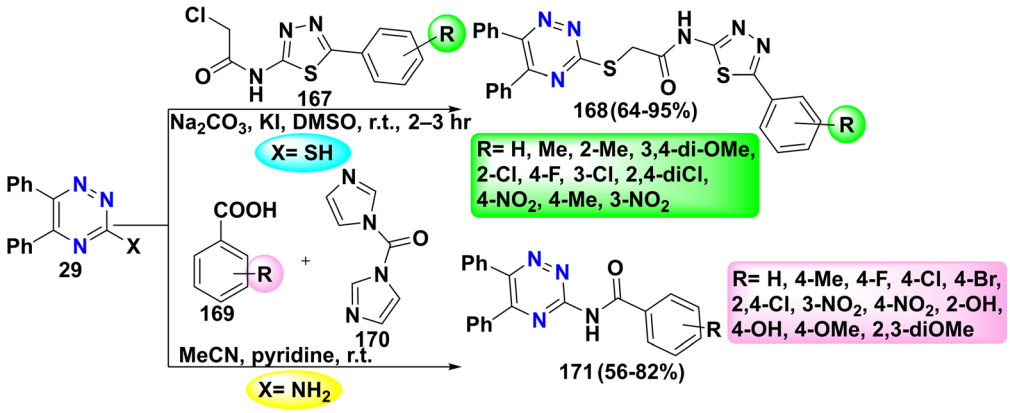
3.2.4 Nucleophilic substitution reaction. Stirring a combination of diphenyl-triazine-amine **29**, chloroacetyl chloride (**162**), and potassium carbonate (K_2CO_3) in DCE led to chloro-(diphenyl-triazin-yl)acetamide **163**. Subsequently, refluxing piperazine derivatives **145** with chloro-(triazin-yl)acetamide derivative **163** in DCM yielded (diphenyl-triazin-yl)-(4-substituted piperazinyl)acetamide scaffold **164**, which acted as



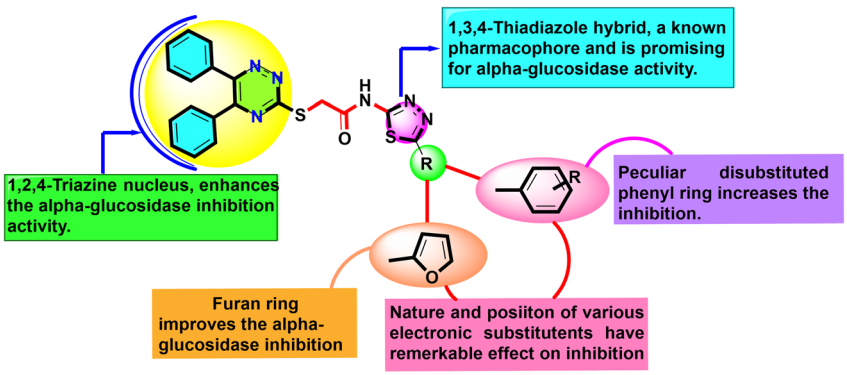
Scheme 63 Formation of binary triazine compounds.

© 2025 The Author(s). Published by the Royal Society of Chemistry

Open Access Article. Published on 21 Oktober 2025. Downloaded on 9/06/2026 1:40:11 PG.
This article is licensed under a Creative Commons Attribution-NonCommercial 3.0 Unported Licence.



Scheme 64 Construction of binary triazine scaffolds.



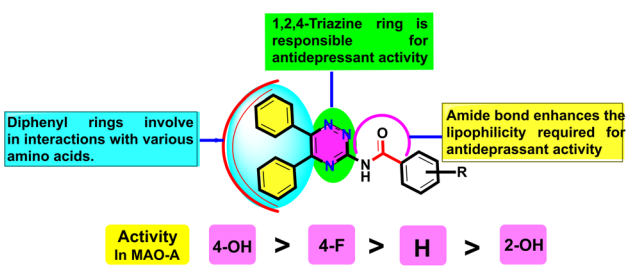
Substituent	IC_{50}(micrometer)	Substituent	IC_{50}(micrometer)
Ph-	743.15 ± 0.86	2,4-diCl-Ph	50.21 ± 0.04
2-Tolyl-	51.55 ± 0.45	4-MeO-Ph	481.84 ± 0.64
4-Tolyl-	109.26 ± 0.84	3,4-di-MeOP	120.65 ± 0.89
4-F-Ph	166.55 ± 1.92	3-NO_2-Ph	68.84 ± 0.70
2-Cl-Ph	14.36 ± 0.70	4-NO_2-Ph	51.29 ± 0.36
4-Cl-Ph	291.35 ± 1.80	Furan-2-yl	61.01 ± 0.78

Fig. 5 SAR studies[118] for thiadiazole-diphenyl-triazine scaffolds **168**.

a potent anticonvulsant agent (Fig. 4).[116] Whereby, (((diphenyl-triazin-yl)thio)methyl)-phenyl-oxadiazole derivatives **166**, which were shown to be dual COX-2/5-LOX inhibitors, were obtained by stirring a combination of diphenyl-triazine-thiol **29** with (chloromethyl)-phenyl-oxadiazole derivative **165** in DMF and KOH (Scheme 63).[117]

Analogously, dissolving an equimolar amount of diphenyl-triazine-thiol **29**, chloroacetyl-thiadiazole amide **167** in DMSO and in the presence of Na_2CO_3 and KI furnished thiadiazole-diphenyl-triazine hybrids **168** with antidiabetic activities (Scheme 64).[118] It is worth mentioning that the amidic linkages between the thiadiazole and triazine pharmacophores show remarkable effects on activity due to their substantial interactions (Fig. 5), which displayed α-glucosidase inhibitory activities. Analogously, MCR of benzoic acid derivatives **169**, thiol compound **29**, and carbonyl diimidazole (CDI) (**170**) in CH_3CN was allowed to stir at room temperature to yield (diphenyl-triazin-yl)benzamide derivatives **171** (Scheme 64), which are antioxidant and antidepressant agents (Fig. 6).[119]

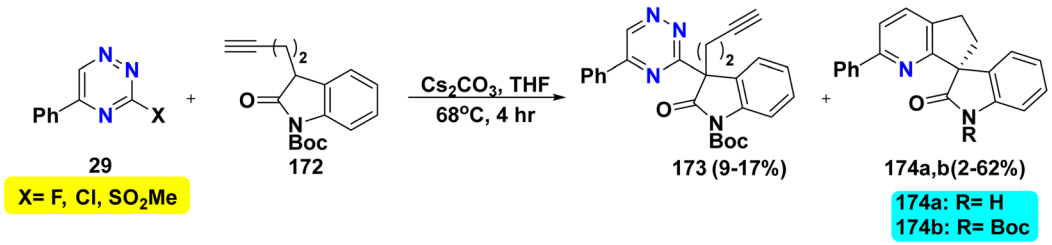
3.2.5 Nucleophilic aromatic substitution (SNAr) as well as inverse-electron-demand hetero-Diels–Alder (ihDA) and retro-



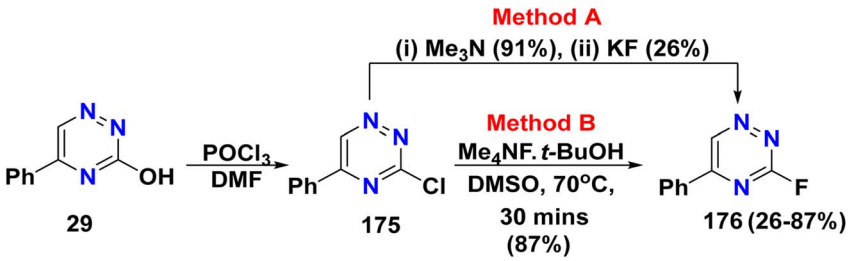
Substituent	IC_{50}(micrometer)	Substituent	IC_{50}(micrometer)
H	0.51 ±0.11	2-OH	0.78 ±0.32
4-F	0.30 ±0.06	4-OH	0.12 ±0.17

Fig. 6 SAR studies[119] of *N*-(diphenyl-triazin-yl)benzamide derivatives **171**.

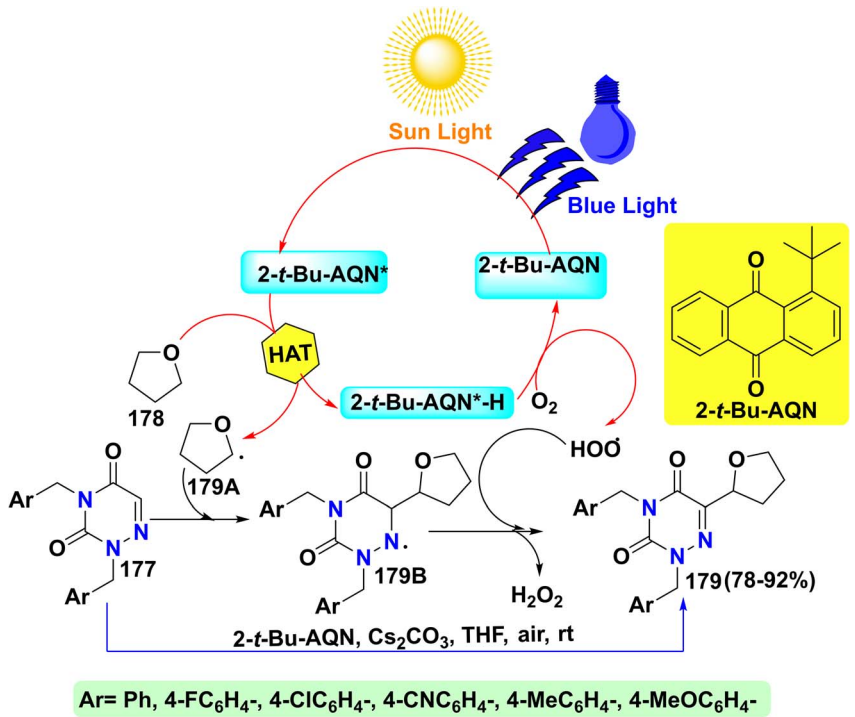
Open Access Article. Published on 21 Oktober 2025. Downloaded on 9/06/2026 1:40:11 PG.
This article is licensed under a Creative Commons Attribution-NonCommercial 3.0 Unported Licence.



Scheme 65 Synthesis pathway toward fused and spirobinary triazines.



Scheme 66 Halogenation of triazine derivative.



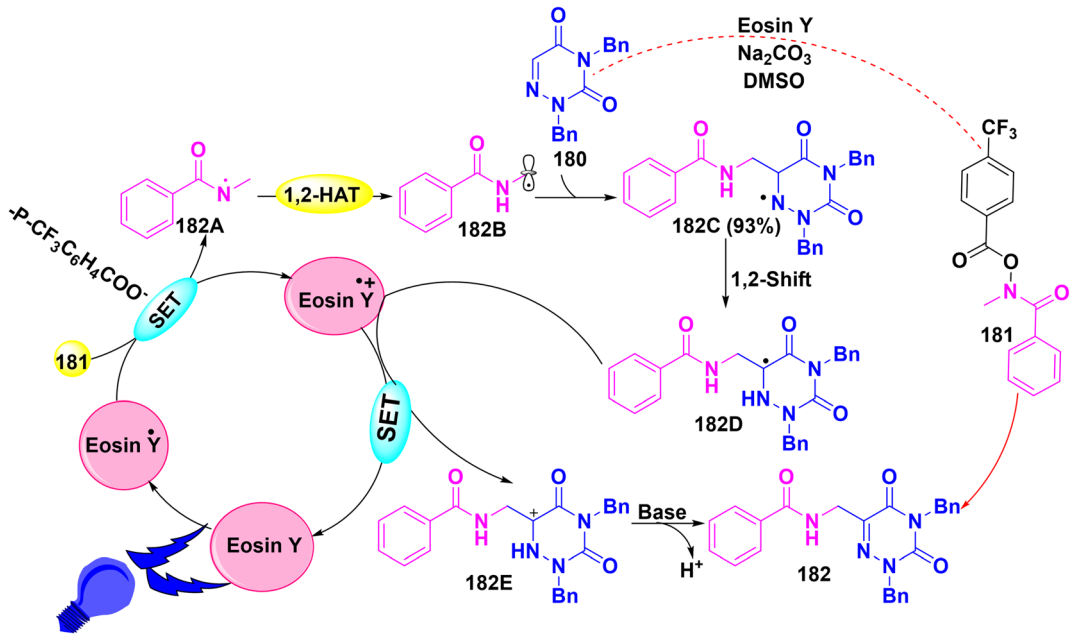
Scheme 67 Plausible mechanism for the synthesis of oxyalkylated-triazine-diones.

Diels–Alder reactions (RDA). SNAr of triazine derivatives **29** with alkyne-tethered oxindole derivatives **172** in the presence of Cs_2CO_3 in THF gave *tert*-butyl-(but-yn-yl)-oxo-(phenyl-triazin-yl) indoline-carboxylate **173**, in addition to spirocyclic products such as phenyl-dihydrospiro[cyclopenta[*b*]pyridine-indolin]-one **174a** and *tert*-butyl-oxo-phenyl-dihydrospiro[cyclopenta[*b*] pyridine-indoline]-carboxylate **174b** through a domino sequence involving SNAr, followed by ihDA and RDA reactions (Scheme 65).[120]

3.2.6 Halogenation reaction followed by SNAr. In 2024, Lapray *et al.*[120] reported a two-step halogen exchange sequence starting from hydroxy-triazine derivative **29** to form a different halogenated triazine scaffold. Initially, the chlorination reaction of compound **29** with $POCl_3$ and DMF transforms the hydroxy group at position 3 to a chloro substituent to afford

© 2025 The Author(s). Published by the Royal Society of Chemistry

Open Access Article. Published on 21 Oktober 2025. Downloaded on 9/06/2026 1:40:11 PG.
This article is licensed under a Creative Commons Attribution-NonCommercial 3.0 Unported Licence.



Scheme 68 Proposed reaction mechanism toward selective C–H-alkylation of triazine-diones.

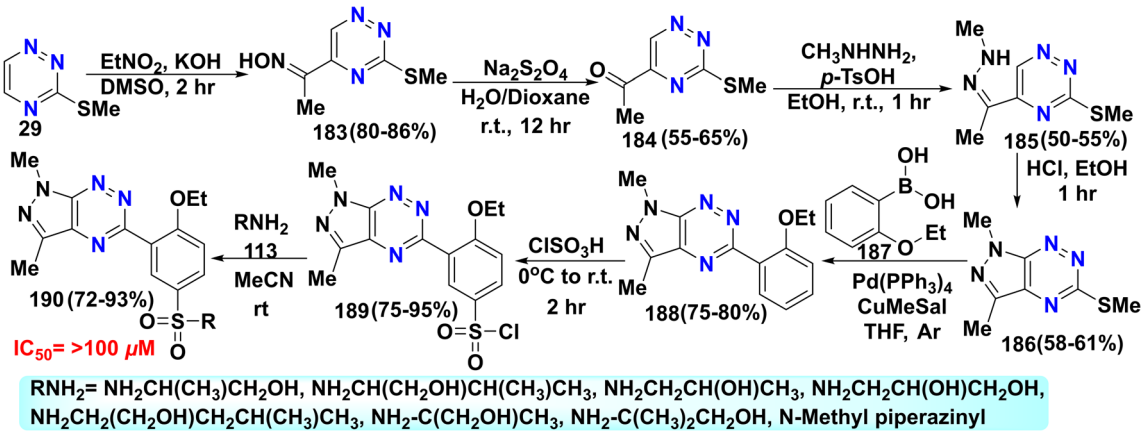
chloro-triazine **175**. The latter readily underwent SNAr with tetramethylammonium fluoride (Me_4NF) and *t*-BuOH in DMSO to replace the chlorine compound **175** with a fluorine atom to furnish fluoro-triazine **176** (Scheme 66).[120] Similarly, the same product **176** was attained *via* two steps; starting with the addition of trimethyl amine, followed by adding potassium fluoride (KF). Method A involves an additional synthetic step and may produce byproducts owing to incomplete methylation or salt formation. In contrast, under mild conditions, method B achieves the transformation in a single step with higher yields (up to 87%) and selectivity.

3.2.7 Visible light-induced C–H alkylation of triazine-diones *via* hydrogen atom transfer (HAT). In 2022, Tan *et al.*[121] postulated the formation of oxyalkylated-triazine-diones **179** through oxidative cross-dehydrogenative coupling between triazine-diones **177** and ether compounds **178** utilizing the metal-free photocatalyst 2-*t*-butyl anthraquinone (2-*t*-Bu-AQN) and air as a green oxidant under visible light or green energy source sunlight. Initially, upon blue light irradiation, excited species 2-*t*-Bu-AQN* is formed from 2-*t*-Bu-AQN, which then undergoes a HAT process between THF **178** and 2-*t*-Bu AQN* to generate an α-oxy radical **179A** as well as 2-*t*-Bu AQN˙H. Subsequently, 2-*t*-Bu-AQN is synthesized again through the oxidation of 2-*t*-Bu-AQN˙-H, accompanied by the formation of hydroperoxyl radical $HO_2^{\bullet}$. In the interim, α-oxy radical **179A** attacks **177** to produce radical intermediate **179B**, which interacts with radical $HO_2^{\bullet}$ to afford H_2O_2 and compound **179** (Scheme 67).

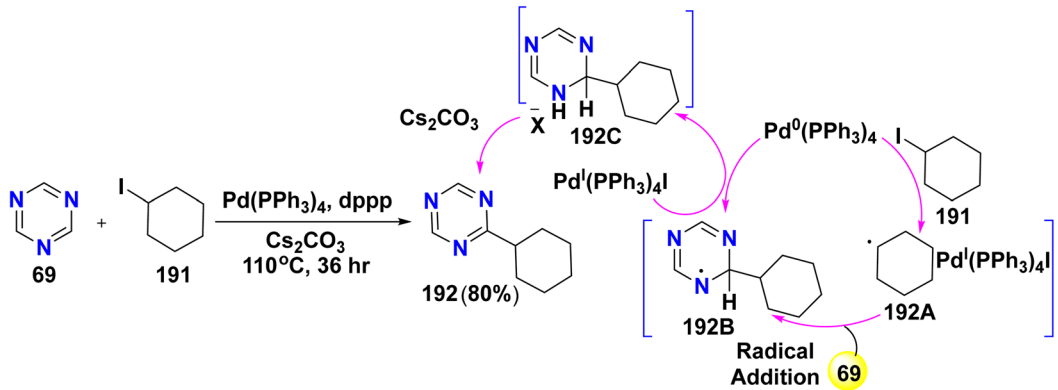
Wang and coworkers[122] proposed the synthesis and mechanism for the formation of (dibenzyl-dioxo-tetrahydro-triazin-yl)-methyl-benzamide **182** through the visible light-driven C–H alkylation of triazine-diones **180** with methyl-((4-(trifluoromethyl)benzoyl)oxy)benzamide derivative **181** using Eosin Y as the photocatalyst, Na_2CO_3, and DMSO under blue LED irradiation. Upon visible-light irradiation, Eosin Y is promoted to its excited-state Eosin Y*, which then undergoes single-electron transfer (SET) with compound **181** to yield Eosin $Y^{\bullet+}$ and N-centered radical intermediate **182A**, while *p*-$CF_3C_6H_4COO^-$ is liberated. Following this, intramolecular 1,2-HAT of intermediate **182A** generates C-centered radical intermediate **182B**. Afterward, adding this intermediate to the C6 position of dibenzyl-triazine-dione **180** furnishes N-centered radical intermediate **182C**, which is subjected to 1,2-hydrogen shift to yield radical **182D**. The latter is oxidized by Eosin $Y^{\bullet+}$ to give intermediate **182E**. Finally, the base-catalyzed deprotonation of intermediate **182E** furnishes compound **182**, with the regeneration of Eosin Y (Scheme 68).

3.2.8 Miscellaneous reaction. Triazine sulfonamides **190** were synthesized *via* several steps, starting from the formation of oxime **183** from the addition of (methylthio)-triazine **29** to nitroethane ($EtNO_2$) in the presence of KOH. In contrast, reductive deoximation of compound **183** with sodium dithionite ($Na_2S_2O_4$) furnished acetyltriazine **184**. Then, hydrazone compound **185** was produced upon stirring acetyltriazine **184** with methyl hydrazine and *p*-TsOH. The latter readily cyclized upon refluxing with HCl/EtOH to generate pyrazolo[4,3-*e*]triazine **186**. Consequently, Suzuki coupling of compound **186** with ethoxyphenylboronic acid **187** in the presence of a catalytic amount of palladium and copper(I)-methylsalicylate derivative produced (ethoxyphenyl)-dimethyl-pyrazolo[4,3-*e*]triazine **188**. Next, chlorosulfonylation at the 5-position of the phenyl ring was accomplished by treating scaffold **188** with chlorosulfonic acid at 0 °C, forming polycyclic triazine-sulfonyl chloride derivative **189**. Finally, nucleophilic substitution reaction of

Open Access Article. Published on 21 Oktober 2025. Downloaded on 9/06/2026 1:40:11 PG.
This article is licensed under a Creative Commons Attribution-NonCommercial 3.0 Unported Licence.



Scheme 69 Synthetic route toward the generation of triazine-sulfonamides **190**.



Scheme 70 Palladium-catalyzed alkylation of *s*-triazine using alkyl halide.

sulfonyl chloride **189** with various amines **113** afforded triazine sulfonamides **190** (Scheme 69), which exhibited salient antiproliferative activity and protein kinase activity against MCF-7 and K-562 cancer cells. The studied pyrazolotriazines underwent metabolic changes by phase I enzymes, forming hydroxylated and dealkylated metabolites, while phase II transformations were absent. These phase I metabolites might impact the final activity of the compounds. Also, the polar nature of these metabolites could improve their distribution in the body and advance their interactions with molecular targets, including specific plasma proteins.[123]

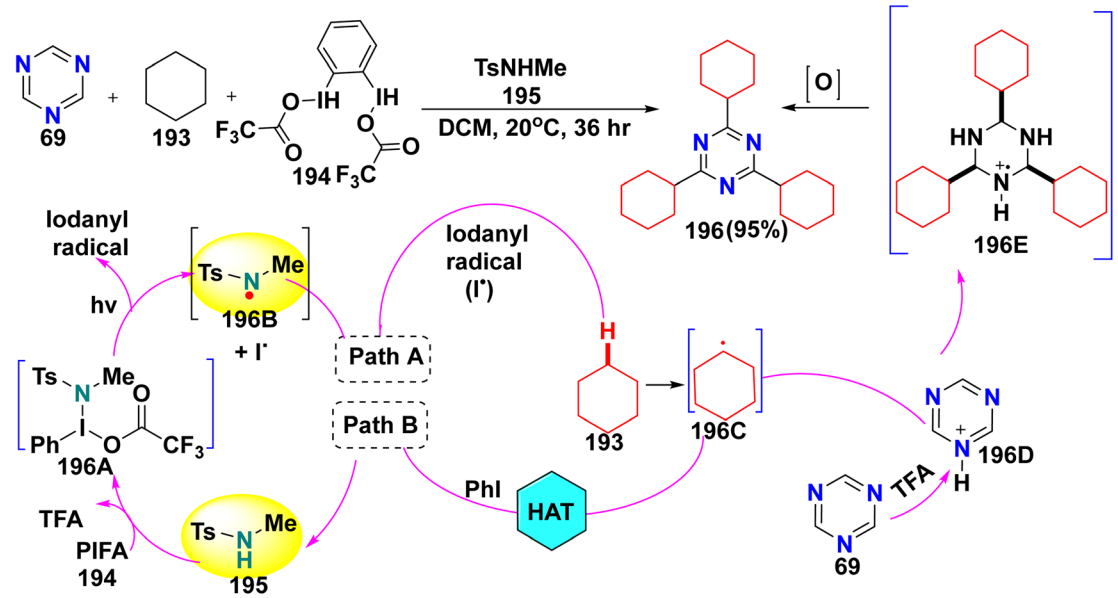
3.3 Reactions of 1,3,5 triazines

3.3.1 Reaction with cycloalkane. The palladium-catalyzed alkylation of heteroarenes is a crucial method in the synthesis of materials and pharmaceuticals. Specifically, the alkylation of triazine **69** with iodocyclohexane (**191**) is executed using tetrakis(triphenylphosphine)palladium(0) ($Pd(PPh_3)_4$) and 1,3-bis(diphenylphosphino)propane (dppp) in the presence of Cs_2CO_3 to obtain binary cyclohexyl-triazine **192**. This process can be detailed through the following mechanism: initiating with single-electron transfer from $Pd(PPh_3)_4$ to iodocyclohexane, forming cyclohexyl radical **192A** and $Pd^{I}(PPh_3)_4I$. Then, this intermediate is added to triazine **69** to furnish intermediate **192B**. Back electron transfer from **192B** to $Pd^{I}(PPh_3)_4I$ leads to the formation of intermediate **192C**. Finally, deprotonation of **192C** produces the alkylated heteroarene (Scheme 70).[124]

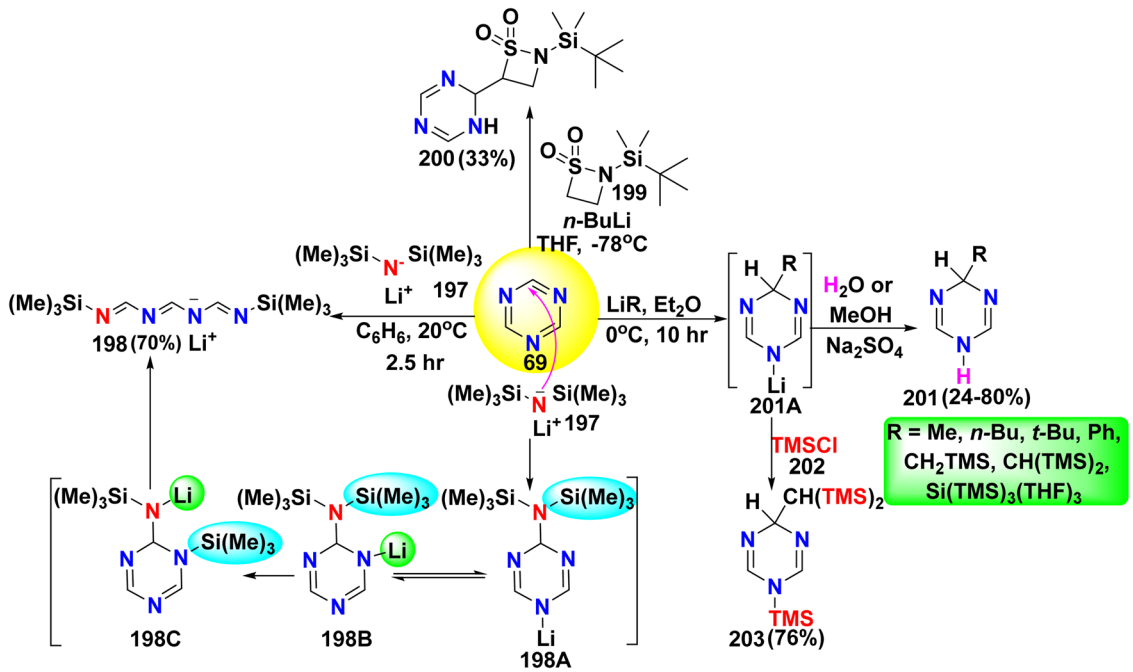
Under blue LED irradiation, tricyclohexyl-triazine **196** was synthesized *via* Minisci reaction as a valuable methodology for the alkylation of triazine **69** with an excess amount of cyclohexane **193** in the presence of phenyliodine(III) bis(trifluoroacetate) (PIFA) **194** as an oxidizing agent, and a catalytic amount of *N*-methyl-*p*-toluenesulfonylamide (TsNHMe) (**195**) as a hydrogen-abstracting agent. The proposed mechanism for the synthesis of trialkylated triazine **196** is illustrated in Scheme 71. Initially, the interaction between PIFA and the amide group of TsNHMe **195** results in the formation of intermediate **196A**, whereby PIFA is converted to TFA at the same time. This intermediate undergoes homolysis upon visible-light irradiation to yield the corresponding amidyl radical **196B** and an iodanyl radical. The nitrogen-centered radical **196B** abstracts a hydrogen atom from alkane **193**, producing alkyl radical **196C** (**path A**). Alternatively, the iodanyl radical may participate in a distinct HAT process to afford intermediate **196C** (**path B**). It is noteworthy that the *in situ*

© 2025 The Author(s). Published by the Royal Society of Chemistry

Open Access Article. Published on 21 Oktober 2025. Downloaded on 9/06/2026 1:40:11 PG.
This article is licensed under a Creative Commons Attribution-NonCommercial 3.0 Unported Licence.



Scheme 71 Synthetic strategy toward tricyclohexyl-triazine formation.

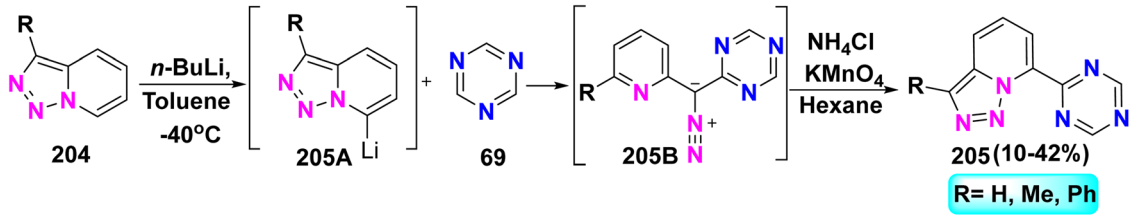


Scheme 72 Reaction of triazine with lithium reagents.

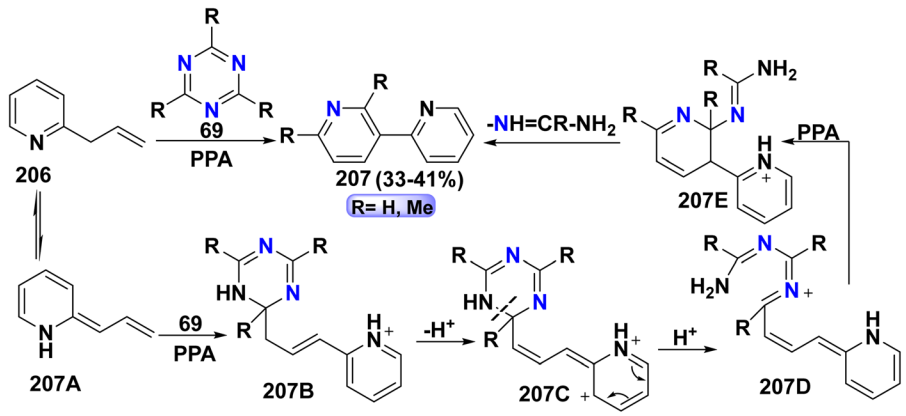
formation of TFA preactivates triazine **69** to proceed to intermediate **196D**. Following this, the nucleophilic addition of alkyl radical **196C** to acidified heteroarene **196D** affords intermediate **196E**, which is subsequently oxidized to yield **196** (Scheme 71).[125]

3.3.2 Lithiation reaction. Tetraazaheptatrienyllithium **198** was synthesized *via* a multistep process, commencing with the 1,4-addition reaction of lithium bis(trimethylsilyl)amide ($LiN(TMS)_2$) (**197**) to triazine **69** to give 1,4-dihydrotriazinyllithium complex **198A**, which is then isomerized to **198B**. Therefore, intermediate **198B** undergoes a 1,3-Me_3Si shift from $N(Me_3Si)_2$ to furnish complex **198C**. Afterward, this complex is subjected to ring scission to afford **198**.[126] Plagge *et al.*[127] reported the synthesis of [(*t*-butyl)dimethylsilyl]-(dihydro-triazinyl)-thiazetidine-dioxide **200** by refluxing a mixture of **69** with (*t*-butyldimethylsilyl)-thiazetidine-dioxide **199** in THF containing *n*-BuLi. Similarly, treatment of **69** with various lithium reagents in Et_2O affords adduct **201A** through 1,4-addition, which is subsequently subjected to further reactions with H_2O or MeOH to give dihydrotriazines **201**.

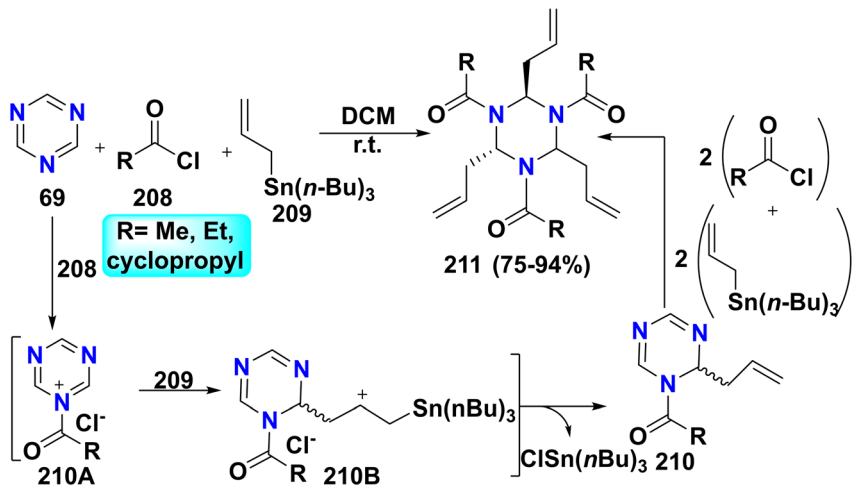
Open Access Article. Published on 21 Oktober 2025. Downloaded on 9/06/2026 1:40:11 PG.
This article is licensed under a Creative Commons Attribution-NonCommercial 3.0 Unported Licence.



Scheme 73 Construction of azinyls *via* lithiation reaction.



Scheme 74 Formation of bipyridyls.



Scheme 75 Triple allylation process for compound 211 synthesis.

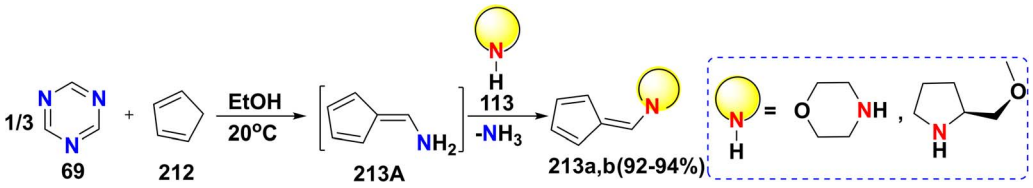
Alternatively, the reaction between **201A** and trimethylsilyl chloride (TMSCl) (**202**) furnishes (bis(trimethylsilyl)methyl)-(trimethylsilyl)-dihydro-triazine **203** (Scheme 72).[128]

The lithiation reaction of triazolo[1,5-*a*] pyridines **204** with *n*-BuLi results in the formation of (triazolo[1,5-*a*]pyridin-7-yl) lithium intermediate **205A.** Subsequently, this intermediate reacts with electrophilic triazine **69**, affording adducts **205B.** Ultimately, these adducts are hydrolyzed, followed by oxidation with $KMnO_4$, yielding azinyl derivatives **205** (Scheme 73).[129]

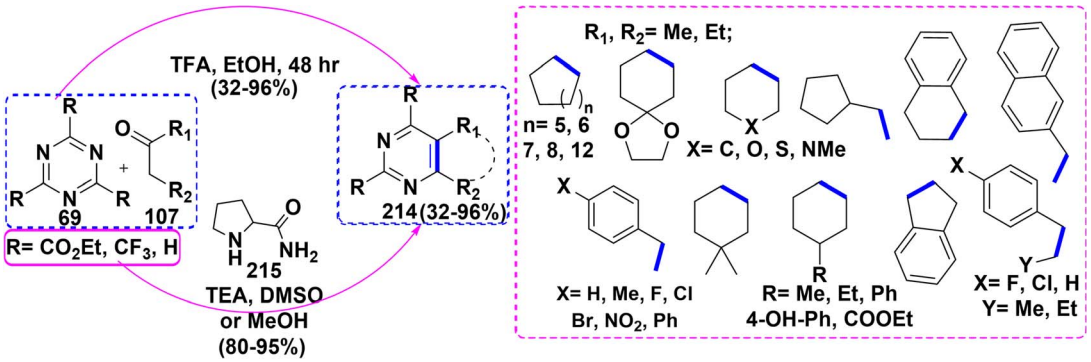
3.3.3 Allylation reaction. Alternatively, treatment of allyl pyridine **206** with triazine **69** in the presence of polyphosphoric acid (PPA) gave bipyridyls **207.** The proposed mechanism for the synthesis of bipyridyls **207** is shown in Scheme 74. Whereby, allyl pyridine **206** exists in equilibrium with its tautomer **207A** under acidic conditions. In contrast, the interaction of **207A** with protonated triazine **69** yields intermediate **207B,** followed by deprotonation to give intermediate **207C.** Additionally, under acidic conditions, compound **207C** undergoes ring opening to form cationic intermediate **207D,** which then undergoes intramolecular electrophilic addition using PPA to yield intermediate **207E.** Finally, elimination of the amidine molecule from **207E** produces **207** (Scheme 74).[130]

© 2025 The Author(s). Published by the Royal Society of Chemistry

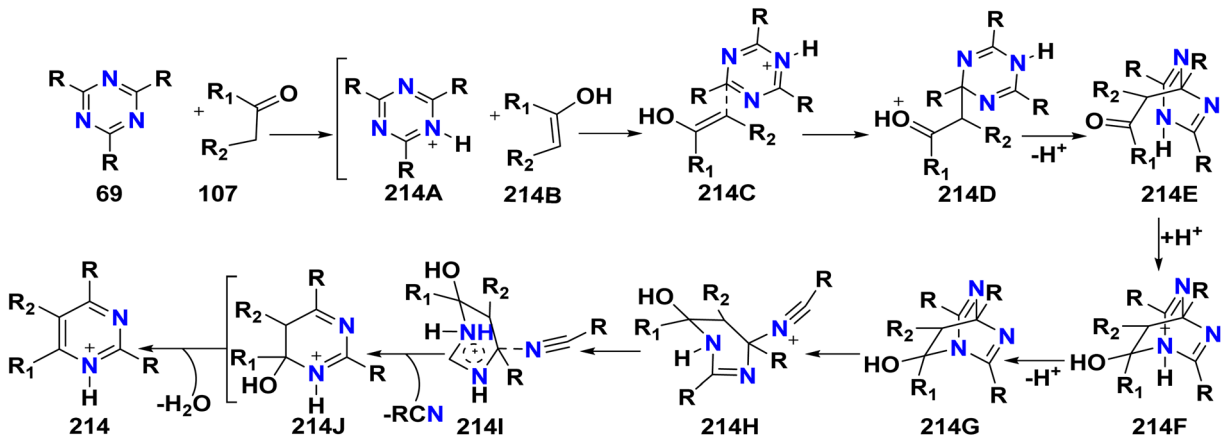
Open Access Article. Published on 21 Oktober 2025. Downloaded on 9/06/2026 1:40:11 PG.
This article is licensed under a Creative Commons Attribution-NonCommercial 3.0 Unported Licence.



Scheme 76 Reaction of cyclopentadiene with 69.



Scheme 77 Formation of cyclic pyrimidines 214.



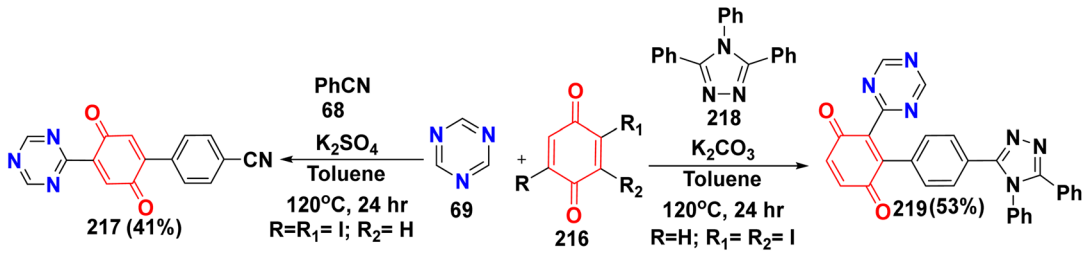
Scheme 78 Mechanistic pathway toward the synthesis of pyrimidines 214.

Hexahydro-1,3,5-triazine is a significant heterocyclic structure employed in various applications, particularly within the domains of energetic materials and polymers. It serves as a crucial component in energetic materials due to its stability and reactivity, which contribute to the performance of explosives.[131,132] Furthermore, hexahydrotriazine derivatives are utilized in polymers[133] as well as in medicine as antimicrobial agents,[134] especially in dental applications for anti-caries formulations.[135] In the same context, Davis *et al.*[132] reported the synthesis of hexahydro-triazines **211** through a one-pot triple allylation reaction involving acid chloride derivatives **208**, triazine **69**, and allyl tributyltin **209**. The proposed mechanism for the formation of triallyl-hexahydro-trialkanoyl-triazines **211** starts with the reaction of acid chloride **208** with triazine **69** to afford *N*-acyliminium ion **210A**. Subsequently, the π electrons from another allyl tin molecule nucleophilically attack the electrophilic carbon generated by the *N*-acylation of **210A** to produce tin-substituted intermediate **210B**. Then, the elimination of tributyltin chloride ($ClSn(nBu)_3$) from intermediate **210B** furnishes mono-allyl-triazine **210**. Ultimately, a series of consecutive double allylation reactions occurs, leading to the formation of compound **211** (Scheme 75).

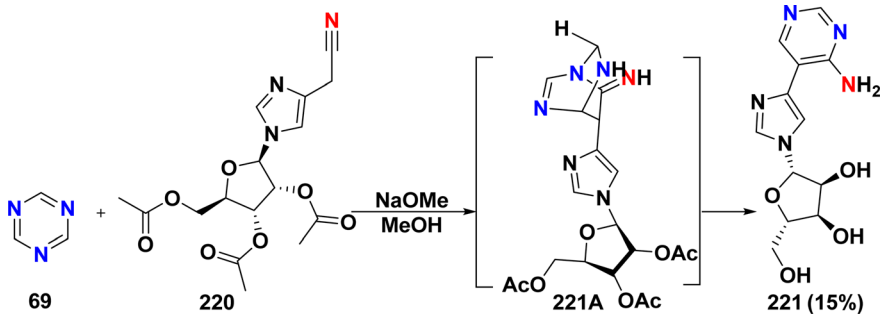
Treatment of triazine **69** and cyclopentadiene (**212**) in EtOH furnished intermediate **213A**, which was then subjected to deamination upon reacting with morpholine or (*S*)-2-(methoxymethyl) pyrrolidine to give 6-(morpholino)fulvene **213a** and (cyclopentadienylidenemethyl)-(methoxymethyl)pyrrolidine **213b** (Scheme 76).[136]

3.3.4 Reaction with ketones through IEDDA. Two distinct synthetic methodologies were developed for the synthesis of fused pyrimidine derivatives **214**. The first methodology employed IEDDA between triazine **69** and cyclic ketones **107**,

Open Access Article. Published on 21 Oktober 2025. Downloaded on 9/06/2026 1:40:11 PG.
This article is licensed under a Creative Commons Attribution-NonCommercial 3.0 Unported Licence.



Scheme 79 Synthesis of N-heterocyclic compounds.

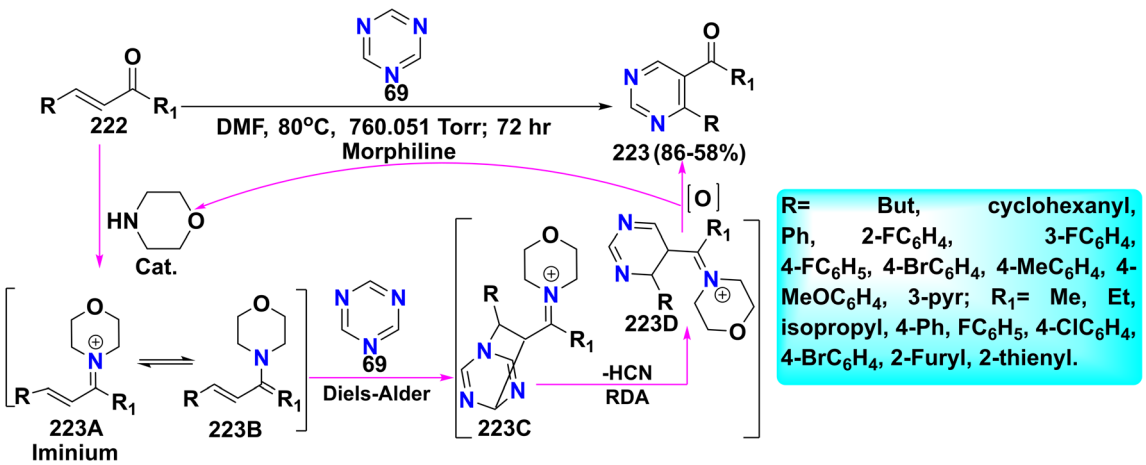


Scheme 80 Reaction of imidazole acetonitrile derivatives with triazine 69.

catalyzed by TFA and EtOH.[137] Alternatively, the second one involved the IEDDA reaction of **69** with **107** in the presence of a catalytic amount of pyrrolidine-2-carboxamide (**215**) and drops of TEA in DMSO.[138] Pyrimidines are widely recognized heterocyclic structures found in various natural products, pharmaceuticals, and functional materials. Numerous pyrimidine derivatives exhibit significant biological activities (Scheme 77).[137]

IEDDA reaction for the formation of pyrimidines **214** occurs through a stepwise mechanism, whereby under neutral conditions, triazines **69** act as a base to promote the enolization of ketone **107**, and during this process, triazines **69** become protonated to give **214A** and ketone in enol form **214B**, while intermediate **214A** undergoes IEDDA reaction with **214B** to proceed to the transition state **214C**. Afterward, **214C** undergoes C–C bond formation to give intermediate **214D**. Subsequently, **214D** is transformed to a more stable intermediate, **214E**, *via* rapid C–C bond rotation. Following this, **214E** is converted to **214F** *via* C2–N1 bond formation. Then, intermediate **214F** is deprotonated to **214G**. Therefore, C3–N1 bond cleavage of **214G** gives **214H**. Afterward, the nitrile moiety leaves **214H** to proceed to **214I**, which needs an activation enthalpy of 6.5 kcal mol^{-1} to generate **214J**. Finally, elimination of a water molecule from **214J** gives protonated cycloadduct **214** (Scheme 78).[137]

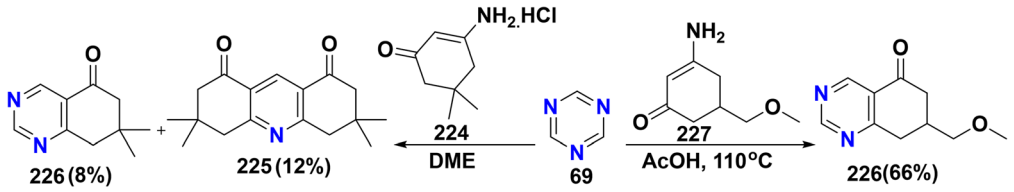
The three-component reaction of triazine **69**, benzonitrile (**68**), and diiodocyclohexa-diene-1,4-dione **216** was refluxed in toluene to furnish dioxo-(triazin-2-yl)-dihydro-[1,1′-biphenyl]-4-carbonitrile **217**. In a similar reaction, MCR of



Scheme 81 Plausible mechanism of the formation of pyrimidine scaffolds **223**.

© 2025 The Author(s). Published by the Royal Society of Chemistry

Open Access Article. Published on 21 Oktober 2025. Downloaded on 9/06/2026 1:40:11 PG.
This article is licensed under a Creative Commons Attribution-NonCommercial 3.0 Unported Licence.



Scheme 82 Treatment of enaminones with **69**.

triphenyltriazole **218**, triazine **69** and diiodocyclohexa-diene-1,4-dione **216** yielded (diphenyl-triazolyl)-(triazinyl)-biphenyl-dione **219** (Scheme 79).[139]

3.3.5 Reaction with nitrile derivative. (4-Aminopyrimidin-yl)-imidazol-(hydroxymethyl)tetrahydrofuran-diol fleximer **221** was prepared through the *in situ* reaction of (acetoxymethyl)-(4-(cyanomethyl)-imidazol-yl)tetrahydrofuran-diyl diacetate **220** with NaOMe and **69** *via* [4 + 2] Diels–Alder cycloaddition reaction, affording intermediate **221A**. Afterward, RDA fragmentation of the resulting intermediate occurred, corresponding with deblocking of the acetate protecting group to furnish (4-(4-aminopyrimidin-5-yl)-imidazol-yl)-(hydroxymethyl) tetrahydrofuran-diol **221** (Scheme 80). Fleximer inhibitors overcome the resistance of drug mutations in HIV. Moreover, scaffold **221** can easily adapt to flexible and unpredictable binding sites, maximizing the structural interactions without losing crucial contacts involved in the mechanism of the enzyme. This flexibility enables them not only to effectively explore enzyme–coenzyme and nucleic acid–protein interactions but also to function as strong inhibitors that can overcome viral mutations by accommodating structural changes in drug targets.[140]

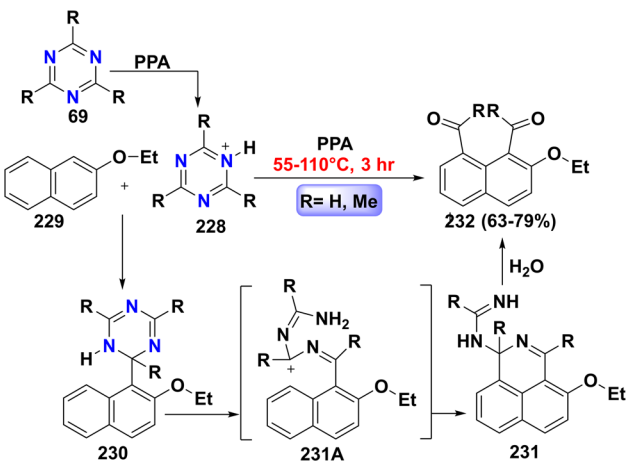
3.3.6 Reaction with chalcones. The morpholine-catalyzed Diels–Alder reaction of chalcones **222** with triazine **69** in DMF led to the formation of pyrimidine scaffolds **223**. A reasonable mechanism is suggested to describe the reaction process, as illustrated in Scheme 81. In the beginning, α,β-unsaturated ketones **222** combine with the morpholino catalyst to produce iminium intermediate **223A**, which converts to enamine form **223B**. After that, intermediate **223C** is synthesized *via* Diels–Alder reaction between iminium intermediate **223A** and triazine **69**. Then, intermediate **223C** is transformed to intermediate **223D** *via* RDA. Lastly, product **223** is produced *via* aerobic oxidation of intermediate **223D**, and the catalyst is released for another catalytic cycle (Scheme 81).[141]

3.3.7 Reaction with enaminone. A mixture of tetramethyl-tetrahydroacridine-dione **225** and quinazolinone **226** was obtained *via* the reaction of dimethylcyclohexenone derivative **224** with triazine **69** in the presence of dimethoxyethane (DME). Then, [4 + 2] cycloaddition reaction of triazine **69** with amino-(methoxymethyl)cyclohex-2-en-one **227** in AcOH furnished methoxymethyl-tetrahydro-quinazolinone **228** (Scheme 82).[142]

3.3.8 Diacetylation reaction. The diacetylation reaction of ethoxynaphthalene **229** with protonated-trisubstituted triazines **288** in PPA furnished diformylated naphthalene derivative **232** through a multi-step reaction. The reaction initiates with the protonation of trisubstituted triazine **69** to give trisubstituted protonated triazine **288**, which then reacts with **229** to furnish (ethoxynaphthalenyl)-triazine **230**. Subsequently, compound **230** undergoes ring opening upon treatment with an acid to form carbocation intermediates **231A**. Afterward, intramolecular electrophilic substitution of **231A** gives (ethoxy-benzo-isoquinolinyl)formimidamide derivatives **231**. Finally, hydrolysis of scaffold **231** yields diformylated naphthalene **232** (Scheme 83).[143]

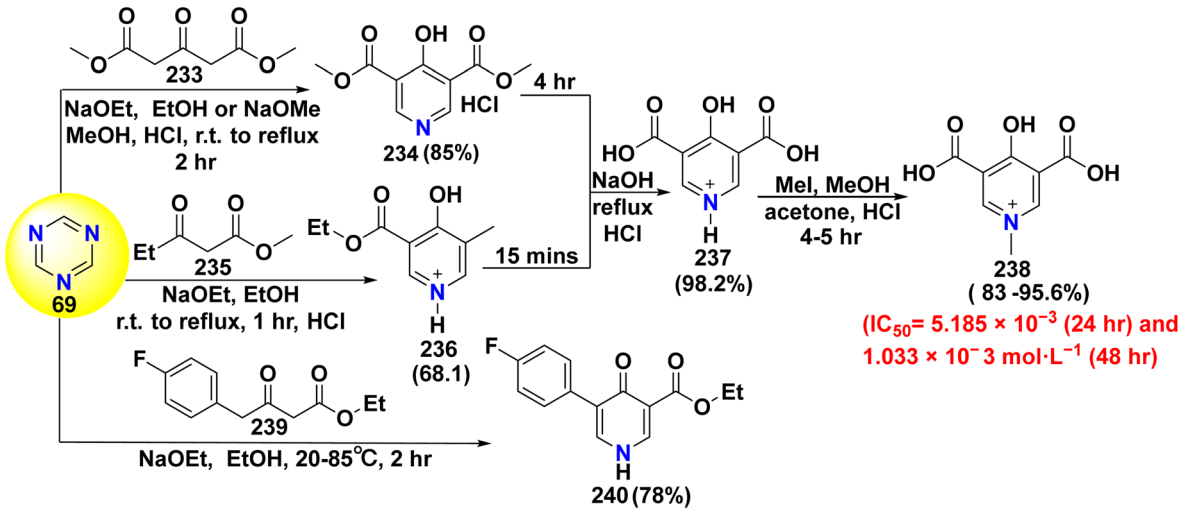
3.3.9 Reaction with ester scaffolds. An equimolar amount of triazine **69** and dimethyl-acetonedicarboxylate **233** was incrementally added to a freshly prepared NaOEt solution in EtOH or NaOMe in MeOH, followed by neutralization with HCl to produce pyridine salts **234** (Scheme 84).[144] Similarly, stirring a mixture of methyl-oxopentanoate **235** with triazine **69** produced ethylhydroxy-methylnicotinate **236**.[145] Then, the scaffold **234** or **236** was added to an NaOH solution, allowed to reflux, and then neutralized with HCl to afford pyridinium-dicarboxylic acid **237**. Afterward, methylation of compound **237** with a large excess of methyl iodide produced dicarboxy-hydroxy-methylpyridinium **238**.[144,145] Hybrid **238** was examined *in vitro* on HEK-293 human embryonic kidney cells with (IC_{50} of 5.185×10^{-3} for 24 h and 1.033×10^{-3} mol L^{-1} for 48 h) with a lack of cytotoxicity. Likewise, treatment of triazine **69** with phenyl-ketoester **239** in the presence of NaOEt in EtOH gave pyridone analog **240**.[146]

Interestingly, substituted isoquinolines play a vital role against Alzheimer's disease and as anti-HIV and antiplasmodial agents.[147–149] Moreover, isoquinoline **242** and its analogs were synthesized through the reaction of *s*-triazine (**69**) with phenyl

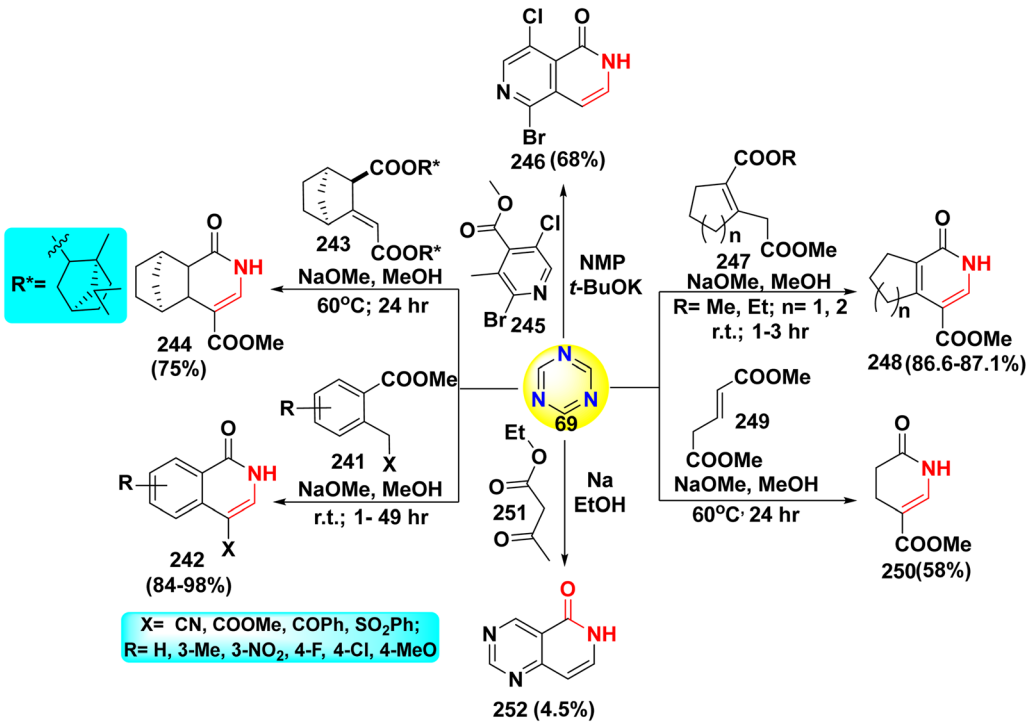


Scheme 83 Formation of diformylated naphthalene.

Open Access Article. Published on 21 Oktober 2025. Downloaded on 9/06/2026 1:40:11 PG.
This article is licensed under a Creative Commons Attribution-NonCommercial 3.0 Unported Licence.



Scheme 84 Synthesis of pyridinone scaffold.



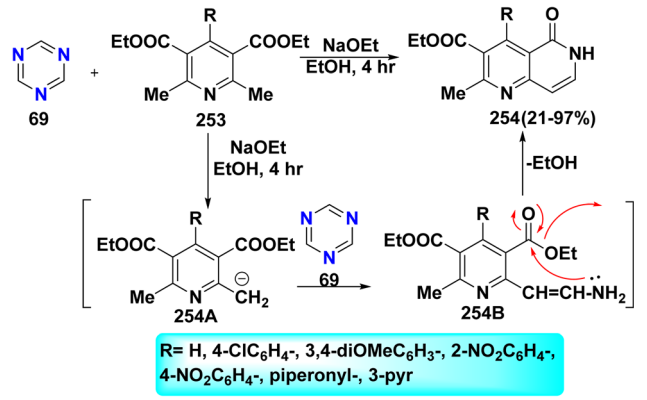
Scheme 85 Reaction of triazine with ester compounds.

ester hybrids **241** in the presence of NaOMe. Alternatively, treatment of triazine **69** with diester derivatives **243** and NaOMe, followed by sequential transesterification, olefin isomerization, and then hydrolysis furnished methanoisoquinoline **244**.[150] Likewise, naphthyridine analog **246** was prepared by stirring a mixture of triazine **69** with a solution of methyl bromo-chloro-3-methylisonicotinate **245** in NMP at 0 °C and *t*-BuOK.[151] 2,6-Naphthyridine alkaloids **246** exert significant effects on the central nervous system as well as showing a wide range of pharmacological actions, including hypnotic, curare-like effects, and neuromuscular inhibition, along with sedative and hypotensive properties.[152] Hayashida *et al.*[150] improved their synthesis to involve the reaction of cyclic **247** or acyclic aliphatic diester **249** with **69** to produce fused 2-pyridone **248** and methyl-oxo-tetrahydropyridine-carboxylate **250**, respectively. In the same context, under a nitrogenous atmosphere, refluxing a mixture of ethyl acetoacetate **251** and triazine **69** in the presence of Na metal furnished pyrido[4,3-*d*] pyrimidine **252** (Scheme 85).[153]

Treatment of dimethyl-pyridine-dicarboxylates **253** with triazine **69** in the presence of NaOEt afforded substituted ethyl-2-methyl-oxo-dihydro-naphthyridine-carboxylate **254**. The

© 2025 The Author(s). Published by the Royal Society of Chemistry

Open Access Article. Published on 21 Oktober 2025. Downloaded on 9/06/2026 1:40:11 PG.
This article is licensed under a Creative Commons Attribution-NonCommercial 3.0 Unported Licence.



Scheme 86 Synthesis of biologically active naphthyridinones.

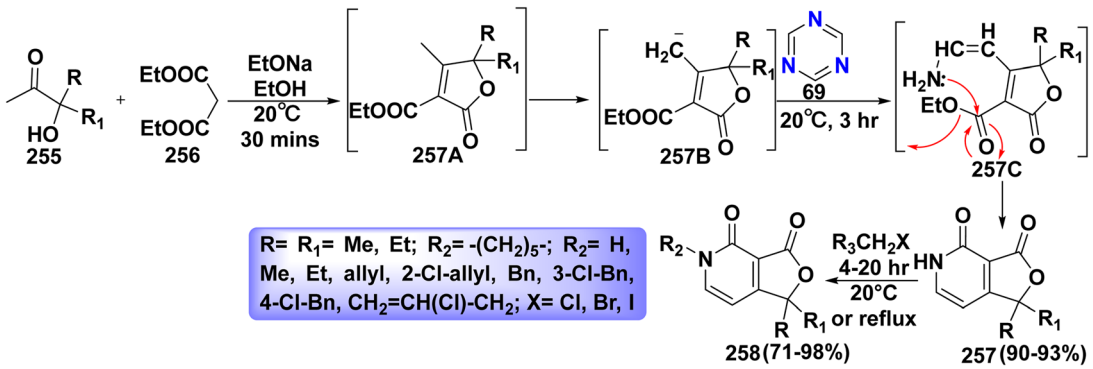
reaction begins with the deprotonation of the acidic proton from the methyl group of dimethyl-pyridine-dicarboxylates **253** using basic NaOEt to form the acidic methylene group of intermediate **254A**, which acts as a nucleophile to attack the electrophilic carbon atom of triazine **69** to furnish amino-methylene intermediate **254B**. Finally, intramolecular nucleophilic attack of the amino group into the carbonyl carbon of the ester group afford ethyl-2-methyl-oxo-dihydro-naphthyridine-carboxylate **254** (Scheme 86). In contrast, naphthyridinones exhibit a wide range of biological activities, such as anticonvulsant, anti-inflammatory, antifungal, insecticidal, antibacterial, and calcium channel antagonistic.[154]

Fused furo[3,4-*c*]pyridine-dione **258** is synthesized through a transesterification process, followed by a Knoevenagel reaction involving the condensation of hydroxy ketone **255** and diethyl malonate (**256**), and this step is facilitated by the use of NaOEt as a base to afford butenolide intermediate **257A**. Then, this intermediate is deprotonated at the methyl group to form carbanion intermediate **257B**, which acts as a nucleophile to attack the electrophilic C atom of **69** to form intermediate **257C**. Ultimately, the amino group of **257C** intramolecularly attacks the carbonyl ester to yield pyridinone lactone **257**. Alkylation of **257** with alkyl halides gives substituted furo[3,4-*c*]pyridine-dione **258** (Scheme 87). Pyridinone derivatives are widely present among naturally occurring alkaloids. For example, cerpegin and its alkaloid analogs are utilized in traditional Indian medicine, recognized for their analgesic, antiulcer, tranquilizing, and anti-inflammatory properties.[155]

3.3.10 Reaction with heterocyclic amine derivatives. Interestingly, pyrrolo[2,3-*d*]pyrimidines are pivotal structural frameworks in numerous natural products; they also exhibit a range of biological activities, including antibacterial, adenosine kinase inhibition, and antiseizure properties. The one-pot synthesis of pyrrolo[2,3-*d*]pyrimidines **260** was achieved by stirring a mixture of triazine **69** with amino-cyanopyrroles **259** at ambient temperature *via* IEDDA. Dang *et al.*[156] suggested a stepwise reaction mechanism for the synthesis of pyrrolo[2,3-*d*] pyrimidines **260**. Initially, the [4 + 2] cycloaddition reaction involving amino-cyanopyrroles **259** as the dienophile and triazine **69** as the diene yields cycloadduct **260A**. In pathway A, this cycloadduct undergoes RDA reaction, resulting in the formation of intermediate **260B** through losing hydrogen cyanide (HCN) gas. After that, intermediate **260B** quickly eliminates the NH_3 molecule to afford pyrrolopyrimidines **260**. Alternatively, in pathway B, the elimination of the ammonia molecule occurs to afford intermediate **260C**, which is superior to liberating HCN gas (Scheme 88).[156]

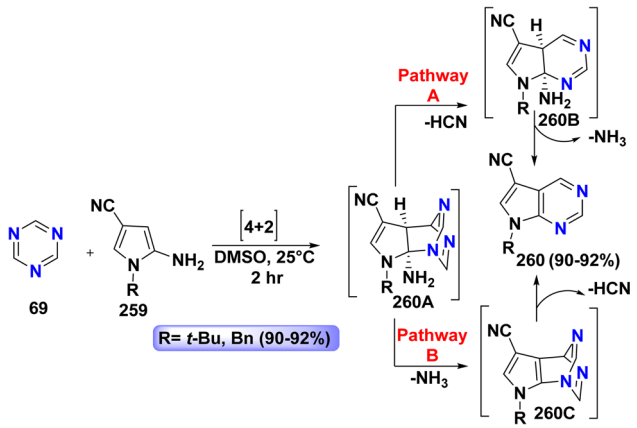
The reaction of *tris*(trifluoromethyl)triazine **69** with amino-pyrrole **259** yielded 2,4-bis(trifluoromethyl)-5*H*-pyrrolo[3,2-*d*] pyrimidine **261**. In the first step, the IEDDA reaction of electron-rich aminopyrrole **259** with azine compound **69** leads to the formation of zwitterion **261A**. Once generated, the zwitterion cyclizes to produce tricyclic adduct **261B**. Subsequently, this adduct undergoes RDA, followed by elimination of trifluoroacetonitrile (CF_3CN) and ammonia to give **261**.[157] Alternatively, tautomerization of Wheland–Meisenheimer intermediate **261A** forms intermediate **261C**, then reacting with CF_3CN to afford intermediate **261D**, which was isolated in 20% yield (Scheme 89).

Iaroshenko *et al.*[158] reported the first attempts to synthesize 9-substituted purine **263** by refluxing an equimolar quantity of triazine **69** with freshly prepared substituted-5-amino-imidazoles **262** in DCM. The postulated mechanism for the synthesis of purine **263** starts with the synthesis of charge transfer complex **263A**, which then forms zwitterion **263B**, followed by a sequence nucleophilic attack by the nitrogen atom on position-4 or position-5 of imidazole to furnish intermediate **263C**, which undergoes C–N bond



Scheme 87 Preparation of fused furo[3,4-c]pyridine-diones.

Open Access Article. Published on 21 Oktober 2025. Downloaded on 9/06/2026 1:40:11 PG.
This article is licensed under a Creative Commons Attribution-NonCommercial 3.0 Unported Licence.

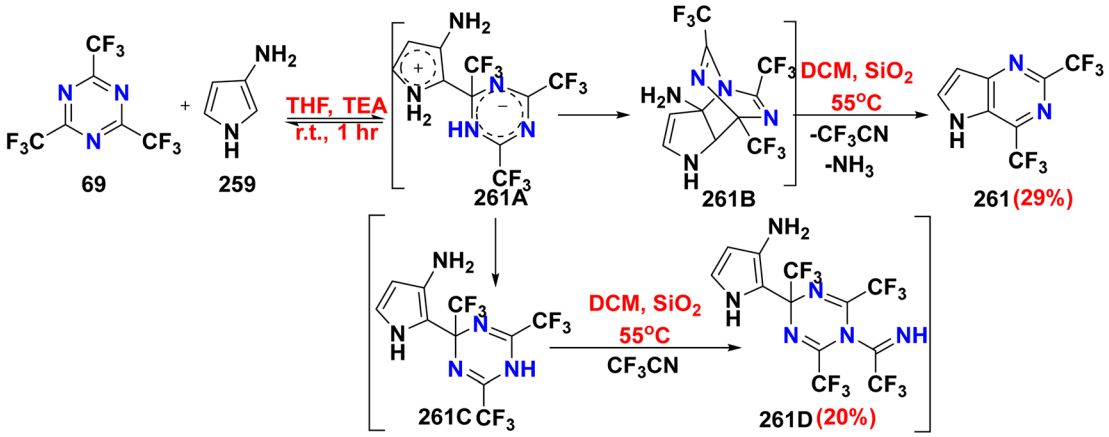


Scheme 88 RDA reaction for the formation of pyrrolo-pyrimidines.

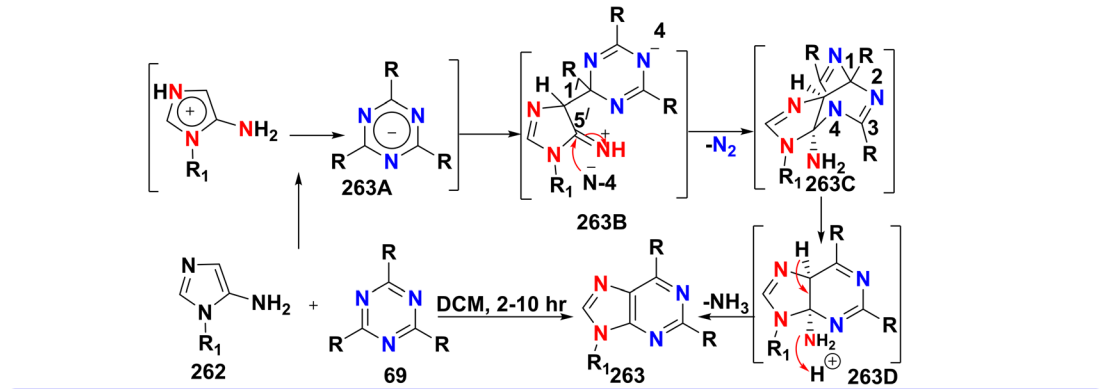
breaking to give intermediates **263D**; ultimately, deamination of the ammonia molecule yields substituted purines **263** (Scheme 90).

Pyrazolo[3,4-*d*]pyrimidine analogues serve as promising therapeutic agents, functioning as inhibitors of adenosine kinase and A1 receptors. The synthesis of purine hybrids **265** was achieved through the reaction of triazine **69** with 5-amino-pyrazolecarboxylic acid derivative **264** in a mixture of DMF/AcOH or DMSO with a Lewis acid such as boron trifluoride diethyl etherate ($BF_3 \cdot OEt_2$), employing a tandem decarboxylation/Diels–Alder reaction (TDDA). The mechanistic pathway for pyrazolo-pyrimidine synthesis **265** starts with the decarboxylation of 5-amino-phenyl-pyrazolecarboxylic acid **264**, yielding 5-amino-pyrazole derivative **153**, which subsequently reacts with triazine **69** *via* [4 + 2] cycloaddition to generate cycloadduct product **265A**. This cycloadduct then undergoes RDA, with the liberation of RCN molecule to form intermediate **265B**. Finally, aromatization of **265B** through the concurrent elimination of an ammonia molecule gives pyrazolo-pyrimidine derivatives **265** (Scheme 91).[159]

Benzoxazole-[phenyl-$^{13}C_6$] **267** was obtained through the reaction of aminophenol **266** with triazine **69** in the presence of



Scheme 89 Reaction of triazine with aminopyrrole.

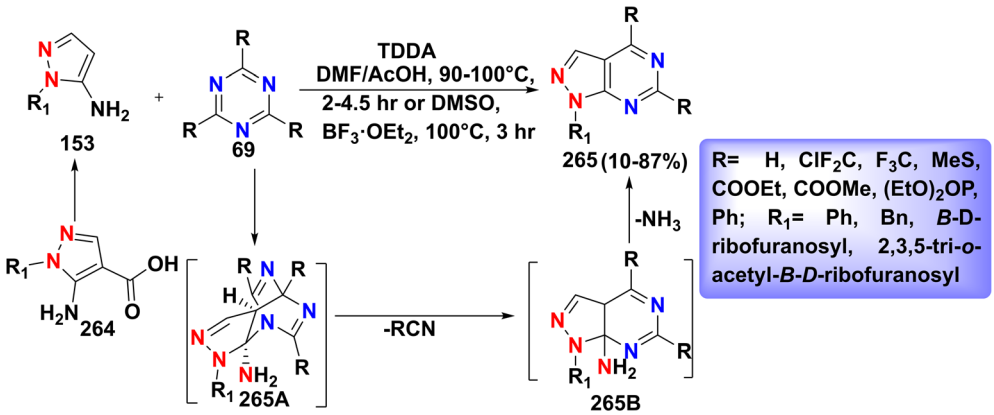


R= H, CF_3; R_1= *t*-Bu, *n*-heptyl, *N*,*N*-dimethyethyl, *N*,*N*-diethyethyl, allyl, cyclopropyl, cyclohexyl, Bn, 4-*N*,*N*-diethylphenyl, (*S*)-1-phenylethyl, 2-ClBn, 2-(2-chlorophenyl)ethyl, 3-BrC_6H_4-, 4-BrC_6H_4-, 2,6-dibromo-4-methylphenyl, 4-methoxybenzyl, 2-methoxyphenylethyl, 2,4,6-trimethylphenyl, 3-Methoxyphenyl, 2,4-Dimethoxyphenyl, 3,4-Dimethoxyphenyl, 3,5-Dimethoxyphenyl, 3,4-dimethoxyphenylethyl, 3,4,5-Trimethoxyphenyl, 4-ethoxyphenyl, pyridin-2-yl, pyridin-4-yl-methyl, thiazol-2-yl, morpholyl, 3-morpholinopropyl, 4-metylpiperazin-1-yl.

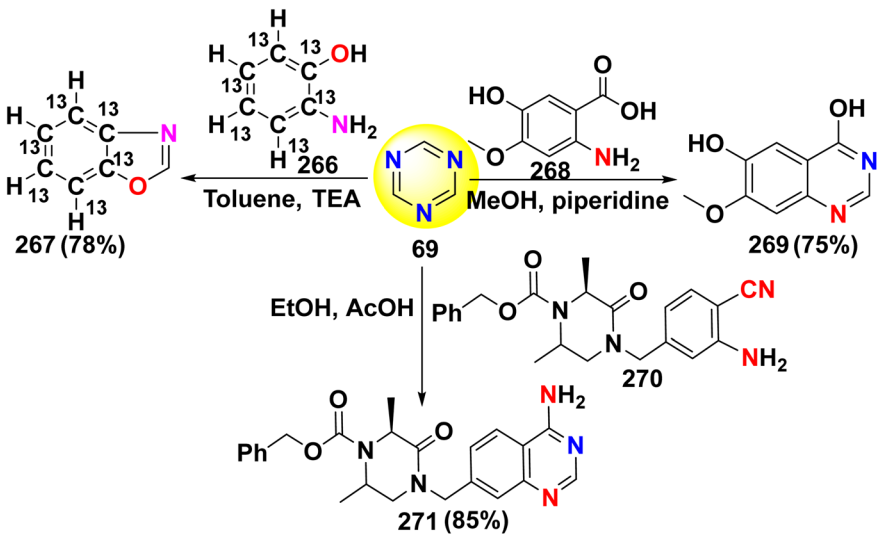
Scheme 90 Proposed mechanism for the formation of purine scaffolds **263**.

© 2025 The Author(s). Published by the Royal Society of Chemistry

Open Access Article. Published on 21 Oktober 2025. Downloaded on 9/06/2026 1:40:11 PG.
This article is licensed under a Creative Commons Attribution-NonCommercial 3.0 Unported Licence.



Scheme 91 Synthetic strategy for pyrazolo[3,4-*d*]pyrimidine synthesis **265**.

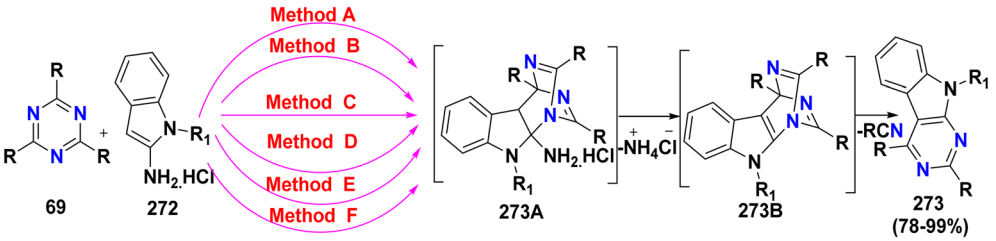


Scheme 92 Treatment of **69** with different amines.

TEA and toluene.[160] Whereby, a combination of amino-hydroxy-methoxybenzoic acid **268** and triazine **69** was dissolved in MeOH, and piperidine was added as a basic catalyst to furnish 7-methoxyquinazoline-4,6-diol (**269**).[161] Quinazolinones have attracted significant attention due to their diverse pharmacological activities, including anticancer effects through the inhibition of various tyrosine kinases and dihydrofolate reductase enzymes, which are crucial targets in cancer therapy. Furthermore, quinazolinone derivatives have demonstrated antimicrobial, anti-inflammatory, and antihypertensive properties.[162] Similarly, benzyl-((4-aminoquinazolin-yl)methyl)-dimethyl-oxopiperazine-carboxylate **271** was synthesized by refluxing a solution of (aminocyanobenzyl)-dimethyl oxopiperazine carboxylic acid benzyl ester **270** with triazine **69** in EtOH and drops of AcOH (Scheme 92).[163]

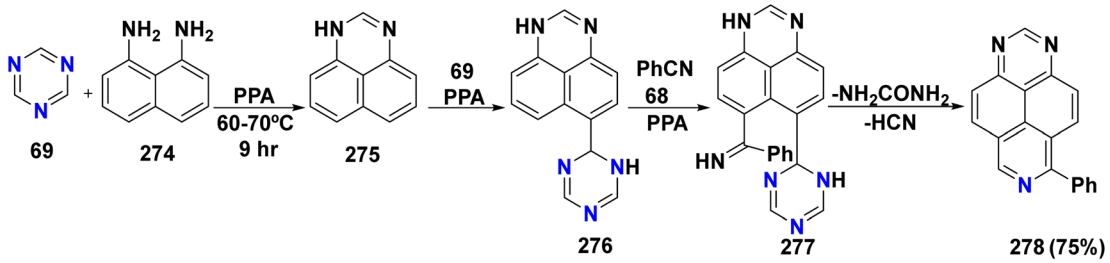
The IEDDA reaction between dienophile aminoindole **272** and diene triazine **69** was performed under various conditions, including MeOH, DMSO, MeOH/TEA, DMSO/MeOH, DMSO/MeOH/TEA and i-PrOH to afford pyrimido[4,5-*b*]indole derivatives **273**. This route can be explained *via* the following reaction mechanism: initially, [4 + 2] cycloaddition reaction of triazines **69** and aminoindoles **272** furnishes intermediate **273A**. Then, the elimination of ammonium chloride from intermediate **273A** gives intermediate **273B**. The reaction culminates in RDA reaction that involves the loss of RCN molecule to form pyrimido[4,5-*b*]indoles **273** (Scheme 93).[164] Method B achieved the highest yield (99%) at room temperature, indicating a mild, efficient process with a fast reaction time of 4.5 h with higher selectivity. Method A consistently delivered high yields (78–97%) across diverse substituents, demonstrating robustness and broad applicability. Both methods benefit from electron-withdrawing groups (COOEt in B and CF_3 in A) that increase ring electrophilicity, and R_1 = H avoids steric hindrance, enabling smooth cyclization. In contrast, methods C and D, using mixed solvents or TEA base, had lower yields (49–79%), with a longer reaction time (18 h) likely due to side reactions or poor solubility. Electron-withdrawing groups such as CF_3 (in methods A and C) slightly lower yields compared to COOEt, owing to the reduced nucleophilicity or intermediate

Open Access Article. Published on 21 Oktober 2025. Downloaded on 9/06/2026 1:40:11 PG.
This article is licensed under a Creative Commons Attribution-NonCommercial 3.0 Unported Licence.

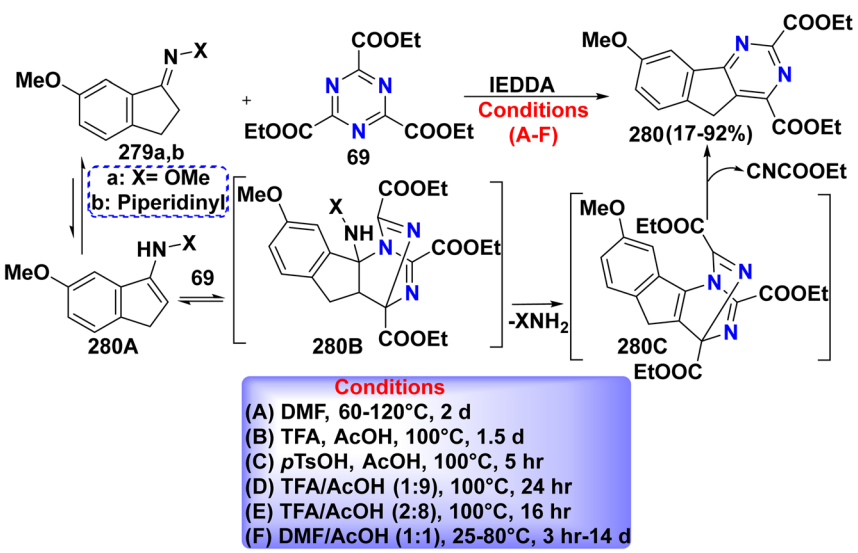


Methods	R	R_1	Conditions	Temp	Time	Yield	Methods	R	R_1	Conditions	Temp	Time	Yield
A	COOEt	Bn	MeOH	50	18	97	B	COOEt	H	DMSO	25	4.5	99
	CF_3	H	MeOH	50	7.5	94	C	CF_3	Me	MeOH, TEA	50	18	79
	CF_3	Me	MeOH	50	17	97	D	COOEt	Me	DMSO, MeOH	50	18	49
	CF_3	Bn	MeOH	50	18	93	E	COOEt	H	DMSO/MeOH / TEA	50	11	82
	H	H	MeOH	50	19	78	F	COOBu	H	*i*-PrOH	50	19	78

Scheme 93 Reaction of triazine with aminoindoles.



Scheme 94 Synthesis of perimidines.



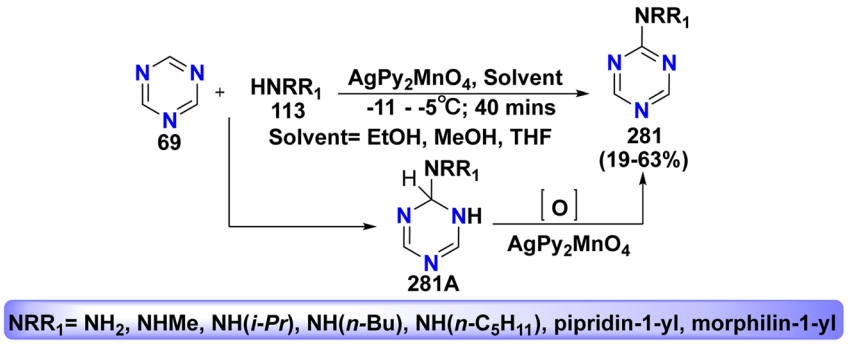
Scheme 95 Reaction of 69 with indanone-oximes and hydrazones.

stabilization, while bulky alkyl esters (COOBu in Method F) also showed slightly decreased yields (78%) owing to steric effects.

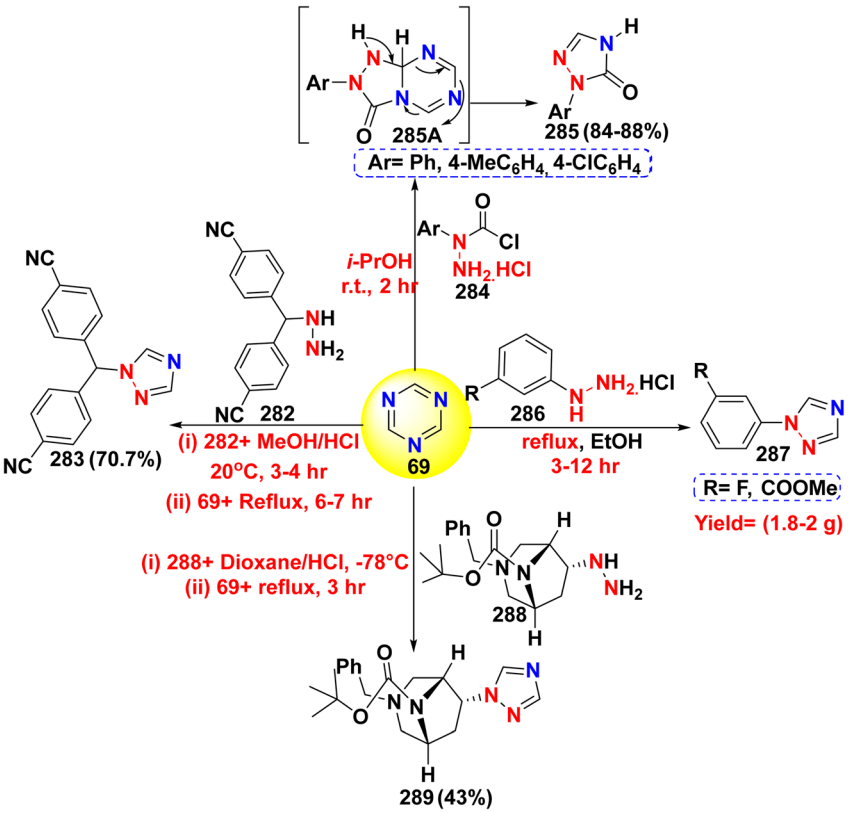
The reaction of naphthalenediamine **274** with triazine **69** in PPA furnished tricyclic system **275**, which, upon reacting with another molecule of triazine **69**, *in situ* formed (dihydrotriazinyl)perimidine **276**. Subsequently, (dihydrotriazinyl)-perimidinyl(phenyl)methanimine **277** was obtained *via* the reaction of **276** with benzonitrile (**68**) in PPA. Alternatively, phenyl pyridoperimidine **278** was produced through the elimination of a urea molecule and HCN gas from scaffold **277** (Scheme 94).[165]

© 2025 The Author(s). Published by the Royal Society of Chemistry

Open Access Article. Published on 21 Oktober 2025. Downloaded on 9/06/2026 1:40:11 PG.
This article is licensed under a Creative Commons Attribution-NonCommercial 3.0 Unported Licence.



Scheme 96 Treatment of *s*-triazine with amine derivatives.



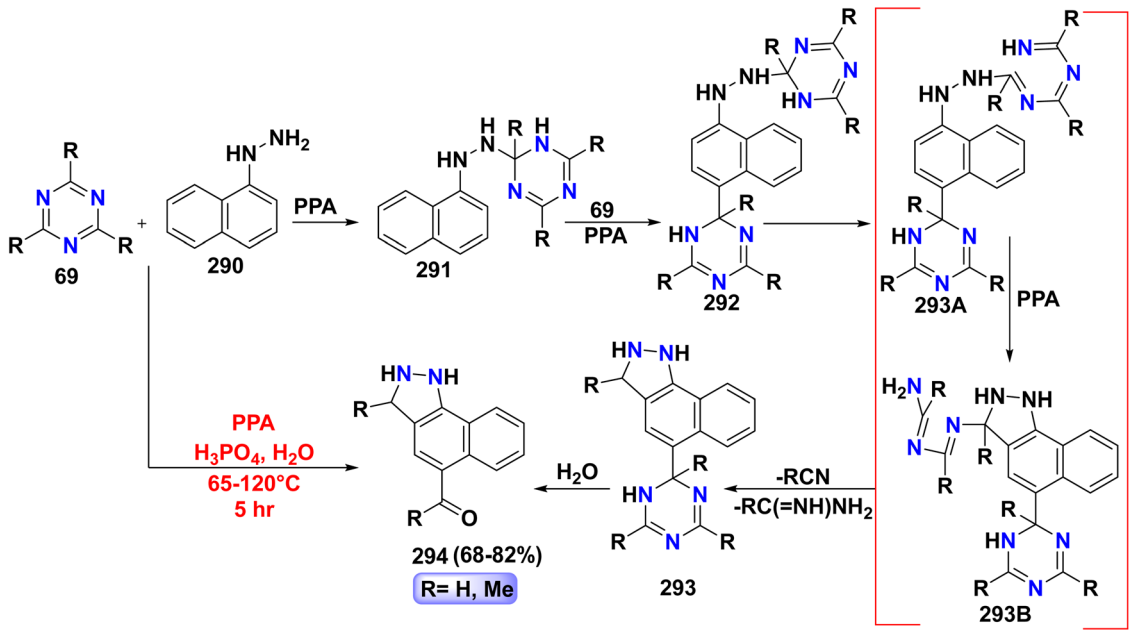
Scheme 97 Reaction of triazine **69** with hydrazine molecules.

IEDDA reaction for the preparation of diethylmethoxy-indeno[1,2-*d*]pyrimidine-dicarboxylates **280** starts with the tautomerization reaction of oxime **279a** or hydrazone scaffolds **279b** into a more reactive nucleophile enamine **280A**. Following this, the [4 + 2] cycloaddition reaction of enamine **280A** with triazine derivatives **69** furnishes intermediate **280B**, which then loses a substituted amine molecule to give intermediate **280C**. Ultimately, intermediate **280C** loses ethyl carbonocyanidate to produce compound **280** (Scheme 95).[166]

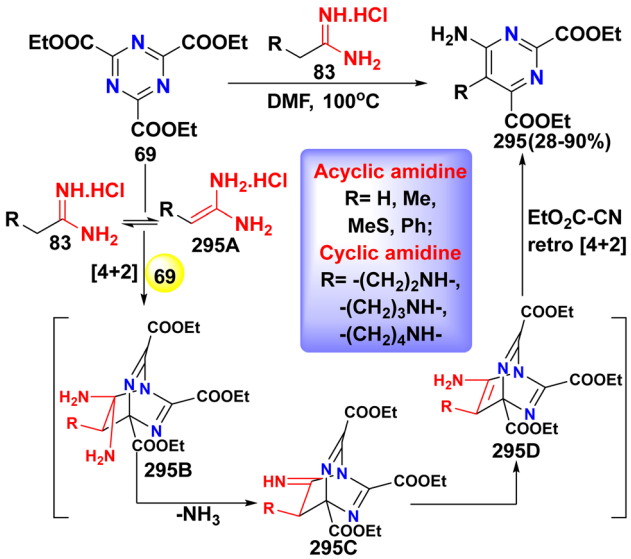
Amino and alkylamino derivatives of triazine have demonstrated significant utility across various domains, including polymers, pharmaceuticals, fiber-reactive dyes, optical brighteners, and agrochemicals. Treatment of triazine **69** with substituted amines **113** affords σ^H adduct **281A**, which then undergoes oxidative (alkyl)amination using bis(pyridine)silver(I)permanganate ($AgPy_2MnO_4$) as the oxidant to afford amino- and alkylamino-triazines **281** (Scheme 96).[167]

3.3.11 Reaction with hydrazine derivatives. Letrozole drug **283**, an aromatase inhibitor, is a crucial pharmacological substance primarily indicated for the treatment of infertility with polycystic ovarian syndrome and hormone-receptor-positive breast cancer in postmenopausal women *via* its ability to decrease oestrogen.[168,169] Whereby, stirring a combination of (hydrazineylmethylene)dibenzonitrile **282** in MeOH/HCl for 3–4 h, then adding triazine **69** and refluxing for 6–7 h furnished letrozole **283**.[170] Also, 1,2,4-triazolones **285** were

Open Access Article. Published on 21 Oktober 2025. Downloaded on 9/06/2026 1:40:11 PG.
This article is licensed under a Creative Commons Attribution-NonCommercial 3.0 Unported Licence.



Scheme 98 Synthesis of benzo-indazole derivatives.



Scheme 99 Diels–Alder reaction for the synthesis of aminopyrimidines.

obtained through the cycloaddition reaction of triazine **69** with α-chloroformyl arylhydrazine hydrochloride **284** to yield cycloadduct **285A**, which is subsequently broken to give compound **285**.[171] Analogously, heating a combination of triazine **69** with substituted phenyl hydrazine hydrochloride **286** in EtOH furnished phenyl triazole derivatives **287**.[172] Under a nitrogen atmosphere, stirring a combination of *t*-butyl-benzyl-hydrazinyl-diazabicyclo[3.2.1]octane-carboxylate **288** with triazine **69** in HCl and dioxane resulted in the formation of *t*-butyl-benzyl-triazolyl-diazabicyclo[3.2.1]octane-carboxylate **289** (Scheme 97).[173]

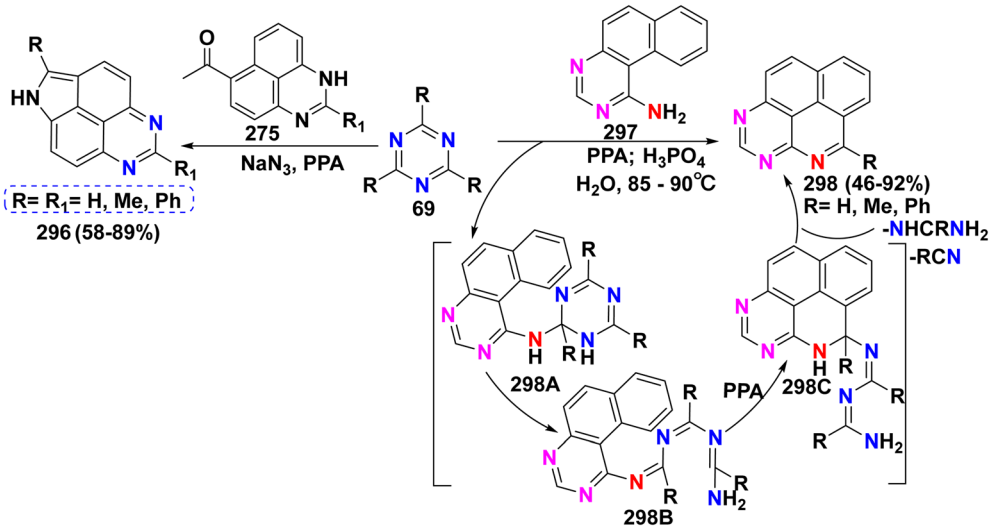
The reaction of naphthyl hydrazine **290** with triazine **69** in PPA generates ((naphthalenyl)hydrazineyl)-triazine **291**. Following this, compound **291** is subjected to further treatment with an additional molecule of **69** in PPA, which leads to ((((dihydro-triazin-yl)hydrazineyl)naphthalen-yl)-dihydro-triazine **292**. During this process, one of the triazine molecules undergoes ring opening to give intermediate **293A**. Subsequently, intramolecular heterocyclization occurs, yielding intermediate **293B**. This reaction culminates in the elimination of a substituted nitrile molecule and formimidamide to form (dihydrotriazinyl)-dihydro-benzo[*g*]indazole **293**. Finally, hydrolysis of compound **293** produces benzoindazoles **294** (Scheme 98).[174]

3.3.12 Reaction with amidine derivatives. Substituted aminopyrimidine derivatives **295** were afforded *via* the reaction of triazines **69** with amidine hydrochloride salts **83** in DMF. The synthesis of substituted 4-aminopyrimidines **295** may be rationalized on the basis of the mechanism involving the tautomerization of amidine hydrochlorides **83** to their corresponding diaminoethene forms **295A**, which then undergo [4 + 2] cycloaddition with triazine **69** to give initial Diels–Alder adduct **295B**. Afterward, this adduct loses an NH_3 molecule to afford imine intermediate **295C**, which subsequently undergoes tautomerization to yield enamine **295D**. In the last step, ethyl cyanoformate is eliminated from the enamine intermediate **295A** *via* RDA reaction to afford 4-aminopyrimidines **295** (Scheme 99).[175]

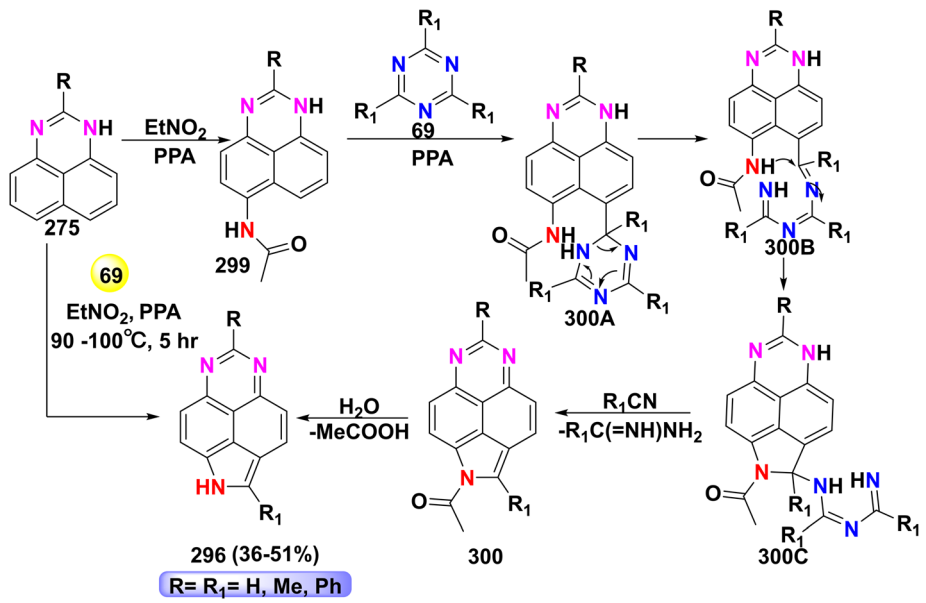
3.3.13 Reaction with perimidines. Schmidt reaction of acetyl-perimidines **275** with triazine **69** in the presence of sodium azide (NaN_3) and PPA furnished pyrrolo-perimidine **296**. Pyrrolo-perimidines have demonstrated effectiveness as inhibitors of thymidylate synthetase.[176] Similarly, treatment of amino-quinazoline derivatives **297** with triazines **69** in PPA afforded triazapyrenes **298**. Scheme 100 depicts the synthetic

© 2025 The Author(s). Published by the Royal Society of Chemistry

Open Access Article. Published on 21 Oktober 2025. Downloaded on 9/06/2026 1:40:11 PG.
This article is licensed under a Creative Commons Attribution-NonCommercial 3.0 Unported Licence.



Scheme 100 Synthetic strategy for the formation of triazapyrenes.



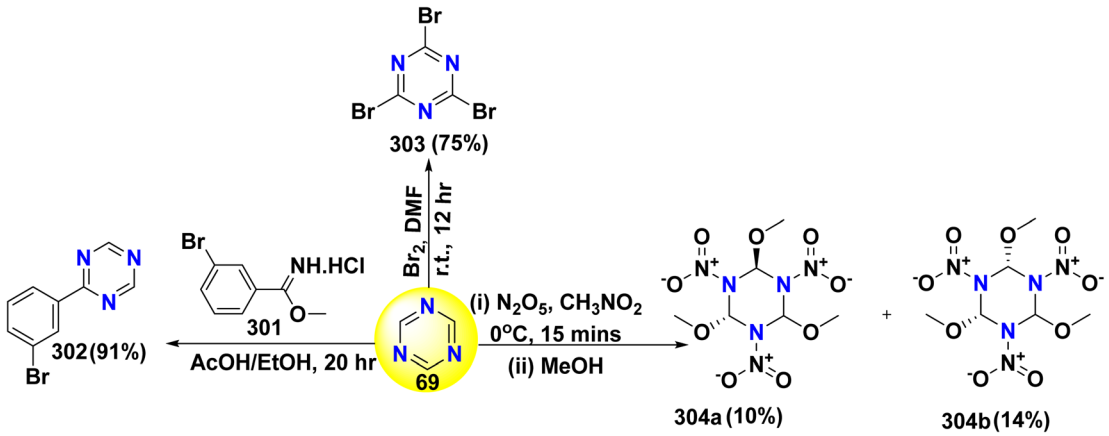
Scheme 101 Mechanistic route for pyrrolo-perimidine generation.

pathway for the formation of triazapyrenes **298**, commencing with the nucleophilic attack of amino quinazoline **297** into the electrophilic carbon of triazine moiety **69**, resulting in the formation of a new C–N bond in intermediate **298A.** Then, this intermediate undergoes ring-opening to yield intermediate **298B.** Following this step, a cyclization reaction occurs to form substituted aminomethylene-(dihydroisoquinolino-quinazolin-5-yl)formimidamide **298C**. Finally, the aromatization reaction of **298C**, accompanied by the elimination of nitrile and amidine molecules, produces triazapyrenes **298** (Scheme 100).[177]

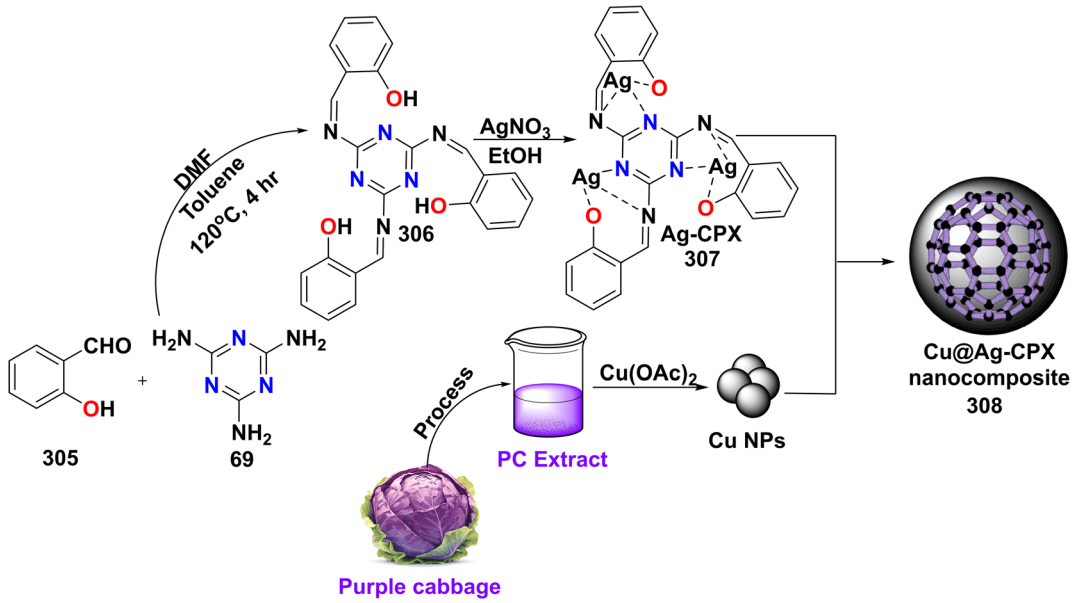
In the same context, heating a mixture of perimidine **275**, $EtNO_2$, and triazine **69** in PPA furnished pyrollo perimidines **296.**[178] The proposed mechanism for pyrrolo-perimidine **296** synthesis is depicted in Scheme 101. Initially, the acetamidation of perimidines **275** with $EtNO_2$, facilitated by the presence of PPA, yields acetamide derivatives **299.** This compound subsequently reacts with triazine **69** to generate intermediate **300A.** Following this, intermediate **300A** undergoes ring-opening to form intermediate **300B**, which then participates in a hetero-cyclization reaction to produce acetyl-pyrrolo-perimidine-iminomethyl-formimidamide intermediate **300C**. Therefore, *N*-acetyl derivatives **300** were produced by losing the nitrile and formimidamide moieties. Ultimately, compound **300** is hydrolyzed in the presence of water, resulting in the formation of scaffold **296** (Scheme 101).[178]

3.3.14 Halogenation and nitration reaction. Bromophenyl triazine **302** was obtained by refluxing a solution of triazine **69** in a combination of AcOH/EtOH with methyl-

Open Access Article. Published on 21 Oktober 2025. Downloaded on 9/06/2026 1:40:11 PG.
This article is licensed under a Creative Commons Attribution-NonCommercial 3.0 Unported Licence.



Scheme 102 Reaction of triazine with halogens and a nitrating agent.



Scheme 103 Formation of the Cu@Ag-CPX nanocomposite.

bromobenzimidate hydrochloride **301**.[179] Similarly, under inert conditions, refluxing a mixture of bromine (Br_2) and triazine **69** in DMF yielded tribromo-triazine **303**.[180] Conversely, the reaction of triazine **69** with a nitrating agent such as dinitrogen pentoxide (N_2O_5), followed by MeOH quenching, afforded a mixture of *cis* and *trans* trinitro-trimethoxyhexahydrotriazine **304a** and **b**, respectively (Scheme 102).[181]

3.3.15 Miscellaneous reactions. The synthesis of Cu@Ag-CPX nanocomposite **308** involves a multistep strategy. Initially, melamine **69** and salicylaldehyde **305** are condensed in DMF/toluene at 120 °C for 4 h, affording ((1,3,5-triazine-2,4,6-triyl)*tris*(azaneylylidene))*tris*(methaneylylidene) triphenol Schiff base **306**. Afterward, the Schiff base reacts with silver nitrate ($AgNO_3$) in EtOH to afford Ag-CPX complex **307** *via* metal chelation and ligand exchange. Parallelly, copper nanoparticles (Cu NPs) are biosynthesized using an aqueous extract of purple cabbage as a stabilizing and reducing agent, reacting with $Cu(OAc)_2$ to form Cu NPs. Then, Cu NPs were added dropwise to the Ag-CPX complex to afford the Cu@Ag-CPX nanocomposite, while copper nanoparticles were immobilized on the Ag-CPX scaffold (Scheme 103).[182]

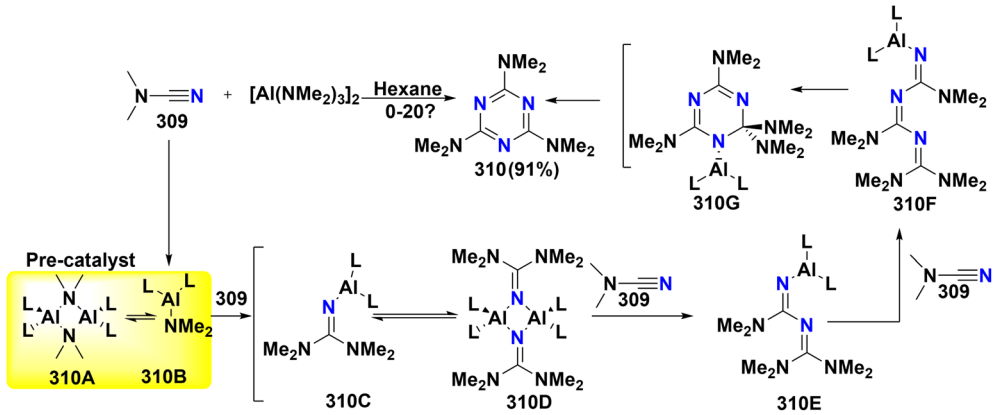
4. Applications

4.1 In medicine

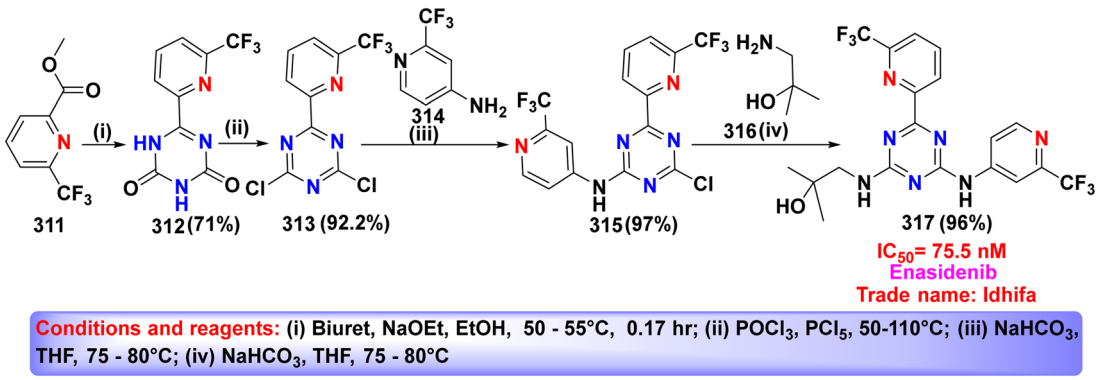
Altretamine **104** is a potent alkylating agent that has been utilized as an antineoplastic in the therapy of diverse cancers as well as a chemosterilant for male houseflies and other insects. The synthesis of altretamine was performed *via* the cyclotrimerization reaction of cyanamide scaffold **309** with a catalytic amount of aluminum amide $[Al(NMe_2)_3]_2$ in hexane. Initially, dimeric Al pre-catalyst **310A** dissociates into the active trivalent aluminium complex Me_2N-Al–L_2 species **310B**. Then, the coordination of nitrogen atom of the cyanamide ligand **309** to Me_2N-

© 2025 The Author(s). Published by the Royal Society of Chemistry

Open Access Article. Published on 21 Oktober 2025. Downloaded on 9/06/2026 1:40:11 PG.
This article is licensed under a Creative Commons Attribution-NonCommercial 3.0 Unported Licence.

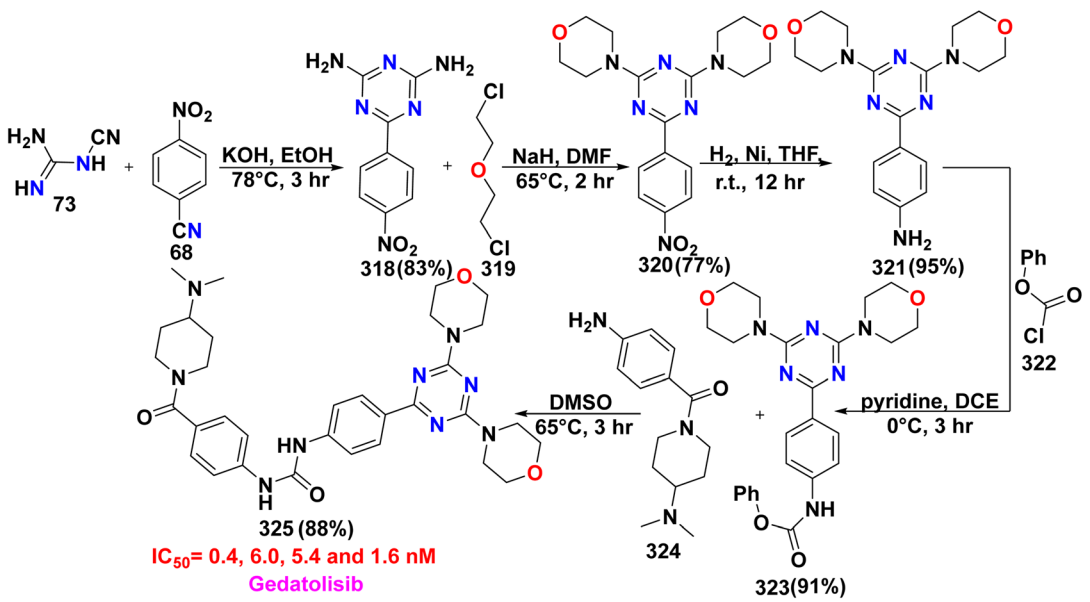


Scheme 104 Formation of the altretamine drug.



Scheme 105 Synthetic strategy for the preparation of enasidenib.

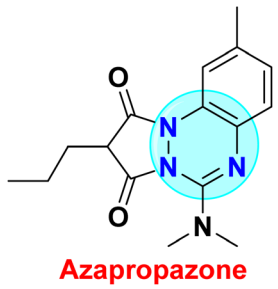
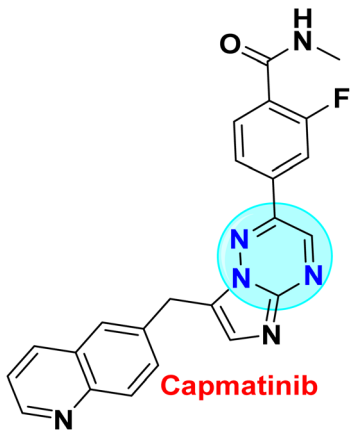
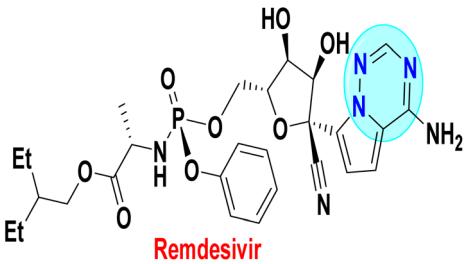
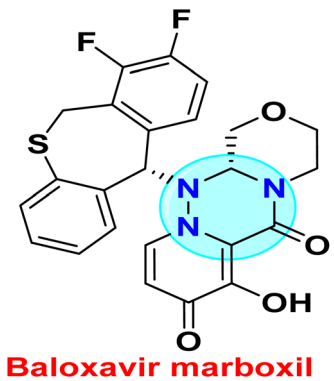
Al–L_2 generates intermediate **310C** *via* a four transition state Afterward, dimerization of intermediate **310C** leads to the formation of intermediate **310D.** Next, a second molecule of cyanamide **309** is introduced to **310D** to yield intermediate **310E**, followed by the third addition of **309** to give intermediate **310F.** Subsequently, intermediate **310F** undergoes cyclization to



Scheme 106 Synthetic methodology toward the gedatolisib drug.

Open Access Article. Published on 21 Oktober 2025. Downloaded on 9/06/2026 1:40:11 PG.
This article is licensed under a Creative Commons Attribution-NonCommercial 3.0 Unported Licence.

Table 3 Examples of a vast array of biologically active molecules for the treatment of some diseases

Structure	Activities	Action mechanism & references
 Azapropazone	❖ Nonsteroidal anti-inflammatory drug (NSAID)[189]	Azapropazone downregulates the synthesis of prostaglandins by impeding cyclooxygenase (COX) enzymes, leading to diminished inflammation and pain.[190,191]
 Capmatinib	❖ Therapy of lung cancer cells.[192,193]	Capmatinib binds to the ATP-binding pocket of the mesenchymal–epithelial transition (MET) receptor, impeding the phosphorylation and activation of downstream signaling pathways. This inhibition disorders the MET-mediated signaling cascade, which is pivotal for the migration, proliferation, and survival of cancer cells.[192,193]
 Remdesivir	❖ Treatment of coronavirus disease[194]	Remdesivir acts as a nucleoside analog that inhibits the RNA polymerase of coronaviruses, as well as it competes with their ATP, which is responsible for their growth. This adds three nucleotides to the RNA chain, causing steric hindrance and a delay in chain elongation. This leads to stalling the enzyme and the termination of RNA synthesis[194]
 Baloxavir marboxil	❖ Treat influenza[195]	Baloxavir marboxil is hydrolyzed to the active form, baloxavir acid, which inhibits the cap-dependent endonuclease activity of polymerase acidic protein, thereby blocking mRNA synthesis and halting viral replication[195]

© 2025 The Author(s). Published by the Royal Society of Chemistry

Open Access Article. Published on 21 Oktober 2025. Downloaded on 9/06/2026 1:40:11 PG.
This article is licensed under a Creative Commons Attribution-NonCommercial 3.0 Unported Licence.

Table 3 (*Contd.*)

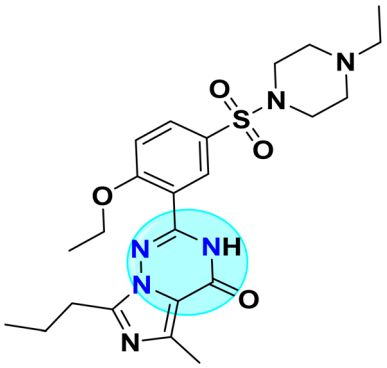
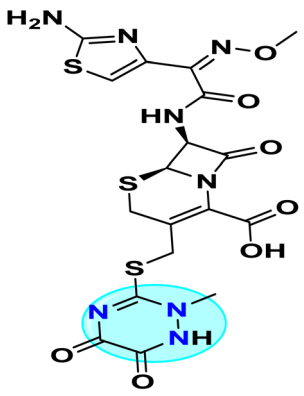
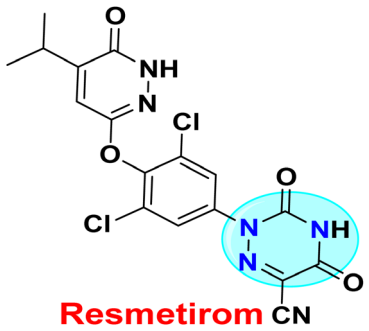
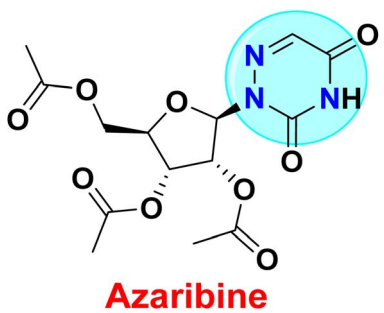
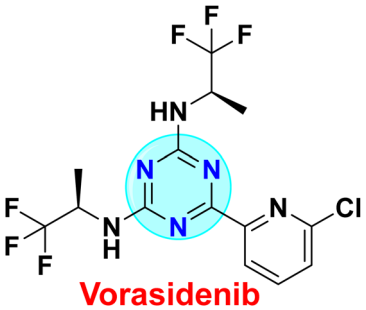
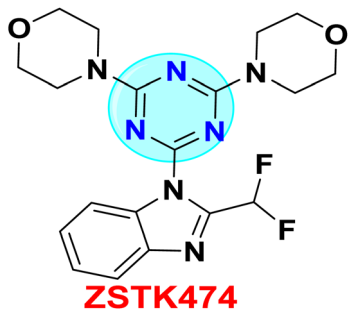
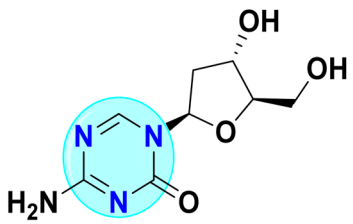
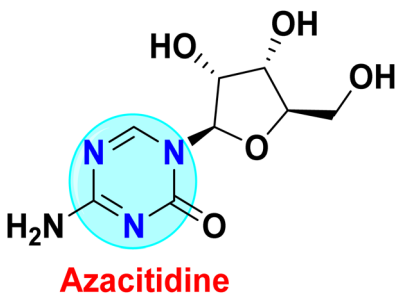
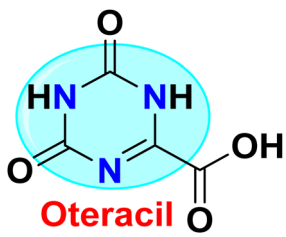
Structure	Activities	Action mechanism & references
 Vardenafil	❖ Treatment of erectile dysfunction[196]	Vardenafil amplifies the natural process of erection by extending the action of cyclic guanosine monophosphate *via* the inhibition of phosphodiesterase-type 5 enzyme, enhancing blood flow, besides sustained erections during sexual activity[196]
 Ceftriaxone	❖ Antibacterial[197]	Ceftriaxone binds to penicillin-binding proteins, stopping the formation of peptide bonds between adjoining peptidoglycan strands, besides enfeebling cell walls, generating osmotic instability and eventual cell lysis, and the death of the bacteria[197,198]
 Resmetirom	❖ Preventing liver scarring[199]	Resmetirom improves lipid metabolism by activating thyroid hormone receptor-β, which promotes genes involved in lipid metabolism. Afterward, fatty acid β-oxidation is increased, and lipogenesis is reduced. As a result, hepatic fat inflammation and accumulation are reduced[200]
 Azaribine	❖ Therapy for psoriasis[201]	Azaribine is metabolized to azauridine, which interferes with thymidylate synthesis to prevent the synthesis of thymidine, which is vital for DNA replication. When DNA synthesis is inhibited, azaribine diminishes the proliferation of keratinocytes, which are overproduced in psoriasis[202]

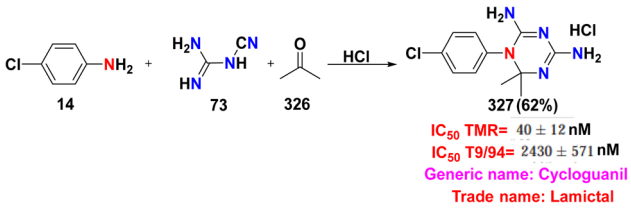
Table 3 (*Contd.*)

Structure	Activities	Action mechanism & references
 Vorasidenib	❖ Treatment of brain tumors[203]	Vorasidenib binds to the mutant isocitrate dehydrogenase 1 and 2 enzymes, preventing them from transforming isocitrate to α-ketoglutarate, which leads to the production of oncometabolite D-2HG. This inhibition decreases the levels of 2-HG in tumor cells[204]
 ZSTK474	❖ PI3K inhibitor.[205,206] ❖ Antineoplastic ❖ Hematopoietic malignancies	ZSTK474 inhibitor blocks the catalytic subunit (p110) of PI3K enzyme, avoiding the transformation of phosphatidylinositol 4,5-bisphosphate to phosphatidylinositol-3,4,5-trisphosphate. This leads to a decrease in the recruitment of downstream effectors, such as 3-phosphoinositide-dependent protein kinase-1 (PDK1) and protein kinase (AKT), which are vital for cell proliferation[207]
 Decitabine	❖ Antineoplastic[208] ❖ Hematopoietic malignancies[209] ❖ AML[210] ❖ Therapy for gastric cancer[211]	Decitabine establishes a covalent bond with DNA methyltransferases (DNMTs) through replication. This irreversible binding reduces the pool of DNMTs, leading to DNA hypomethylation as well as DNA methyltransferases.[212,213] Additionally, it reactivates the apoptosis-related genes, such as RUNX3, PYCARD, TNF, FAS, and FASLG[211]
 Azacitidine	❖ Therapy for myelodysplastic syndrome[214–216]	Azacitidine promotes apoptosis in malignant cells and develops cellular differentiation, which can enhance blood cell counts as well as decrease the risk of progression to AML[216] Also, the inhibition of DNA methyltransferase enzyme decreases DNA methylation, which reactivates tumor suppressor genes, as well as genes implicated in apoptosis and cellular differentiation that are silenced by hypermethylation[214–217]
 Oteracil	❖ Therapy for gastric cancer[218]	Oteracil blocks the phosphoribosyltransferase enzyme, essential for 5-fluorouracil (5-FU) metabolism, leading to a reduction in the activity of 5-FU in the gut and decreasing its toxicity to the normal gastrointestinal mucosa[218]

Open Access Article. Published on 21 Oktober 2025. Downloaded on 9/06/2026 1:40:11 PG.
This article is licensed under a Creative Commons Attribution-NonCommercial 3.0 Unported Licence.

© 2025 The Author(s). Published by the Royal Society of Chemistry

Open Access Article. Published on 21 Oktober 2025. Downloaded on 9/06/2026 1:40:11 PG.
This article is licensed under a Creative Commons Attribution-NonCommercial 3.0 Unported Licence.



Scheme 107 Synthesis of cycloguanil.

afford intermediate **310C**. Finally, deinsertion of the Al complex from intermediate **310G** affords the triazine scaffold **310** (Scheme 104).[183]

Enasidenib drug, known as AG-221, is employed to treat acute myeloid leukemia (AML) with the isocitrate dehydrogenase 2 arginine 140 (IDH2 R140Q) mutation by inhibiting the mutant IDH2 enzyme. Initially, IDH2 converts isocitrate to α-ketoglutarate in the Krebs cycle. However, the R140Q mutation causes the enzyme to produce an oncometabolite, 2-hydroxyglutarate (2-HG), which results in DNA and histone hypermethylation, blocking the differentiation of myeloid precursor cells and promoting leukemia. Enasidenib binds to the allosteric site of the mutant enzyme, preventing the structural changes needed for 2-HG production. By lowering the 2-HG levels, enasidenib relieves the differentiation block, enabling maturation of myeloid cells and reducing leukemic blasts, which result in a clinical improvement in acute myeloid leukemia (AML) patients with this mutation.[184] Enasidenib **317** was synthesized through a series of steps, commencing from the condensation of methyl (trifluoromethyl)picolinate **311** with biuret in the presence of NaOEt and EtOH to furnish (trifluoromethyl)pyridinyl-triazine-dione **312**. Afterward, compound **312** undergoes chlorination using a mixture of $POCl_3$ and phosphorus pentachloride (PCl_5), affording dichloro-(trifluoromethyl)pyridinyl-triazine **313**. Subsequently, one of the chlorine atoms on the triazine core is subjected to nucleophilic substitution with aminopyridine **314** to proceed chloro-(trifluoromethyl)pyridinyl-(trifluoromethyl)pyridine-yl-triazinamine **315**. Ultimately, the remaining chlorine atom on scaffold **315** is replaced with amino-methylpropanol **316**, forming enasidenib **317** (Scheme 105).[184,185]

Gedatolisib (PF-05212384 or PKI-587) is a powerful dual inhibitor targeting both PI3K and mTOR in the PI3K/mTOR pathway. It inhibits all class I PI3K isoforms (α, β, γ, δ) with very low nanomolar IC_{50} values (0.4–6.0 nM) and suppresses mTOR at 1.6 nM. By binding their catalytic subunits, gedatolisib disrupts key signaling controlling cell growth and survival, showing strong antitumor potential. It is a valuable therapeutic agent against numerous cancers and tumors, including AML, by inhibiting the growth of cells and survival pathways. The synthesis of gedatolisib has been achieved through multiple steps. Initially, the condensation reaction of cyanoguanidine **73** and nitrobenzonitrile **68** in EtOH produces nitrophenyl-triazine-diamine **318**. Following this, (nitrophenyl)-triazine-dimorpholine **320** is afforded through the reaction of dichlorodiethyl-ether **319** with scaffold **318** in DMF and NaH. Subsequently, the reduction of scaffold **320** with RANEY® nickel in THF affords (dimorpholino-triazinyl)aniline **321**. Afterward, compound **321** is coupled with phenyl carbonochloridate **322** to give phenyl(dimorpholino-triazinyl)phenylcarbamate **323**. Finally, gedatolisib **325** is synthesized through the reaction of carbamate derivative **323** with (aminophenyl)(dimethylamino) piperidinyl-methanone **324** in DMSO (Scheme 106).[186]

The one-pot-three-component reaction of chloroaniline **14** with cyanoguanidine **73** and acetone **326** in the presence of HCl afforded cycloguanil drug **327**. Cycloguanil is a strong inhibitor of *Plasmodium falciparum* dihydrofolate reductase (pfDHFR), an enzyme crucial for parasite DNA synthesis. It binds tightly to the active site of pfDHFR, blocking the conversion of dihydrofolate to tetrahydrofolate, which is essential for nucleotide production (Table 3). This interruption halts DNA replication and kills the parasite. Cycloguanil targets pfDHFR specifically over the human enzyme, but resistance can develop through pfDHFR mutations that reduce drug binding (Scheme 107).[187,188]

4.2 In industry

4.2.1 CFTs. Triazine serves as a fundamental building block in CTFs,[219] which is due to its three nitrogen atoms, improving their gas interaction and catalytic activity. Additionally, the aromatic nature of triazine provides structural stability, while its planar π-conjugation imparts semiconductive properties, making CFTs suitable for photocatalysis and energy storage applications.[220,221] Also, triazine rings can be functionalized to tailor CTF properties for specific applications. The porous nature of CTFs makes them appropriate for applications such as catalysis,[222] gas adsorption,[223] and separation.[221] In the same context, triazine scaffolds are highly effective in various reactions, including water splitting, H_2 evolution, O_2 evolution, CO_2 reduction, and ammonia production.[224] Alternatively, CTFs can facilitate the integration of renewable energy and its storage, thereby reducing the dependence on fossil fuels and decreasing greenhouse gas emissions. SF-CFT-1 is used in high-performance ion batteries owing to its porosity and abundance of nitrogen atoms.[221] In addition, CTF-HUST-A1 shows exceptional efficiency in photocatalytic water splitting due to its desirable optoelectronic properties as well as chemical stability.[225] Whereby, porous triazine frameworks such as NRPOP-1 and NRPOP-2 exhibit impressive iodine adsorption capacity through host–guest interactions, which is vital for nuclear waste management (Fig. 7).[226]

Salahvarzi *et al.*[227] introduced an innovative gram-scale method for constructing heteroaromatic covalent organic frameworks (COFs) through a catalyst-free, electron-deficient [2 + 2 + 2] cyclotrimerization of alkynes at room temperature. This strategy enables the size-selective intercalation of molecules and offers a rapid approach to water treatment. The process involves the treatment of sodium acetylide (**328**) with cyanuric chloride (**101**) to generate highly reactive triethynyl-triazine intermediate **329A**, which subsequently undergoes *in situ* cyclotrimerization to form COFs **329** composed of benzene and triazine rings (Scheme 108).[227] The triazine ring plays a critical role in enhancing the reactivity of ethynyl groups toward

Open Access Article. Published on 21 Oktober 2025. Downloaded on 9/06/2026 1:40:11 PG.
This article is licensed under a Creative Commons Attribution-NonCommercial 3.0 Unported Licence.

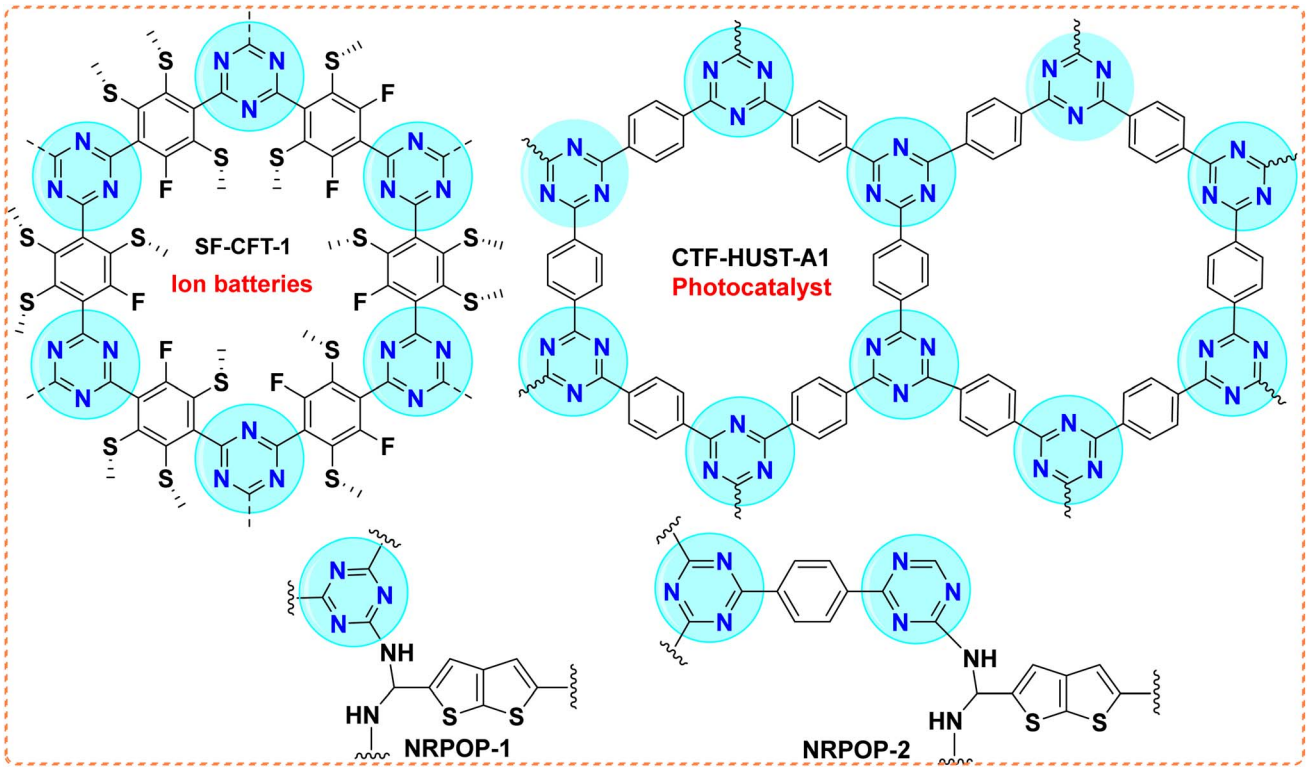
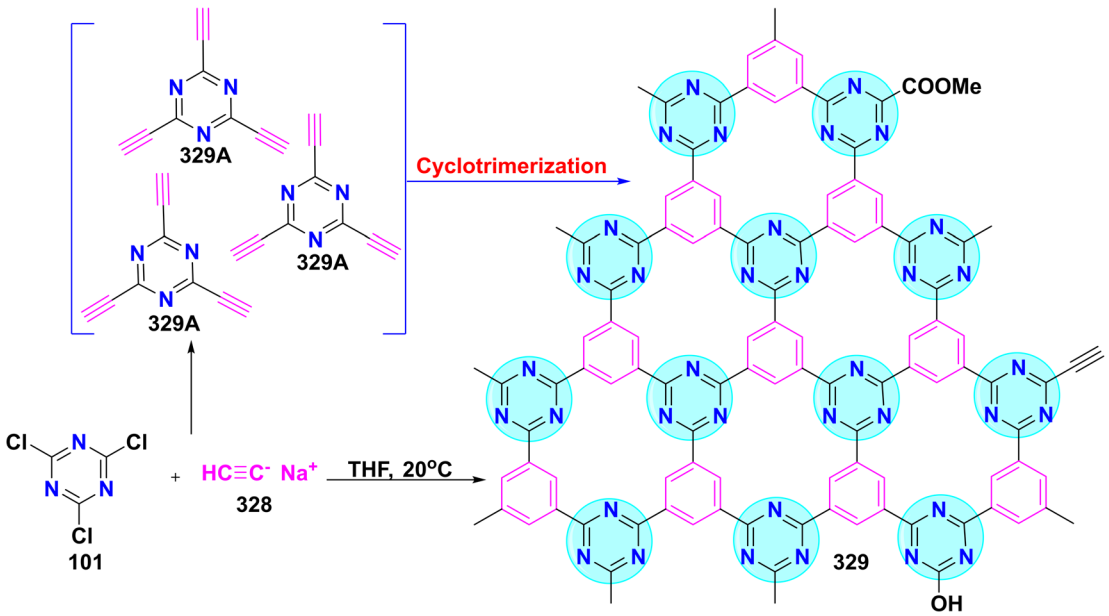


Fig. 7 Examples of some triazine frameworks.



Scheme 108 Synthesis of a triazine framework **329**.

cyclotrimerization. COFs were effectively utilized for molecular intercalation and water purification applications.

4.2.2 In polymers. Additionally, triazine-based polymers, such as *s*-triazine bishydrazino/bishydrazido polymers, are employed to enhance flame retardancy in polypropylene composites.[228] Furthermore, triazine-based porous organic polymers (T-POPs), characterized by high surface area, are utilized to remove pollutants. Remarkably, T-POP1 and T-POP2 exhibit high efficiency in eliminating ~99.4% of methylene blue (cationic dye) and >99% of methyl orange (anionic dye) through electrostatic interactions and functional group coordination (Fig. 8).[229]

© 2025 The Author(s). Published by the Royal Society of Chemistry

Open Access Article. Published on 21 Oktober 2025. Downloaded on 9/06/2026 1:40:11 PG.
This article is licensed under a Creative Commons Attribution-NonCommercial 3.0 Unported Licence.

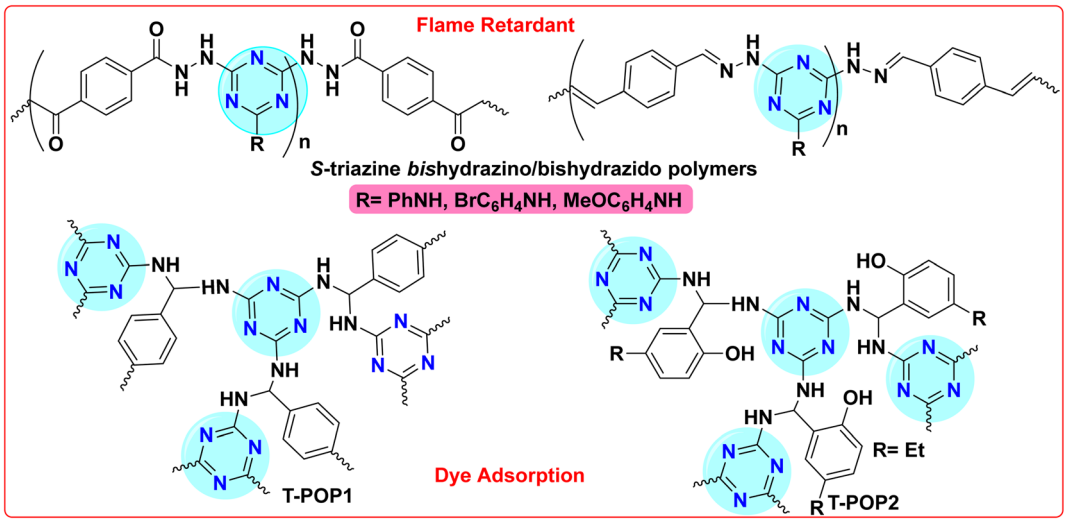


Fig. 8 Applications of some triazine-based polymers.

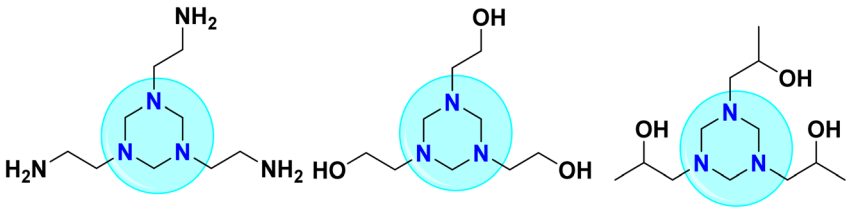
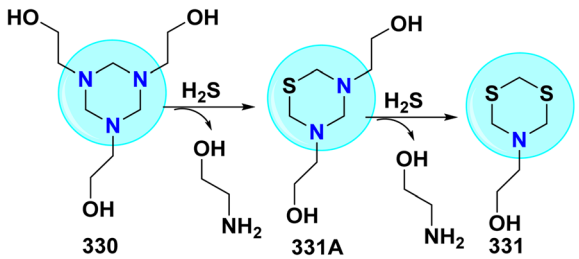


Fig. 9 Some examples of triazine scavengers.



Scheme 109 Postulated mechanism for the stepwise removal of H_2S by triazine scavenger.

4.2.3 In oil & gas. Hydrogen sulfide (H_2S) is a common and problematic contaminant encountered during oil and water processing.[230] Its presence poses significant challenges to the industry due to its high toxicity,[231,232] strong corrosive properties,[233,234] and status as an undesirable byproduct.[235] In certain areas, produced industrial gases contain H_2S concentrations of many thousands of parts per million.[236,237] One of the main methods to control sulfide production is the use of H_2S scavengers, among which triazine-based compounds are the most prevalent.[238] Triazines not only act as effective desulfurizing agents but also synergistically serve as corrosion inhibitors[239,240] owing to the presence of nitrogen atoms with lone electron pairs, a stable ring structure, and abundant π-electrons that are responsible for their strong adsorption onto steel surfaces.[241,242] Hexahydro-1,3,5-*tris*(hydroxyethyl)-*s*-triazine (MEA-triazine) (Fig. 9) dominates the most common class of chemical scavenger in current use today,[243] owing to its superiority in terms of low toxicity, rapid H_2S absorption, low price, high sulfur capacity, efficiency, and biodegradability, which are suitable for offshore oil and gas fields.[244] Additionally, some oil-soluble triazine sulfur remover XN are demonstrated in Fig. 9.[244]

Scheme 109 illustrates the proposed mechanism by which triazine derivatives effectively capture and remove hazardous H_2S from industrial gas streams. Initially, the H_2S ion acts as a nucleophile, attacking one of the ethanolamine side chains of triazine ring **330** to yield (thiadiazinanediyl)bis(ethanol) intermediate **331A**, in which a sulfur atom substitutes one of the nitrogen positions. This process is subsequently repeated with another H_2S molecule, ultimately leading to the generation of the safer (dithiazinanyl)ethanol **331** (Scheme 109).[245]

4.2.4 In agriculture. Plant diseases, insect pests, and invasive weeds represent the main challenges to crop quality and productivity, posing significant risks to food security and the sustainability of agriculture.[246–251] Among them, globally, plant pathogens are responsible for over $220 billion in annual economic losses. Notably, the use of pesticides recovers approximately one-third of these agricultural losses.[252,253] Recently, triazine-based compounds have made great progress in the discovery of new pesticides, especially novel insecticides,[254] herbicides,[255] and fungicides,[256] such as simazine,[257]

Open Access Article. Published on 21 Oktober 2025. Downloaded on 9/06/2026 1:40:11 PG.
This article is licensed under a Creative Commons Attribution-NonCommercial 3.0 Unported Licence.

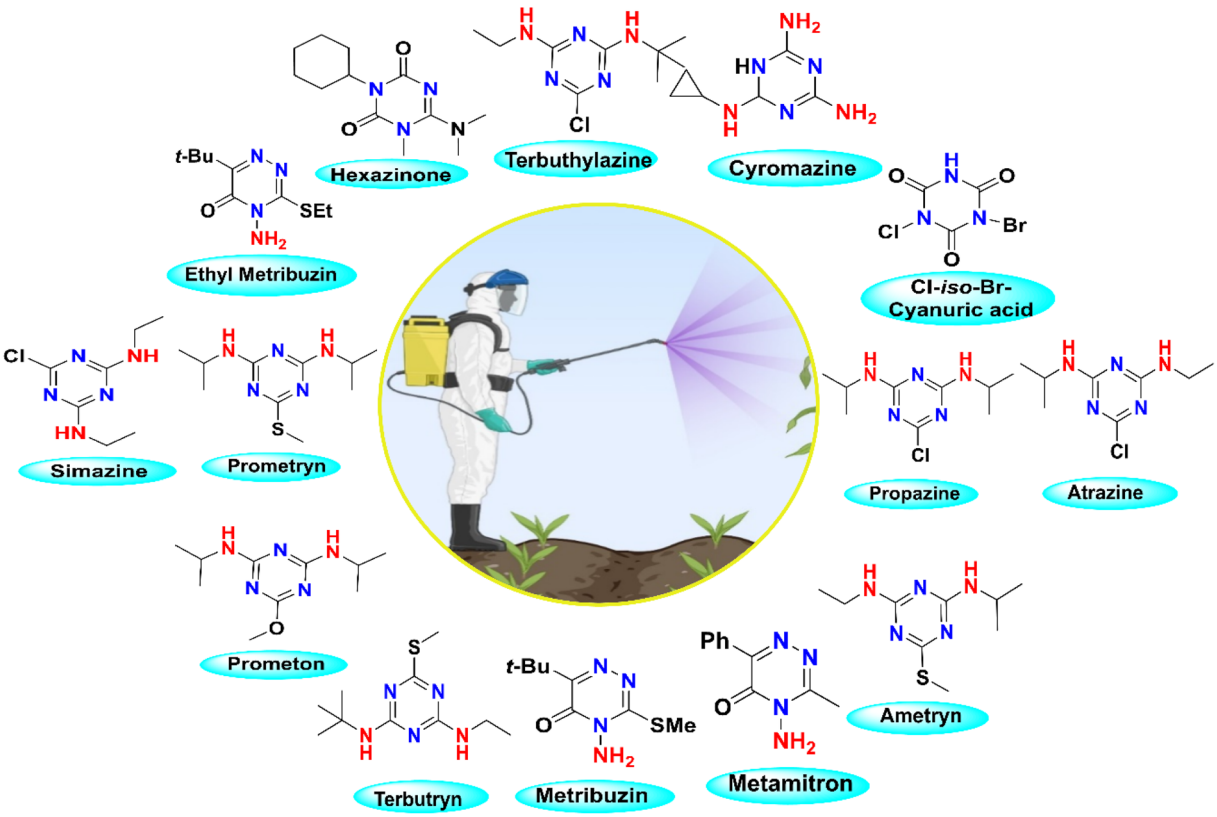


Fig. 10 Chemical structures of some pesticides containing triazine.

prometryn,[258] ethyl metribuzin,[259] hexazinone,[260] terbuthylazine,[261] cyromazine,[262] chloroisobromine cyanuric acid,[263] propazine,[264] atrazine,[265] ametryn,[266] metamitron,[267] metribuzin,[268,269] terbutryn,[270–272] and prometon.[273–275] Their pesticidal efficacy primarily stems from their unique ability to disrupt key biological processes in target pests, most notably by inhibiting photosynthesis[276–279] through interference with electron transport within photosystem II[280,281] and impeding protein, RNA, and lipid synthesis (Fig. 10).[282,283]

Furthermore, the environmental persistence and degradation of triazine-based pesticides, such as atrazine, have been widely studied, with particular focus on microbial enzymatic

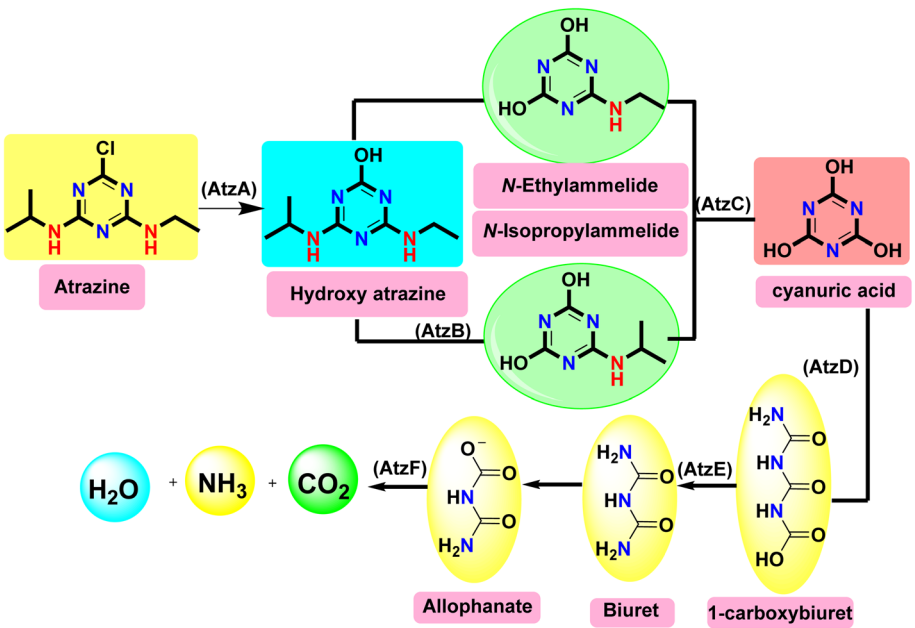


Fig. 11 Biodegradation of atrazine pesticide.

© 2025 The Author(s). Published by the Royal Society of Chemistry

Open Access Article. Published on 21 Oktober 2025. Downloaded on 9/06/2026 1:40:11 PG.
This article is licensed under a Creative Commons Attribution-NonCommercial 3.0 Unported Licence.

degradation pathways. Key enzymes play sequential roles in the biodegradation process, where atrazine chlorohydrolase (AtzA) initiates the pathway by removing chlorine from atrazine to produce hydroxyatrazine. Then, hydroxyatrazine hydrolase (AtzB) deaminates hydroxyatrazine, yielding *N*-isopropylammelide or *N*-ethylammelide. Afterward, *N*-isopropylammelide amidohydrolase (AtzC) deaminates these intermediates to generate cyanuric acid and isopropylamine. Subsequently, cyanuric acid amidohydrolase (AtzD) cleaves the triazine ring of cyanuric acid, generating 1-carboxybiuret, which is then hydrolyzed to biuret by 1-carboxybiuret hydrolase (AtzE). Biuret is further converted to allophanate by biuret hydrolase. Finally, allophanate hydrolase (AtzF) hydrolyzes allophanate to release ammonia (NH_3), water (H_2O), and carbon dioxide (CO_2) (Fig. 11).[284–290]

4.3 In metal complex formation

The deliberate design of expansive coordination networks from precisely engineered molecular units has become a major focus in contemporary research, driven by both the visual appeal and

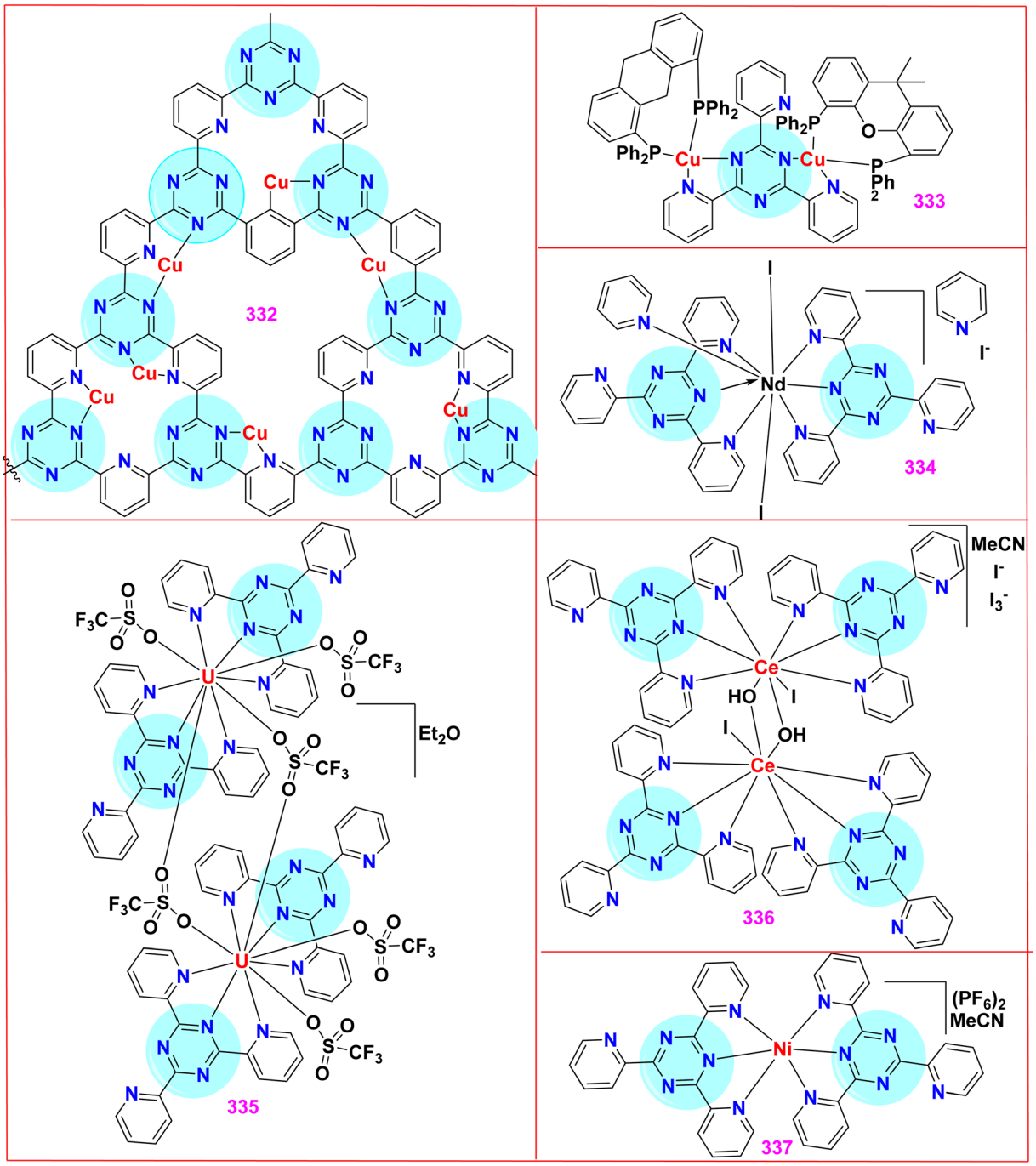


Fig. 12 Coordination modes of TPTZ complexes with their applications.

Open Access Article. Published on 21 Oktober 2025. Downloaded on 9/06/2026 1:40:11 PG.
This article is licensed under a Creative Commons Attribution-NonCommercial 3.0 Unported Licence.

the functional promise of metallosupramolecular assemblies. These structures show potential for a wide range of uses, including molecular magnets, photonic devices, and porous frameworks for gas capture and storage. Achieving the desired physical and chemical properties requires precise regulation of the polymeric architecture, often addressed through the creation of multidentate ligands capable of organizing metal centers in defined geometries. The 1,3,5-triazine moiety, particularly in the form of 2,4,6-*tris*(pyridin-2-yl)-*s*-triazine (TPTZ), stands out for its compartmental structure and the meta disposition of nitrogen donor sites, which facilitates not only a range of coordination geometries from tridentate to bidentate binding for the formation of mononuclear pincer complexes but also encourages strong ferromagnetic interactions between paramagnetic metal ions due to spin-polarization effects. TPTZ has also been widely utilized as a spectroscopic ligand for the analytical detection of transition metals. Advancements in this area include the development of highly efficient and stable copper-modified covalent triazine frameworks **332**, hybridized with carbon nanoparticles, serving as robust cathodic catalysts for electrochemical applications such as nitrate and carbon dioxide reduction in fuel cell technologies.[291–293] Keller and co-workers[294] synthesized copper cyclometallated complex **333**, which is suitable for use in OLED and LEC devices. Additionally, Berthet *et al.*[295] reported the preparation of a series of mono-, bis-, and *tris*-TPTZ complexes with metals such as Nd, U, and Ce, such as in complexes **334**, **335**, and **336**, respectively, expanding the diversity of triazine-based architectures. Also, Hadadzadeh *et al.*[296] synthesized Ni(II)-TPTZ complexes **337** and revealed interesting photophysical behaviors, given that the typical π–π* and n–π* fluorescence of TPTZ is quenched upon

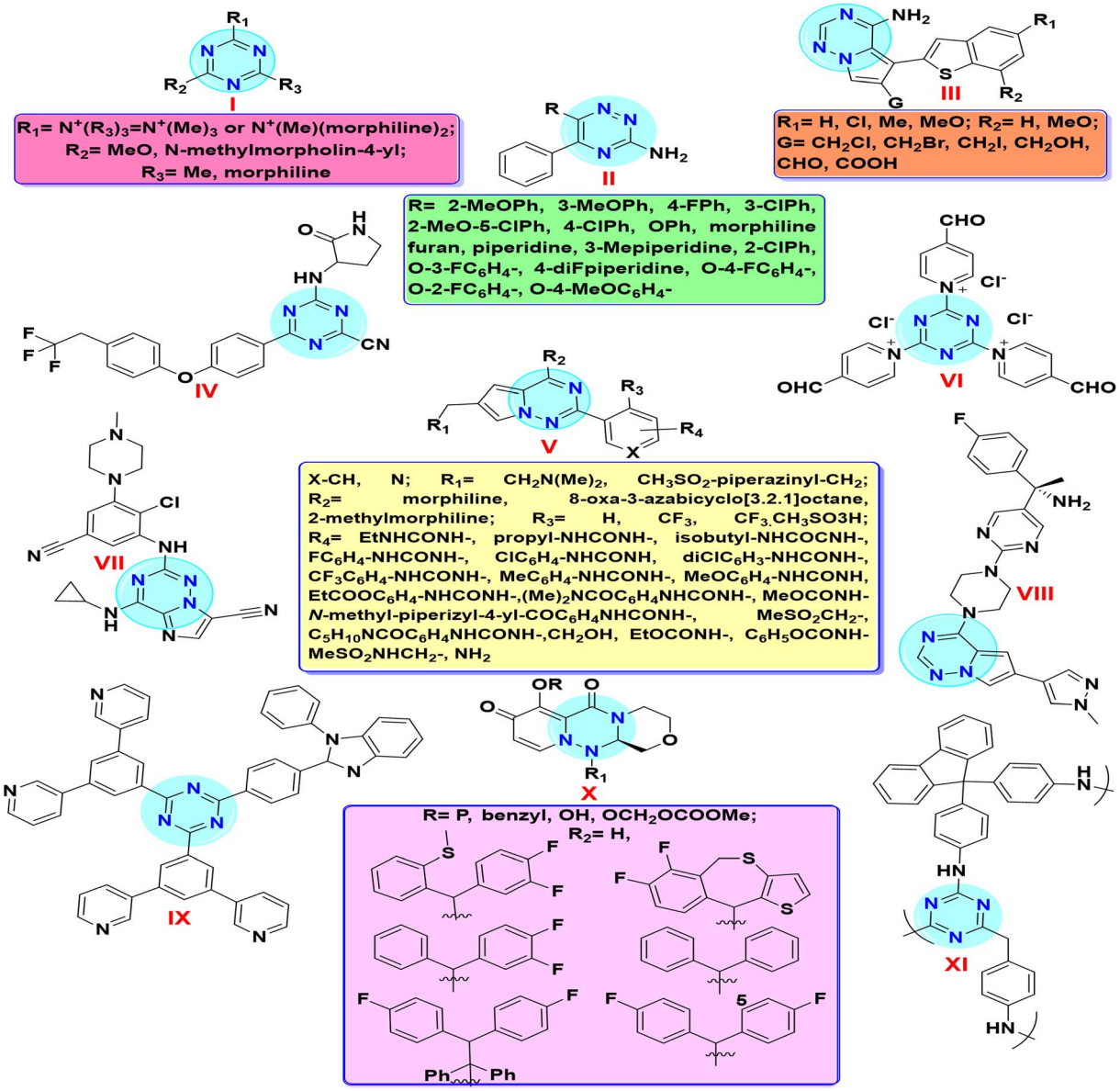


Fig. 13 Reported triazine hybrids in patents.

© 2025 The Author(s). Published by the Royal Society of Chemistry

Open Access Article. Published on 21 Oktober 2025. Downloaded on 9/06/2026 1:40:11 PG. This article is licensed under a Creative Commons Attribution-NonCommercial 3.0 Unported Licence.

complexation due to efficient energy transfer, and exhibit notable paramagnetic properties (Fig. 12).

5. Patents

Triazine hybrids represent a diverse class of heterocyclic molecules, and a significant number of these compounds has been the subject of patent filings worldwide. The vast patent activity involving triazines reflects their large utility across various industries, including materials science, pharmaceuticals, polymers, and agrochemicals. For instance, 1,3,5-triazine derivatives including quaternary amine **I** have been patented and utilized as an effective water-surfactant in various industrial applications.[297] Alternatively, substituted phenyl-[1,2,4] triazine derivatives **II** have been investigated for their potential as a therapeutic agent in the treatment of Parkinson's disease (PD).[298] Also, 5-(1-benzothiophen-2-yl)pyrrolo[2,1-*f*] triazin-amine derivatives **III** have been identified as potent inhibitors of protein tyrosine kinases.[299] Scaffold ((2-oxopyrrolidin-3-yl)amino)-4-(4-trifluoroethyl-phenoxy)phenyl-1,3,5-triazine-2-carbonitrile **IV** exhibits efficacy in the management of sodium channel-related disorders.[300] Pyrrolo[2,1-*f*]triazine scaffolds **V** act as inhibitors of the PI3K signaling cascade.[301] Chlorinated 1,3,5-*tris*(4-formylpyridyl)triazine **VI** serves as a key building block for constructing conjugated microporous polymers, enabling advanced materials with tunable porosity and functional properties.[302] In addition, imidazotriazine carbonitrile **VII** acts as a potent kinase inhibitor.[303] Compound **VIII**, a (4-fluorophenyl)-(2-(4-(6-(methyl-pyrazol-yl)pyrrolo-triazin) piperazinyl)pyrimidinyl)ethan-amine, exhibits notable promise as a therapeutic agent for disorders driven by abnormal tyrosine-protein kinase (KIT) activity.[304] In addition, ((bis(3,5-di(pyridin-3-yl)phenyl)-1,3,5-triazin-2-yl)phenyl)-1-phenyl-dihydro-3*H*-benzo[*d*]imidazole **IX** has been developed as an advanced material for use in organic electroluminescent devices.[305] Substituted 1,4-dihydropyridine-triazine derivatives **X** represent promising antiviral agents for influenza, given that they integrate cap-dependent endonuclease inhibition.[306,307] Furthermore, substituted (9*H*-fluoren-9-yl)phenyl-1,3,5-triazin-2-amine **XI** exhibits excellent optical clarity, high refractive index, good solubility, thermal stability, and low shrinkage, making it suitable for use in advanced film-forming applications (Fig. 13).[308]

6. Conclusion and future perspectives

This review consolidates recent synthetic approaches and reactions for three triazine isomers, in contrast to prior reviews, which focus on only one isomer. Additionally, this review encompasses various chemical approaches for functionalizing the triazine core. Moreover, this review elucidates the mechanistic aspects of diverse reactions to give a deep scope for a nuanced understanding. Also, we reviewed the applications of triazines in drug discovery as anti-inflammatory, anticonvulsant, anticancer, antiviral, and antibacterial agents. In agriculture, triazine derivatives, which are widely commercially used as herbicides, insecticides, and fungicides, are discussed alongside their environmental impacts and biodegradability to less toxic compounds, highlighting opportunities for developing environmentally safer alternatives. Also, this review encompasses industrial applications spanning metal complexes and corrosion inhibition, where mechanistic insights into the role of triazines as sulfur scavengers, mitigating metal corrosion, are elaborated. Furthermore, this review emphasizes the significance of triazines as critical raw materials in the fabrication of CFTs and polymers, showcasing their versatility in materials science. In addition, the emerging utilization of triazines in solar cells and sensors with biological relevance is highlighted, expanding their scope beyond traditional uses. Remarkably, an extensive compilation of recently patented triazine compounds provides a forward-looking perspective on emerging innovations and future research directions. Despite the broad scope of current research, significant gaps remain, including limited strategies for the selective synthesis of triazines at various substitution positions and insufficient systematic exploration of their roles as key intermediates in synthesizing biologically active compounds. Consequently, there is a lack of comprehensive understanding regarding structure–activity relationships across diverse applications of triazine scaffolds. Therefore, future research should prioritize developing innovative, regioselective, and environmentally friendly synthetic methodologies for triazines and improving the mechanistic understanding of their structure–activity relationships. Conversely, efforts should focus on expanding their applications in drug development, especially antifungal, anti-Alzheimer's, anticancer therapies, and advanced material technologies. Integration of computational tools and novel drug design approaches will also be crucial to unlocking the full potential of triazine chemistry.

Conflicts of interest

The authors confirm that this review's contents have no conflict of interest.

Abbreviations

CH_3CN	Acetonitrile
AcOH	Acetic acid
AML	Acute myeloid leukemia
dppp	Bis(diphenylphosphino)propane
$AgPy_2MnO_4$	Bis(pyridine)silver(I)permanganate
Br_2	Bromine
Cs_2CO_3	Caesium carbonate
CuCN	Cuprous cyanide
CTFs	Covalent triazine frameworks
$CuCl_2$	Cupper(II)chloride
CuI	Copper(I)iodide
CO_2	Carbon dioxide
CDI	Carbonyl diimidazole
$Cu(OAc)_2$	Copper(II) acetate

© 2025 The Author(s). Published by the Royal Society of Chemistry

Open Access Article. Published on 21 Oktober 2025. Downloaded on 9/06/2026 1:40:11 PG. This article is licensed under a Creative Commons Attribution-NonCommercial 3.0 Unported Licence.

COX	Cyclooxygenase
DCM	Dichloromethane
DCE	Dichloroethane
DMF	Dimethyl formamide
DCB	Dichlorobenzene
N_2O_5	Dinitrogen pentoxide
DABCO	1,4-Diazabicyclo[2.2.2]octane
DNMTs	DNA methyltransferases
2HG	D-2-Hydroxyglutarate
(EDC)	1-Ethyl-3-(3-dimethylaminopropyl)carbodiimide
HCOOH	Formic acid
CH_2O	Formaline
5-FU	5-Fluorouracil
HFIP	Hexafluoro-iso-propanol
HATU	Hexafluorophosphate azabenzotriazole tetramethyl uronium
HDA	Hetero-Diels–Alder
ihDA	Inverse-electron-demand hetero-Diels–Alder
HAT	Hydrogen atom transfer
HCl	Hydrogen chloride
HCN	Hydrogen cyanide
NH_2OH	Hydroxyl amine
NH_2NH_2	Hydrazine hydrate
HAT	Hydrogen atom transfer
H_2S	Hydrogen sulfide
I^-	Iodide ions
I_2	Iodine
IEDDA	Inverse electron demand Diels–Alder
IDH2	Isocitrate dehydrogenase 2
$(LiN(TMS)_2)$	Lithium bis(trimethylsilyl)amide
MCR	Multicomponent reaction
mTOR	Mammalian target of rapamycin
MET	Mesenchymal–epithelial transition
NLOs	Nonlinear optics
N_2O	Nitrous oxide
$EtNO_2$	Nitroethane
SNAr	Nucleophilic aromatic substitution
NMP	*N*-Methyl-pyrrolidone
TsNHMe	*N*-Methyl-*p*-toluenesulfonylamide
NSAID	Nonsteroidal anti-inflammatory drug
DMEA	*N*,*N*-Dimethylethanolamine
DMA	*N*,*N*-Dimethylacetamide
OLEDs	Organic light-emitting diodes
OSCs	Organic solar cells
PSCs	Perovskite solar cells
$KHCO_3$	Potassium bicarbonate
Pd/C	Palladium/carbon
PI3K	Phosphatidylinositol 3-kinase
K_3PO_4	Potassium phosphate
$POCl_3$	Phosphorous oxychloride
PPA	Polyphosphoric acid
t-BuOK	Potassium *tert*-butoxide
K_3PO_4	Potassium phosphate
K_2CO_3	Potassium carbonate
KF	Potassium fluoride
PIFA	Phenyliodine(III) bis(trifluoroacetate)
PCl_5	Phosphorus pentachloride
pfDHFR	Plasmodium falciparum dihydrofolate reductase
$(COCl)_2$	Phosgene gas
p-TsOH	*p*-Toluene sulfonic acid
PD	Parkinson's disease
RDA	Retro-Diels–Alder
$NaNO_2$	Sodium nitrite
$Na_2S_2O_3$	Sodium hyposulfite
NaHNCN	Sodium hydrogen cyanamide
MeONa	Sodium methoxide
$AgNO_3$	Silver nitrate
t-BuONa	Sodium-*tert*-butoxide
H_2SO_4	Sulfuric acid
Na_2CO_3	Sodium carbonate
$NaBH_4$	Sodium borohydride
NaOEt	Sodium ethoxide
SET	Single-electron transfer
$Na_2S_2O_4$	Sodium dithionite
NaN_3	Sodium azide
NaH	Sodium hydride
v-Triazine	1,2,3-Triazine
α-Triazine	1,2,4-Triazine
s-Triazine	1,3,5-Triazine
TFA	Trifluoroacetic acid
t-BuONO	*Tert*-butyl nitrite
PPh_3	Triphenylphosphine
Me_4NF	Tetramethylammonium fluoride
TBAB	Tetrabutylammonium bromide
t-Bu-AQN	*t*-Butyl anthraquinone
THF	Tetrahydrofuran
Tf_2O	Triflic anhydride
TfOH	Triflic acid
HSCN	Thiocyanic acid
t-butylMgCl	*Tert*-butyl magnesium chloride
$P(OMe)_3$	Trimethyl phosphite
$TMSN_3$	Trimethylsilyl azide
TFE	Trifluoroethanol
$Pd(PPh_3)_4$	Tetrakis(triphenylphosphine)palladium(0)
TMSCl	Trimethylsilyl chloride
$ClSn(nBu)_3$	Tributyl tin chloride
CF_3CN	Trifluoroacetonitrile
$BF_3 \cdot OEt_2$	Trifluoride diethyl etherate
TDDA	Tandem decarboxylation/Diels–Alder reaction
T-POPs	Triazine-based porous organic polymers
Tos(MIC)	Tosylmethyl isocyanide
MEA-triazine	Hexahydro-1,3,5-*tris*(2-hydroxyethyl)-*s*-triazine
TPTZ	2,4,6-*tris*(Pyridin-2-yl)-*s*-triazine
KIT	Tyrosine-protein kinase

Data availability

No primary research results, software, or code has been included, and no new data were generated or analyzed as part of this review.

Acknowledgements

The authors are grateful to Mansoura University, Egypt, for its support under project ID MU-SCI-25-73.

© 2025 The Author(s). Published by the Royal Society of Chemistry

Open Access Article. Published on 21 Oktober 2025. Downloaded on 9/06/2026 1:40:11 PG. This article is licensed under a Creative Commons Attribution-NonCommercial 3.0 Unported Licence.

References

1 A. Ansari, A. Ali, M. Asif and Shamsuzzaman, *New J. Chem.*, 2017, **41**, 16–41.

2 (*a*) N. Vats, A. Parveen, M. Shafeeque, A. Choudhary, S. Yahya and M. S. Yar, *Arch. Pharm.*, 2025, **358**, e12004; (*b*) S. Talbi, S. Hamri, S. Rabi, A. Hafid and M. Khouili, *Curr. Org. Chem.*, 2025, 2070–2096.

3 D. Maliszewski and D. Drozdowska, *Pharmaceuticals*, 2022, **15**, 221.

4 (*a*) R. E. Abdelwahab, A. H. M. Elwahy, N. S. Ibrahim, A. M. Abdelmoniem and I. A. Abdelhamid, *BMC Chem.*, 2025, **19**, 61; (*b*) F.-G. Zhang, Z. Chen, X. Tang and J.-A. Ma, *Chem. Rev.*, 2021, **121**, 14555–14593.

5 (*a*) N. Kushwaha and C. S. Sharma, *Mini-Rev. Med. Chem.*, 2020, **20**, 2104–2122; (*b*) C. F. M. Silva, A. P. D. de, M. S. Guerrinha, S. Carvalho, D. C. G. A. Pinto and A. M. S. Silva, *Int. J. Mol. Sci.*, 2025, **26**, 882.

6 (*a*) R. Kumar, N. Kumar, R. K. Roy and A. Singh, *Curr. Med. Drug Res.*, 2017, **1**, 173; (*b*) X. Li, Y. Li, R. Wang, Q. Wang and L. Lu, *Appl. Environ. Microbiol.*, 2019, **85**, e00106–e00119; (*c*) P. Ruanpanun, H. Laatsch, N. Tangchitsomkid and S. Lumyong, *World J. Microbiol. Biotechnol.*, 2011, **27**, 1373–1380; (*d*) Z. Jiahao, I. Yohei, O. Yasuhiro, O. Kouharu, K. Takashi, L. Wei and A. Yojiro, *J. Nat. Med.*, 2025, **79**, 608–620.

7 B. Rathod, S. Pawar, S. Puri, A. Diwan and K. Kumar, *ChemistrySelect*, 2024, **9**, e202303655.

8 D. Yadav, Subodh and S. K. Awasthi, *Mater. Chem. Front.*, 2022, **6**, 1574–1605.

9 (*a*) S. Zhu, C. Wu, Y. He, Y. Song, Z. Chen, L. Hu, Q. Cheng, R. Liu and H. Zhu, *J. Photochem. Photobiol., A*, 2025, **462**, 116193; (*b*) L. Nayak, S. Acharya, S. Routray, S. Pattnaik and R. Satapathy, *RSC Adv.*, 2025, **15**, 27951–27994.

10 Q. Dai, Q. Sun, X. Ouyang, J. Liu, L. Jin, A. Liu, B. He, T. Fan and Y. Jiang, *Molecules*, 2023, **28**, 4278.

11 J. D. Georgiades, D. A. Berkovich, S. R. McKee, A. R. Smith, B. Sankaran, K. N. Flentie, C. H. Castañeda, D. G. Grohmann, R. Rohatgi, C. Lask, T. A. Mason, J. E. Champine, P. A. Miller, U. Möllmann, G. C. Moraski, S. G. Franzblau, M. J. Miller, C. L. Stallings, J. M. Jez, B. A. Hathaway and T. A. Wencewicz, *ACS Infect. Dis.*, 2025, **11**, 689–702.

12 (*a*) G. Garcia-Manero, J. McCloskey, E. A. Griffiths, K. W. L. Yee, A. M. Zeidan, A. Al-Kali, H. J. Deeg, M. Sabloff, M.-M. Keating, N. Zhu, N. Y. Gabrail, S. Fazal, J. Maly, O. Odenike, A. E. DeZern, C. L. O'Connell, G. J. Roboz, L. Busque, R. Buckstein, H. Amin, B. Leber, A. Shastri, A. Oganesian, H. N. Keer, M. Azab and M. R. Savona, *Future Oncol.*, 2025, **21**, 929–941; (*b*) N. Kim, K. J. Norsworthy, S. Subramaniam, H. Chen, M. L. Manning, E. Kitabi, J. Earp, L. A. Ehrlich, O. O. Okusanya, J. Vallejo, B. J. Gehrke, R. A. de Claro and R. Pazdur, *Clin. Cancer Res.*, 2022, **28**, 3411–3416; (*c*) H. Liu, H. Jiang, H. Tong, R. Xia, L. Yang, H. Zhao, J. Ouyang, H. Bai, H. Sun, L. Hou, M. Jiang, Y. Zeng, Z. Liu, A. Liang, Y. Xie, K. Yu, Z. Zhai, L. Liu, J. Jia, R. Fu and Z. Shao, *Cancer Med.*, 2023, **12**, 13885–13893.

13 (*a*) F. Alirezapour and A. Khanmohammadi, *Acta Crystallogr.*, 2020, **76**, 982–991; (*b*) N. Keldsen, H. Havsteen, I. Vergote, K. Bertelsen and A. Jakobsen, *Gynecol. Oncol.*, 2003, **88**, 118–122; (*c*) H. Liao, M. Liu, M. Wang, D. Zhang, Y. Hao and F. Xie, *Pharmaceuticals*, 2025, **18**, 690.

14 (*a*) E. C. Pham, B.-N. T. Le, A. M. Ngo, L. B. Vong and T. N. Truong, *RSC Adv.*, 2025, **15**, 9968–9984; (*b*) Y. Li, *J. Med. Chem.*, 2024, **67**, 5113–5143; (*c*) D. K. Basedia, B. K. Dubey and B. Shrivastava, *Am. J. PharmTech Res.*, 2011, **1**, 174–193.

15 (*a*) C. J. Bethencourt-Estrella, A. López-Arencibia, J. Lorenzo-Morales and J. E. Piñero, *Pathogens*, 2025, **14**, 127; (*b*) M. G. Jelodar, M. Malek-Ahmadi, A. Sahebnasagh, F. Mohammadi and F. Saghafi, *BMC Pulm. Med.*, 2025, **25**, 107; (*c*) D. Górecka, P. Śliwiński, G. Pałasiewicz, R. Pachocki and J. Zieliński, *Respiration*, 2003, **70**, 275–283.

16 D. Payen, *Crit. Care Med.*, 2021, **49**, 387–389.

17 L.-C. Li, Y.-Y. Han, Z.-H. Zhang, W.-C. Zhou, H.-M. Fang, J. Qu and L.-D. Kan, *Drug Des., Dev. Ther.*, 2021, **15**, 111–124.

18 G. P. Collins, T. A. Eyre, D. Schmitz-Rohmer, W. Townsend, R. Popat, L. Giulino-Roth, P. A. Fields, F. Krasniqi, C. Soussain, A. Stathis, N. Andjelkovic, D. Cunningham, D. Mandic, S. Radulovic, I. Tijanic, N. A. Horowitz, S. Kurtovic, E. Schorb, C. Schmidt, S. Dimitrijević and M. Dreyling, *Hemasphere*, 2021, **5**, e656.

19 S.-J. Wang, T. S. Sihra and P.-W. Gean, *Neuroreport*, 2001, **12**, 2255–2258.

20 (*a*) L. Tu, J. Xiao, Q. Hong, A. Ouyang, Y. Tu and S. Wang, *Expert Opin. Drug Saf.*, 2025, **24**, 805–814; (*b*) H. A. Ebrahimi and F. Ebrahimi, *Iran. J. Neurol.*, 2012, **11**, 162–163.

21 D. Niu, L. Zhang, B. Zhang, Q. Zhang, S. Ding, H. Wei and Z. Li, *Complex Intell. Syst.*, 2025, **11**, 68.

22 O. N. Chupakhin, V. L. Rusinov, M. V. Varaksin, E. N. Ulomskiy, K. V. Savateev, I. I. Butorin, W. Du, Z. Sun and V. N. Charushin, *Int. J. Mol. Sci.*, 2022, **23**, 14537.

23 G. A. Artem'ev, V. L. Rusinov, D. S. Kopchuk, M. I. Savchuk, S. Santra, E. N. Ulomsky, G. V. Zyryanov, A. Majee, W. Du, V. N. Charushin and O. N. Chupakhin, *Org. Biomol. Chem.*, 2022, **20**, 1828–1837.

24 (*a*) L. Tang, J. Wang and Y. Liu, *Molecules*, 2025, **30**, 879; (*b*) G. Sathiyan, G. Venkatesan, S. K. Ramasamy, J. Lee and S. Barathi, *J. Environ. Chem. Eng.*, 2024, **12**, 112804.

25 (*a*) X. Zhao, X. Zhou, Q. Cheng and Y. Liu, *Nano Today*, 2025, **60**, 102561; (*b*) R. S. Chouhan, I. Jerman, D. Heath, S. Bohm, S. Gandhi, V. Sadhu, S. Baker and M. Horvat, *Nano Select*, 2021, **2**, 712–743.

26 (*a*) Y. Feng, L. Wang, H. Gao, J. Zhou, M. Stolte, H. Qiu, L. Liu, V. Adebayo, M. Boggio-Pasqua and F. Würthner, *Angew. Chem.*, 2025, **137**, e202416425; (*b*) H. Irshad, M. A. Assiri, Khadija, S. Rafique, A. M. Khan, M. Imran and S. A. Shahzad, *Spectrochim. Acta, Part A*, 2023, **300**, 122934.

27 Z. Seferoğlu, *Org. Prep. Proced. Int.*, 2017, **49**, 293–337.

Open Access Article. Published on 21 Oktober 2025. Downloaded on 9/06/2026 1:40:11 PG. This article is licensed under a Creative Commons Attribution-NonCommercial 3.0 Unported Licence.

28 P. Šimon, M. Klikar, Z. Burešová, C. Vourdaki, A. Katsidas, J. Tydlitát, J. Kulhánek, J. Zelenka, M. Fakis and F. Bureš, *J. Mater. Chem. C*, 2023, **11**, 7252–7261.
29 E. Baştürk, *Arabian J. Sci. Eng.*, 2024, **49**, 7829–7849.
30 (*a*) S. Singh, M. K. Mandal, A. Masih, A. Saha, S. K. Ghosh, H. R. Bhat and U. P. Singh, *Arch. Pharm.*, 2021, **354**, 2000363; (*b*) V. S. Padalkar, V. S. Patil and N. Sekar, *Chem. Cent. J.*, 2011, **5**, 77.
31 (*a*) X. Fan, J. Chen, J. Wang, J. Wang, J. Zeng, F. Wei, S. Gao, J. Li, J. Zhang, F. Yan and W. Song, *Energy Environ. Sci.*, 2025, **18**, 2905–2917; (*b*) V. D. Cerón, L. A. Illicachi and B. Insuasty, *Molecules*, 2023, **28**, 257.
32 E. V. Nosova, G. N. Lipunova, G. V. Zyryanov, V. N. Charushin and O. N. Chupakhin, *Org. Chem. Front.*, 2022, **9**, 6646–6683.
33 H. Zhang, X.-F. Zang, Y.-P. Hong and Z.-E. Chen, *Synth. Met.*, 2021, **280**, 116882.
34 U. K. Aryal, S. S. Reddy, J. Choi, C. Y. Woo, S. Jang, Y. Lee, B. S. Kim, H. W. Lee and S.-H. Jin, *Macromol. Res.*, 2020, **28**, 727–732.
35 Y. Sun, J. Zhang, H. Yu, C. Huang and J. Huang, *ACS Appl. Mater. Interfaces*, 2022, **14**, 6625–6637.
36 H. T. Nguyen, T. T. Nguyen, V. T. C. Doan, T. H. Nguyen and M. H. Tran, *RSC Adv.*, 2025, **15**, 9676–9755.
37 B. V. Manjushree, G. S. P. Matada, R. Pal, M. A. Sk, M. P. Viji, N. V. S. S. Aishwarya, P. K. Das, I. Aayishamma and S. Mounika, *ChemistrySelect*, 2024, **9**, e202402766.
38 S. Cascioferro, B. Parrino, V. Spano, A. Carbone, A. Montalbano, P. Barraja, P. Diana and G. Cirrincione, *Eur. J. Med. Chem.*, 2017, **142**, 74–86.
39 H. Sugimura, R. Takeuchi, S. Ichikawa, E. Nagayama and I. Sasaki, *Org. Lett.*, 2018, **20**, 3434–3437.
40 L. De Angelis, H. Zheng, M. T. Perz, H. Arman and M. P. Doyle, *Org. Lett.*, 2021, **23**, 6542–6546.
41 M. T. Migawa and L. B. Townsend, *J. Org. Chem.*, 2001, **66**, 4776–4782.
42 F. Maqueda-Zelaya, J. L. Acena, E. Merino, J. J. Vaquero and D. Sucunza, *J. Org. Chem.*, 2023, **88**, 14131–14139.
43 A. O. Gurenko, O. V. Shablykin, A. P. Kozachenko and V. S. Brovarets, *Chem. Heterocycl. Compd.*, 2012, **48**, 1423–1424.
44 X.-W. Zhao, D. Liu, S.-L. Luan, G.-D. Hu, J.-L. Lv, Y.-K. Jing and L.-X. Zhao, *Bioorg. Med. Chem.*, 2013, **21**, 7807–7815.
45 Z. Zeng, C. Chen, X. Xu, Y. Liu, W. Huang and Y. Tang, *J. Org. Chem.*, 2024, **89**, 9516–9520.
46 M. Arshad, T. A. Khan and M. A. Khan, *Int. J. Pharm. Sci. Res.*, 2014, **5**, 149–162.
47 Y. K. Gummadi and L. Y. C. Chen, *Blood*, 2024, **144**, 5373.
48 A. M. Palmer, B. Grobbel, C. Brehm, P. J. Zimmermann, W. Buhr, M. P. Feth, H. C. Holst and W. A. Simon, *Bioorg. Med. Chem.*, 2007, **15**, 7647–7660.
49 F. Z. Nouaytia, N. Oufkira, S. Lahmidic, M. Rehiouid, E.-H. Anouare, I. Filalie, H. Hajjig, M. El Yazidib, J. T. Maguef and E.-M. Essassic, *J. Mol. Struct.*, 2025, **1336**, 142064.
50 S. A. Khan, A. Y. Obaid, L. M. Al-Harbi, M. N. Arshad, O. Şahin, C. C. Ersanlı, R. M. Abdel-Rehman, A. M. Asiri and M. B. Hursthouse, *J. Mol. Struct.*, 2015, **1096**, 29–37.
51 A. P. Krinochkin, A. F. Khasanov, M. I. Valieva, E. A. Kudryashova, M. R. Guda, D. S. Kopchuk, O. V. Shabunina, N. N. Mochulskaya, P. A. Slepukhin, G. V. Zyryanov and O. N. Chupakhin, *Chem. Heterocycl. Compd.*, 2024, **60**, 289–298.
52 J. Meng, M. Wen, S. Zhang, P. Pan, X. Yu and W.-P. Deng, *J. Org. Chem.*, 2017, **82**, 1676–1687.
53 L. Crespin, L. Biancalana, T. Morack, D. C. Blakemore and S. V. Ley, *Org. Lett.*, 2017, **19**, 1084–1087.
54 W. Hamama, G. El-Bana, S. Shaaban, O. M. O. Habib and H. Zoorob, *J. Heterocycl. Chem.*, 2017, **54**, 1384–1390.
55 (*a*) M. Marzi, K. Pourshamsian, F. Hatamjafari, A. Shiroudi and A. R. Oliaey, *Russ. J. Bioorg. Chem.*, 2019, **45**, 391–397; (*b*) H. A. Zamani, G. Rajabzadeh, A. Firouz and A. A. Ariaii-Rad, *J. Braz. Chem. Soc.*, 2005, **16**, 1061–1067.
56 H. A. Ali, M. M. Hammouda, M. A. Ismail and E. A. Ghaith, *RSC Adv.*, 2025, **15**, 17516–17534.
57 A. Hassner and C. Stumer, *Organic Syntheses Based on Name Reactions*, Elsevier, 2002, vol. 22, ISBN 0-08-043260-3.
58 A. Hassner and I. Namboothiri, *Organic Syntheses Based on Name Reactions: a Practical Guide to 750 Transformations*, Elsevier, 2012, pp. 46–47.
59 Y. Cheng, H. Pang and W. Zhang, *J. Am. Chem. Soc.*, 2025, **147**, 12075–12081.
60 R. Yang, Q. Shi, T. Huang, Y. Yan, S. Li, Y. Fang, Y. Li, L. Liu, L. Liu, X. Wang, Y. Peng, J. Fan, L. Zou, S. Lin and G. Chen, *Nat. Commun.*, 2023, **14**, 734.
61 M. A. Kadhim, M. G. Mukhlif, E. W. Gayadh, E. K. M. Zangana, M. A. Mohaisen, M. M. Matar and S. A. Rizk, *J. Mol. Struct.*, 2025, **1322**, 140384.
62 M. T. Helmy, M. A. M. Teleb, D. H. Hanna, M. W. El-Maadawy, H. M. Hassaneen and M. G. Kame, *Tetrahedron*, 2025, **177**, 134557.
63 A. Herrera, A. Riano, R. Moreno, B. Caso, Z. D. Pardo, I. Fernandez, E. Saez, D. Molero, A. Sanchez-Vazquez and R. Martinez-Alvarez, *J. Org. Chem.*, 2014, **79**, 7012–7024.
64 J.-J. Shie and J.-M. Fang, *J. Org. Chem.*, 2007, **72**, 3141–3144.
65 A. Díaz-Ortiz, A. de la Hoz, A. Moreno, A. Sánchez-Migallón and G. Valiente, *Green Chem.*, 2002, **4**, 339–343.
66 P. Debnath and K. C. Majumdar, *Tetrahedron Lett.*, 2014, **55**, 6976–6978.
67 Á. Díaz-Ortiz, J. Elguero, C. Foces-Foces, A. de la Hoz, A. Moreno, M. d. C. Mateo, A. Sánchez-Migallón and G. Valiente, *New J. Chem.*, 2004, **28**, 952–958.
68 P. Zuo, C. Ye, Z. Jiao, J. Luo, J. Fang, U. S. Schubert, N. B. McKeown, T. L. Liu, Z. Yang and T. Xu, *Nature*, 2023, **617**, 299–305.
69 M. Yan, R. Ma, R. Chen, L. Wang, Z. Wang and Y. Ma, *Chem. Commun.*, 2020, **56**, 10946–10949.
70 X. Xu, M. Zhang, H. Jiang, J. Zheng and Y. Li, *Org. Lett.*, 2014, **16**, 3540–3543.
71 J. Xiao, S. Ren and Q. Liu, *RSC Adv.*, 2020, **10**, 22230–22233.
72 A. R. Tiwari and B. M. Bhanage, *Green Chem.*, 2016, **18**, 144–149.

© 2025 The Author(s). Published by the Royal Society of Chemistry

Open Access Article. Published on 21 Oktober 2025. Downloaded on 9/06/2026 1:40:11 PG. This article is licensed under a Creative Commons Attribution-NonCommercial 3.0 Unported Licence.

73 A. M. Ganai, T. K. Pathan, G. A. Hampannavar, C. Pawar, V. A. Obakachi, V. A. Obakachi, B. Kushwaha, N. D. Kushwaha and R. Karpoormath, *ChemistrySelect*, 2021, **6**, 1616–1660.
74 Z.-C. Wu and D. L. Boger, *J. Org. Chem.*, 2022, **87**, 16829–16846.
75 C. Liu, J. Lin and K. Leftheris, *Tetrahedron Lett.*, 2007, **48**, 435–437.
76 L. Pan, Z. Li, T. Ding, X. Fang, W. Zhang, H. Xu and Y. Xu, *J. Org. Chem.*, 2017, **82**, 10043–10050.
77 H. Chen, P. Dao, A. Laporte and C. Garbay, *Tetrahedron Lett.*, 2010, **51**, 3174–3176.
78 C. Zhang, M.-T. Ban, K. Zhu, L.-Y. Zhang, Z.-Y. Luo, S.-N. Guo, D.-M. Cui and Y. Zhang, *Org. Lett.*, 2017, **19**, 3947–3949.
79 B. L. Mylari, G. J. Withbroe, D. A. Beebe, N. S. Brackett, E. L. Conn, J. B. Coutcher, P. J. Oates and W. J. Zembrowski, *Bioorg. Med. Chem.*, 2003, **11**, 4179–4188.
80 (*a*) A. Sethiya, D. K. Jangid, J. Pradhan and S. Agarwal, *J. Heterocycl. Chem.*, 2023, **60**, 1495–1516; (*b*) M. I. Ali and M. M. Naseer, *RSC Adv.*, 2023, **13**, 30462–30490.
81 M. Bashiri, A. Jarrahpour, B. Rastegari, A. Iraji, C. Irajie, Z. Amirghofran, S. Malek-Hosseini, M. Motamedifar, M. Haddadi, K. Zomorodian, Z. Zareshahrabadi and E. Turos, *Monatsh. Chem.*, 2020, **151**, 821–835.
82 A. El-Faham, S. M. Osman, H. A. Al-Lohedan and G. A. El-Mahdy, *Molecules*, 2016, **21**, 714.
83 B. Viira, A. Selyutina, A. T. García-Sosa, M. Karonen, J. Sinkkonen, A. Merits and U. Maran, *Bioorg. Med. Chem.*, 2016, **24**, 2519–2529.
84 J. Senapathi, A. Bommakanti, S. Vangara and A. K. Kondapi, *Bioorg. Chem.*, 2021, **116**, 105313.
85 Y. Karuo, K. Yamada and M. Kunishima, *Chem. Pharm. Bull.*, 2018, **66**, 303–308.
86 K. M. Al-Zaydi, H. H. Khalil, A. El-Faham and S. N. Khattab, *Chem. Cent. J.*, 2017, **11**, 39.
87 K. Huthmacher and D. Most, *Ullmann's Encycl. Ind. Chem.*, 2000.
88 J. Santos, J. Pereira, N. Paiva, J. Ferra, F. D. Magalhães, J. M. Martins and L. H. De Carvalho, *Proc. Inst. Mech. Eng., Part C*, 2021, **235**, 484–496.
89 V. Nemanič, B. Zajec, M. Žumer, N. Figar, M. Kavšek and I. Mihelič, *Appl. Energy*, 2014, **114**, 320–326.
90 C. Hoffendahl, G. Fontaine, S. Duquesne, F. Taschner, M. Mezger and S. Bourbigot, *Polym. Degrad. Stab.*, 2015, **115**, 77–88.
91 M. Badila, M. Kohlmayr, E. M. Zikulnig-Rusch, E. Dolezel-Horwath and A. Kandelbauer, *J. Appl. Polym. Sci.*, 2014, **131**, 40964.
92 H. Zhu, Y. Wang, H. Sun and K. Kannan, *Environ. Sci. Technol. Lett.*, 2019, **6**, 55–61.
93 M. L. Stewart, G. J. Bueno, A. Baliani, B. Klenke, R. Brun, J. M. Brock, I. H. Gilbert and M. P. Barrett, *Antimicrob. Agents Chemother.*, 2004, **48**, 1733–1738.
94 F. Cataldo and Y. Keheyan, *Polyhedron*, 2002, **21**, 1825–1835.
95 Y. Zhang, H. Luo, Q. Lu, Q. An, Y. Li, S. Li, Z. Tang and B. Li, *Chin. Chem. Lett.*, 2021, **32**, 393–396.
96 L. De Angelis, G. C. Haug, G. Rivera, S. Biswas, A. Al-Sayyed, H. Arman, O. Larionov and M. P. Doyle, *J. Am. Chem. Soc.*, 2023, **145**, 13059–13068.
97 I. I. F. Boogaerts and S. P. Nolan, *J. Am. Chem. Soc.*, 2010, **132**, 8858–8859.
98 C.-H. O. Yang, W.-H. Liu, S. Yang, Y.-Y. Chiang and J.-J. Shie, *Eur. J. Org. Chem.*, 2022, e202200209.
99 R. E. Quiñones, C. M. Glinkerman, K. Zhu and D. L. Boger, *Org. Lett.*, 2017, **19**, 3568–3571.
100 E. D. Anderson and D. L. Boger, *J. Am. Chem. Soc.*, 2011, **133**, 12285–12292.
101 E. D. Anderson and D. L. Boger, *Org. Lett.*, 2011, **13**, 2492–2494.
102 L. Baosheng, L. Han, Z. Yuan, A. Qiaoyu, X. Mingchuan, L. Qixing, T. Zongyuan and L. Shanshan, *CN Pat.*, CN111004284, 2020.
103 Q.-K. Yang, T. Chen, S.-Q. Wang, X.-J. Zhang and Z.-X. Yao, *Angiogenesis*, 2020, **23**, 279–298.
104 Z. Long, M. Huang, K. Liu, M. Li, J. Li, H. Zhang, Z. Wang and Y. Lu, *Front. Oncol.*, 2021, **11**, 662318.
105 S. Li, *Front. Oncol.*, 2021, **11**, 664853.
106 H. Luo, Q. Lu, M. Xu, M. Gu and B. Li, *Synthesis*, 2022, **54**, 4472–4480.
107 G. Rivera, L. De Angelis, A. Al-Sayyed, S. Biswas, H. Arman and M. P. Doyle, *Org. Lett.*, 2022, **24**, 6543–6547.
108 S. Biswas, L. D. Angelis, G. Rivera, H. Arman and M. P. Doyle, *Org. Lett.*, 2023, **25**, 1104–1108.
109 A. M. Ghanim, S. Rezq, T. S. Ibrahim, D. G. Romero and H. Kothayer, *Eur. J. Med. Chem.*, 2021, **219**, 113457.
110 A. I. Khodair, A. A. El-Barbary, D. R. Imam, N. A. Kheder, F. Elmalki and T. B. Hadda, *Carbohydr. Res.*, 2021, **500**, 108246.
111 T. N. Lohith, Chandra, B. H. Gayathri, S. Kumar, C. M. Shivaprasad, K. Divya, M. A. Sridhar and M. Mahendra, *J. Mol. Struct.*, 2024, **1317**, 139133.
112 A. V. Zaytsev, P. Distler, J. John, A. Wilden, G. Modolo, M. Sims and F. W. Lewis, *ChemistryOpen*, 2025, **14**, e202400306.
113 A. P. Krinochkin, Y. K. Shtaitz, A. Rammohan, I. I. Butorin, M. I. Savchuk, I. A. Khalymbadzha, D. S. Kopchuk, P. A. Slepukhin, V. V. Melekhin, A. V. Shcheglova, G. V. Zyryanov and O. N. Chupakhin, *Eur. J. Org Chem.*, 2022, e202200227.
114 (*a*) R. Jasiński, *Chem. Heterocycl. Compd.*, 2022, **58**, 260–262; (*b*) M. Ernd, M. Heuschmann and H. Zipse, *Helv. Chim. Acta*, 2005, **88**, 1491–1518.
115 S. E. Creegan, M. Zeller, E. F. C. Byrd and D. G. Piercey, *Cryst. Growth Des.*, 2021, **21**, 3922–3927.
116 R. Pal, M. J. Akhtar, K. Raj, S. Singh, P. Sharma, S. Kalra, P. A. Chawla and B. Kumar, *J. Mol. Struct.*, 2022, **1257**, 132587.
117 P. Saraf, P. N. Tripathi, M. K. Tripathi, A. Tripathi, H. Verma, D. K. Waiker, R. Singh and S. K. Shrivastava, *Bioorg. Chem.*, 2022, **129**, 106147.

Open Access Article. Published on 21 Oktober 2025. Downloaded on 9/06/2026 1:40:11 PG. This article is licensed under a Creative Commons Attribution-NonCommercial 3.0 Unported Licence.

118 H. Kumar, M. Dhameja, S. Kurella, A. Uma and P. Gupta, *J. Mol. Struct.*, 2023, **1273**, 134339.
119 R. Pal, B. Kumar, G. Swamy P M and P. A. Chawla, *Bioorg. Chem.*, 2023, **131**, 106284.
120 A. Lapray, T. Martzel, M.-A. Hiebel, S. Oudeyer, F. Suzenet and J.-F. Brière, *Adv. Synth. Catal.*, 2024, **366**, 316–322.
121 Y. Tan, W. Xuekun, Y.-P. Han, Y. Zhang, H.-Y. Zhang and J. Zhao, *J. Org. Chem.*, 2022, **87**, 8551–8561.
122 M. Wang, Y. Wang, J. Wang, Y. Zhu, P. Zhang, C. Zhang, J. Chen, L. Guo, G. Lv and Y. Wu, *J. Org. Chem.*, 2025, **90**, 7049–7061.
123 Z. Bernat, A. Mieszkowska, Z. Mazerska, J. Matysiak, Z. Karczmarzyk, K. Kotwica-Mojzych and M. Mojzych, *Appl. Sci.*, 2021, **11**, 2660.
124 X. Wu, J. W. T. See, K. Xu, H. Hirao, J. Roger, J.-C. Hierso and J. Zhou, *Angew. Chem., Int. Ed.*, 2014, **53**, 13573–13577.
125 X. Shao, X. Wu, S. Wu and C. Zhu, *Org. Lett.*, 2020, **22**, 7450–7454.
126 W. M. Boesveld, P. B. Hitchcock and M. F. Lappert, *J. Chem. Soc., Dalton Trans.*, 1999, 4041–4046.
127 H. Plagge, N. Manicone and H.-H. Otto, *Helv. Chim. Acta*, 2004, **87**, 1574–1590.
128 W. M. Boesveld, P. B. Hitchcock and M. F. Lappert, *J. Chem. Soc., Perkin Trans. 1*, 2001, 1103–1108.
129 R. Adam, B. Abarca and R. Ballesteros, *Synthesis*, 2017, **49**, 5059–5066.
130 A. V. Aksenov, I. V. Aksenova, I. V. Malikova and N. A. Aksenov, *Russ. Chem. Bull.*, 2009, **58**, 254–255.
131 G. Bikelytė, M. A. C. Härtel and T. M. Klapötke, *Propellants, Explos., Pyrotech.*, 2020, **45**, 1573–1579.
132 M. C. Davis, T. J. Groshens and G. H. Imler, *Tetrahedron Lett.*, 2020, **61**, 151776.
133 M. S. Khan, M. Ahsan, S. Farrukh, E. Pervaiz and A. Q. Malik, *Polymers*, 2024, **16**, 841.
134 N. B. Ayrim, F. R. Hafedh, Y. M. Kadhim, A. S. Hussein, A. M. Abdula, G. L. Mohsen and M. M. Sami, *Indones. J. Chem.*, 2024, **24**, 141–151.
135 J. C. Monteiro, M. Stürmer, I. M. Garcia, M. A. Melo, S. Sauro, V. C. B. Leitune and F. M. Collares, *Polymers*, 2020, **12**, 895.
136 G. E. Herberich, U. Englert and T. Wirth, *Eur. J. Inorg. Chem.*, 2005, 4924–4935.
137 K. Yang, Q. Dang, P.-J. Cai, Y. Gao, Z.-X. Yu and X. Bai, *J. Org. Chem.*, 2017, **82**, 2336–2344.
138 G. Yang, Q. Jia, L. Chen, Z. Du and J. Wang, *RSC Adv.*, 2015, **5**, 76759–76763.
139 W. Lei, L. Panpan, M. Guangyuan and Z. Shaoqing, *CN Pat.*, CN110372540, 2019.
140 K. L. Seley, S. Salim and L. Zhang, *Org. Lett.*, 2005, **7**, 63–66.
141 G. Yang, L. Chen, J. Wang, Q. Jia, J. Wei and Z. Du, *Tetrahedron Lett.*, 2015, **56**, 5889–5891.
142 E. R. Bilbao, M. Alvarado, C. F. Masaguer and E. Raviña, *Tetrahedron Lett.*, 2002, **43**, 3551–3554.
143 A. V. Aksenov, I. V. Aksenova, I. V. Borovlev and A. A. Zamorkin, *Russ. Chem. Bull.*, 2008, **57**, 215–216.
144 A. Dean, M. G. Ferlin, D. Carta, T. Jakusch, T. Kiss, F. F. Faccioli, S. Parrasia, D. Marton, A. Venzo and V. B. Di Marco, *J. Solution Chem.*, 2018, **47**, 92–106.
145 A. Dean, É. Sija, É. Zsigó, M. G. Ferlin, D. Marton, V. Gandin, C. Marzano, D. Badocco, P. Pastore, A. Venzo, R. Bertani, T. Kiss and V. Di Marco, *Eur. J. Inorg. Chem.*, 2013, 1310–1319.
146 K. S. Kim, L. Zhang, R. Schmidt, Z.-W. Cai, D. Wei, D. K. Williams, L. J. Lombardo, G. L. Trainor, D. Xie, Y. Zhang, Y. An, J. S. Sack, J. S. Tokarski, C. Darienzo, A. Kamath, P. Marathe, Y. Zhang, J. Lippy, R. Jeyaseelan, Sr., B. Wautlet, B. Henley, J. Gullo-Brown, V. Manne, J. T. Hunt, J. Fargnoli and R. M. Borzilleri, *J. Med. Chem.*, 2008, **51**, 5330–5341.
147 L. Cahlíková, R. Vrabec, F. Pidaný, R. Peřinová, N. Maafi, A. Al Mamun, A. Ritomská, V. Wijaya and G. Blunden, *Molecules*, 2021, **26**, 5240.
148 S. Hu, J. Chen, J.-X. Cao, S.-S. Zhang, S.-X. Gu and F.-E. Chen, *Bioorg. Chem.*, 2023, **136**, 106549.
149 S. Theeramunkong, A. Thiengsusuk, O. Vajragupta and P. Muhamad, *Med. Chem. Res.*, 2021, **30**, 109–119.
150 J. Hayashida and S. Yoshida, *Tetrahedron Lett.*, 2018, **59**, 3876–3879.
151 N. Kaila, I. Linney, S. Ward, G. Wishart, B. Whittaker, W. Sinko, S. Watts, M. A. Ashwell and B. S. Delabarre, *WO Pat.*, WO2022/174253, 2022.
152 G. Chabowska, E. Barg and A. Wójcicka, *Molecules*, 2021, **26**, 4324.
153 J. J. Marugan, W. Zheng, O. Motabar, N. Southall, E. Goldin, E. Sidransky, R. A. Aungst, K. Liu, S. K. Sadhukhan and C. P. Austin, *Eur. J. Med. Chem.*, 2010, **45**, 1880–1897.
154 M. Balogh, I. Hermecz, K. Simon and L. Pusztay, *J. Heterocycl. Chem.*, 1989, **26**, 1755–1769.
155 D. Villemin, N. Cheikh, L. Liao, N. Bar, J.-F. Lohier, J. Sopkova, N. Choukchou-Braham and B. Mostefa-Kara, *Tetrahedron*, 2012, **68**, 4906–4918.
156 Q. Dang and J. E. Gomez-Galeno, *J. Org. Chem.*, 2002, **67**, 8703–8705.
157 M. De Rosa, D. Arnold and D. Hartline, *J. Org. Chem.*, 2013, **78**, 8614–8623.
158 V. O. Iaroshenko, A. Maalik, D. Ostrovskyi, A. Villinger, A. Spannenberg and P. Langer, *Tetrahedron*, 2011, **67**, 8321–8330.
159 Q. Dang, Y. Liu and Z. Sun, *Tetrahedron Lett.*, 2001, **42**, 8419–8422.
160 V. Derdau, *J. Labelled Compd. Radiopharm.*, 2004, **47**, 19–24.
161 E. Wallace, G. Topolov, Q. Zhao and J. P. Lyssikatos, *US Pat.*, US2005/101617, 2005.
162 R. Rezaeinasab, E. Jafari and G. Khodarahmi, *J. Res. Med. Sci.*, 2022, **27**, 68.
163 W. Ewing, M. Becker, Y. Choi-Sledeski, H. Pauls, W. He, S. Condon, R. Davis, B. Hanney, A. Spada, C. Burns, J. Jiang, A. Li, M. Myers, W. Lau, G. Poli, M. Bobko, R. Morris, J. Karpinski, T. Gallagher, K. Neuenschwander, R. Groneberg and J.-F. Sabuco, *US Pat.*, US2004/102450, 2004.

© 2025 The Author(s). Published by the Royal Society of Chemistry

Open Access Article. Published on 21 Oktober 2025. Downloaded on 9/06/2026 1:40:11 PG. This article is licensed under a Creative Commons Attribution-NonCommercial 3.0 Unported Licence.

164 G. Xu, L. Zheng, S. Wang, Q. Dang and X. Bai, *Synlett*, 2009, 3206–3210.
165 A. V. Aksenov, I. V. Aksenova, A. S. Lyakhovnenko and N. A. Aksenov, *Chem. Heterocycl. Compd.*, 2008, **44**, 1379–1383.
166 K. Yang, Z. Yang, Q. Dang and X. Bai, *Eur. J. Org Chem.*, 2015, 4344–4347.
167 A. V. Gulevskaya, B. U. W. Maes and C. Meyers, *Synlett*, 2007, 71–74.
168 P. Zhang, Q. Zhang, Z. Tong, T. Sun, W. Li, Q. Ouyang, X. Hu, Y. Cheng, M. Yan, Y. Pan, Y. Teng, X. Yan, Y. Wang, W. Xie, X. Zeng, X. Wang, C. Hu, C. Geng, H. Zhang, W. Li, X. Wu, J. Zhong, J. Xu, Y. Shi, W. Wei, N. Bayaxi, X. Zhu and B. Xu, *Lancet Oncol.*, 2023, **24**, 646–657.
169 B. I. Rose and S. E. Brown, *J. Assist. Reprod. Genet.*, 2020, **37**, 2093–2104.
170 V. G. Gore, V. K. Shukla, S. Bhandari, S. Hasbe and S. Mekde, *WO Pat.*, WO2010/146391, 2010.
171 C.-Y. Chiu, C.-N. Kuo, W.-F. Kuo and M.-Y. Yeh, *J. Chin. Chem. Soc.*, 2002, **49**, 239–249.
172 J. Hu, K. Siokos, S. Makam and L. Zhong, *WO Pat.*, WO2021/41671, 2021.
173 X. Wang, A. C. Burns, J. G. Christensen, J. M. Ketcham, J. D. Lawson, M. A. Marx, C. R. Smith, S. Allen, J. F. Blake and M. J. Chicarelli, *WO Pat.*, WO2021/41671, 2021.
174 I. V. Aksenova, A. V. Aksenov and N. A. Aksenov, *Chem. Heterocycl. Compd.*, 2009, **45**, 117–118.
175 D. L. Boger and M. J. Kochanny, *J. Org. Chem.*, 1994, **59**, 4950–4955.
176 A. V. Aksenov, A. S. Lyakhovnenko, A. V. Andrienko and I. I. Levina, *Tetrahedron Lett.*, 2010, **51**, 2406–2408.
177 A. V. Aksenov, I. V. Aksenova and A. S. Lyakhovnenko, *Chem. Heterocycl. Compd.*, 2009, **45**, 119–120.
178 A. V. Aksenov, N. A. Aksenov, A. N. Smirnov, V. I. Goncharov, S. N. Ovcharov and I. V. Aksenova, *Russ. Chem. Bull.*, 2014, **63**, 1643–1645.
179 R. T. Skerlj, E. M. J. Bourque, P. T. Lansbury, W. J. Greenlee and A. C. Good, *WO Pat.*, WO2017/176961, 2017.
180 F. Jiazheng, *CN Pat.*, CN113264951, 2021.
181 A. Chafin and L. Merwin, *J. Org. Chem.*, 2000, **65**, 4743–4744.
182 E. Pormohammad, P. Ghamari Kargar, G. Bagherzade and H. Beyzaei, *Sci. Rep.*, 2023, **13**, 20421.
183 P. Dornan, C. N. Rowley, J. Priem, S. T. Barry, T. J. Burchell, T. K. Woo and D. S. Richeson, *Chem. Commun.*, 2008, 3645–3647.
184 (*a*) C.-H. Gu, H. Yang, L. GUO, Z. Tang, J. Wang, Y. Zhang and Y. Zhou, *WO Pat.*, WO2015/018060, 2015; (*b*) A. F. Khalil, T. F. El-Moselhy, E. A. El-Bastawissy, R. Abdelhady, N. S. Younis and M. H. El-Hamamsy, *J. Enzyme Inhib. Med. Chem.*, 2023, **38**, 2157411.
185 S. V. Agresta, *WO Pat.*, WO2016/053850, 2016.
186 X. Liu, G. Zhu, L. Li, Y. Liu, F. Wang, X. Song and Y. Mao, *Org. Process Res. Dev.*, 2018, **22**, 62–66.
187 (*a*) N. Saesaengseerung, T. Vilaivan and Y. Thebtaranonth, *Synth. Commun.*, 2002, **32**, 2089–2100; (*b*) O. A. Agede, M. O. Bojuwoye, A. F. Adenike, O. A. Mokuolu and C. O. Falade, *Discovery*, 2022, **58**, 1097–1108.
188 Y. Yuthavong, T. Vilaivan, N. Chareonsethakul, S. Kamchonwongpaisan, W. Sirawaraporn, R. Quarrell and G. Lowe, *J. Med. Chem.*, 2000, **43**, 2738–2744.
189 Z. A. Al-Ahmed, A. Hameed, A. Alharbi, R. A. Pashameah, T. M. Habeebullah and N. M. El-Metwaly, *J. Taibah Univ. Sci.*, 2023, **17**, 2163583.
190 J. Balamurugan and M. Lakshmanan, *Introduction to Basics Pharmacology and Toxicology: Volume 2: Essentials of Systemic Pharmacology: from Principles to Practice*, Non-steroidal anti-inflammatory medicines, 2021, pp. 335–352.
191 R. Nagi, S. S. Reddy and N. Rakesh, *Adverse Drug Reactions and Drug Interactions with Nonsteroidal Anti-inflammatory Drugs (NSAIDs): Adverse Drug Reactions to Nonsteroidal Anti-inflammatory Agents*, OrangeBooks Publication, 2021.
192 R. Hsu, D. J. Benjamin and M. Nagasaka, *Cancers*, 2023, **15**, 3561.
193 H. M. Zhang, P. B. Zhao and H. M. Huang, *Medicine*, 2025, **104**, e41460.
194 G. Kokic, H. S. Hillen, D. Tegunov, C. Dienemann, F. Seitz, J. Schmitzova, L. Farnung, A. Siewert, C. Höbartner and P. Cramer, *Nat. Commun.*, 2021, **12**, 279.
195 S. C. Locke, L. M. Splawn and J. C. Cho, *Drugs Today*, 2019, **55**, 359–366.
196 K. Nagao, N. Ishii, S. Kamidono and T. Osada, *Int. J. Urol.*, 2004, **11**, 515–524.
197 A. J. Heffernan, F. B. Sime, S. M. S. Lim, S. Adiraju, S. C. Wallis, J. Lipman, G. D. Grant and J. A. Roberts, *Int. J. Antimicrob. Agents*, 2022, **59**, 106537.
198 M. K. Bhattacharjee, Antibiotics That Inhibit Cell Wall Synthesis, in *Chemistry of Antibiotics and Related Drugs*, Springer, 2016, pp. 49–94, ISBN: 978-3-319-40746-3.
199 Y.-H. Zhang, R. Xie, C.-S. Dai, H.-W. Gao, G. Zhou, T.-T. Qi, W.-Y. Wang, H. Wang and Y.-M. Cui, *J. Hepatol.*, 2025, **82**, 189–202.
200 R. Suvarna, S. Shetty and J. M. Pappachan, *Sci. Rep.*, 2024, **14**, 19790.
201 S. Ravindra, C. P. I. Jesin, A. Shabashini and G. C. Nandi, *Adv. Synth. Catal.*, 2021, **363**, 1756–1781.
202 (*a*) W. Drell, *EP Pat.*, EP0495270B1, 1996; (*b*) E. Poduch, A. M. Bello, S. Tang, M. Fujihashi, E. F. Pai and L. P. Kotra, *J. Med. Chem.*, 2006, **49**, 4937–4945; (*c*) R. C. Deconti and P. Calabresi, *Ann. Intern. Med.*, 1970, **73**, 575–579.
203 I. K. Mellinghoff, M. Penas-Prado, K. B. Peters, H. A. Burris, E. A. Maher, F. Janku, G. M. Cote, M. I. de la Fuente, J. L. Clarke, B. M. Ellingson, S. Chun, R. J. Young, H. Liu, S. Choe, M. Lu, K. Le, I. Hassan, L. Steelman, S. S. Pandya, T. F. Cloughesy and P. Y. Wen, *Clin. Cancer Res.*, 2021, **27**, 4491–4499.
204 Z. Konteatis, E. Artin, B. Nicolay, K. Straley, A. K. Padyana, L. Jin, Y. Chen, R. Narayaraswamy, S. Tong, F. Wang, D. Zhou, D. Cui, Z. Cai, Z. Luo, C. Fang, H. Tang, X. Lv, R. Nagaraja, H. Yang, S.-S. M. Su, Z. Sui, L. Dang, K. Yen, J. Popovici-Muller, P. Codega, C. Campos,

Open Access Article. Published on 21 Oktober 2025. Downloaded on 9/06/2026 1:40:11 PG. This article is licensed under a Creative Commons Attribution-NonCommercial 3.0 Unported Licence.

I. K. Mellinghoff and S. A. Biller, *ACS Med. Chem. Lett.*, 2020, **11**, 101–107.
205 H. Y. Lim and A. V. Dolzhenko, *Eur. J. Med. Chem.*, 2024, **276**, 116680.
206 J. Jiang, W. Wang, W. Xiang, L. Jiang and Q. Zhou, *Bioengineered*, 2021, **12**, 11847–11857.
207 P. Castel, E. Toska, J. A. Engelman and M. Scaltriti, *Nat. Cancer*, 2021, **2**, 587–597.
208 S. Thota, A. Oganesian, M. Azab and E. A. Griffiths, *Future Oncol.*, 2021, **17**, 2077–2087.
209 E. R. Plimack, H. M. Kantarjian and J.-P. Issa, *Leuk. Lymphoma*, 2007, **48**, 1472–1481.
210 P. Malik and A. F. Cashen, *Cancer Manage. Res.*, 2014, **6**, 53–61.
211 A. Majchrzak-Celińska, A. Warych and M. Szoszkiewicz, *Genes*, 2021, **12**, 208.
212 R. Prasad, T. J. Yen and A. Bellacosa, *Adv. Genet.*, 2021, **2**, e10033.
213 V. Davalos and M. Esteller, *Ca-Cancer J. Clin.*, 2023, **73**, 376–424.
214 S.-C. Wang, C.-T. Wu, D.-Y. Wu, C. G.-S. Chen, K.-M. Chang and C.-C. Chang, *Cancers*, 2019, **11**, 1294.
215 Y. Yang, J. Li, Y. Geng, L. Liu and D. Li, *J. Clin. Lab. Anal.*, 2021, **35**, e23597.
216 H. T. T. Tran, H. N. Kim, I.-K. Lee, Y.-K. Kim, J.-S. Ahn, D.-H. Yang, J.-J. Lee and H.-J. Kim, *J. Korean Med. Sci.*, 2011, **26**, 207–213.
217 M. Tobiasson, H. Abdulkadir, A. Lennartsson, S. Katayama, F. Marabita, A. De Paepe, M. Karimi, K. Krjutskov, E. Einarsdottir, M. Grövdal, M. Jansson, A. Ben Azenkoud, L. Corddedu, S. Lehmann, K. Ekwall, J. Kere, E. Hellström-Lindberg and J. Ungerstedt, *Oncotarget*, 2017, **8**, 28812–28825.
218 P. Matt, B. v. Zwieten-Boot, G. C. Rojas, H. t. Hofstede, R. Garcia-Carbonero, J. Camarero, E. Abadie and F. Pignatti, *Oncologist*, 2011, **16**, 1451–1457.
219 Y. Ren, S. Yang and Y. Xu, *Acc. Chem. Res.*, 2025, **58**, 474–487.
220 (*a*) M. Chen, Z. Sun, T. Wei, B. Zhang, K. Guo, Y. Feng and B. Zhang, *Chem. Eng. J.*, 2025, **508**, 160982; (*b*) Y. Wei, Q. Zhou, X. Wang, Y. Liao, J. Meng, Y. Huang, L. Gao and W. Dai, *Catalysts*, 2025, **15**, 562.
221 M. Liu, L. Guo, S. Jin and B. Tan, *J. Mater. Chem. A*, 2019, **7**, 5153–5172.
222 (*a*) Y. Wen, F. Zhang, J. Dou, S. Wang, F. Gao, F. Shan, J. Dong and G. Chen, *Sep. Purif. Technol.*, 2025, **359**, 130579; (*b*) J. Aslam, M. A. Waseem, Y. Wu, W. Sun and Y. Wang, *Adv. Colloid Interface Sci.*, 2025, **341**, 103479.
223 X. Wang, L. Guan, W. Wang, B. Tan and S. Jin, *Sep. Purif. Technol.*, 2025, **364**, 132485.
224 O. Lebedeva, D. Kultin, V. Zakharov, I. Kuznetsova, L. Aslanov and L. Kustov, *Sustainable Energy Fuels*, 2025, **9**, 1464–1479.
225 W. Huang, W. Luo and Y. Li, *Mater. Today*, 2020, **40**, 160–172.
226 A. Mohan, M. H. Al-Sayah, A. Ahmed and O. M. El-Kadri, *Sci. Rep.*, 2022, **12**, 2638.
227 M. Salahvarzi, A. Setarob, S. Beyranvanda, M. Nematia, G. Gordeevb, A. Fieborb, K. Ludwigd, R. Ghanbarie, N. Nasirie and V. Ahmadi, *Mater. Today Chem.*, 2024, **39**, 102155.
228 A. Aldalbahi, B. S. AlOtaibi, B. M. Thamer and A. El-Faham, *Polymers*, 2022, **14**, 784.
229 P. M. C. Matias, D. Murtinho and A. J. M. Valente, *Polymers*, 2023, **15**, 1815.
230 M. Vakili, P. Koutník and J. Kohout, *Sustainability*, 2024, **16**, 1661.
231 A. G. Buret, T. Allain, J.-P. Motta and J. L. Wallace, *Antioxid. Redox Signaling*, 2022, **36**, 211–219.
232 H. Kimura, *Biomolecules*, 2021, **11**, 896.
233 M. S. Khoma, K. B. Vasyliv and M. R. Chuchman, *Mater. Sci.*, 2021, **57**, 308–318.
234 K. Li, Y. Zeng and J.-L. Luo, *Corros. Sci.*, 2021, **190**, 109639.
235 J. J. Wylde, G. N. Taylor, K. S. Sorbie and W. N. Samaniego, *Energy Fuels*, 2022, **36**, 851–860.
236 W. Zhu, H. Ye, X. Zou, Y. Yang and H. Dong, *Sep. Purif. Technol.*, 2021, **276**, 119301.
237 K. Ofori, Hydrogen Sulphide, in *Biogas in the 21st Century: Developments and Perspectives*, ed. L. Montuori and M. Alcázar-Ortega, Springer, Cham, 2023.
238 O. W. Agbroko, K. Piler and T. J. Benson, *ChemBioEng Rev.*, 2017, **4**, 339–359.
239 D. S. Chauhan, M. A. Quraishi, W. B. W. Nik and V. Srivastava, *J. Mol. Liq.*, 2021, **321**, 114747.
240 C. Verma, A. Thakur, R. Ganjoo, S. Sharma, H. Assad, A. Kumar, M. A. Quraishi and A. Alfantazi, *Coord. Chem. Rev.*, 2023, **488**, 215177.
241 H. H. Hammud, N. S. Sheikh, I. Shawish, H. A. Bukhamsin, D. E. Al-Hudairi, A. L. X. Wee, M. H. S. A. Hamid, S. A. Maache, H. H. Al-Rasheed, A. Barakat, A. El-Faham and H. M. Abd El-Lateef, *R. Soc. Open Sci.*, 2024, **11**, 231229.
242 X. Wang, W. L. Xu, Z. Y. Liu and G. A. Zhang, *Corros. Sci.*, 2023, **220**, 111288.
243 J. J. Wylde, G. N. Taylor, K. S. Sorbie and W. N. Samaniego, *Energy Fuels*, 2020, **34**, 13883–13892.
244 P. Wang, X. Gu, Q. Wang, J. Dong, S. Dong, J. Zhang, S. Zhu and G. Chen, *Desalin. Water Treat.*, 2021, **235**, 107–116.
245 N. Montesantos, M. N. Fini, J. Muff and M. Maschietti, *Chem. Eng. J.*, 2022, **427**, 131020.
246 S. D. Meena, M. Susank, T. Guttula, S. H. Chandana and J. Sheela, *Procedia Comput. Sci.*, 2023, **218**, 2369–2382.
247 B. Richard, A. Qi and B. D. L. Fitt, *Plant Pathol.*, 2022, **71**, 187–206.
248 J. Benjamin, O. Idowu, O. K. Babalola, E. V. Oziegbe, D. O. Oyedokun, A. M. Akinyemi and A. Adebayo, *Agric. Food Secur.*, 2024, **13**, 18.
249 B. A. Khan, M. A. Nadeem, H. Nawaz, M. M. Amin, G. H. Abbasi, M. Nadeem, M. Ali, M. Ameen, M. M. Javaid, R. Maqbool, M. Ikram and M. A. Ayub, Pesticides: impacts on agriculture productivity, environment, and management strategies, in *Emerging Contaminants and Plants: Interactions, Adaptations and Remediation Technologies*, ed. T. Aftab, Springer International Publishing, 2023, pp. 109–134.

© 2025 The Author(s). Published by the Royal Society of Chemistry

Open Access Article. Published on 21 Oktober 2025. Downloaded on 9/06/2026 1:40:11 PG. This article is licensed under a Creative Commons Attribution-NonCommercial 3.0 Unported Licence.

250 V. Balaska, Z. Adamidou, Z. Vryzas and A. Gasteratos, *Machines*, 2023, **11**, 774.
251 (*a*) M. Shoaib, A. Sadeghi-Niaraki, F. Ali, I. Hussain and S. Khalid, *Front. Plant Sci.*, 2025, **16**, 1538163; (*b*) L. P. Gianessi, *The Triazine Herbicides: Role of Triazine Herbicides in Sustaintable Agriculture*, ed. H. M. LeBaron, J. M. Farland and O. C. Burnside, Elsevier, Amsterdam (The Netherlands), 1st edn, 2008, ch. 34. vol. 2, pp. 527–538.
252 T. Du, S. Lu, Z. Zhu, M. Zhu, Y. Zhang, J. Zhang and J. Chen, *Chin. Chem. Lett.*, 2025, **36**, 110912.
253 M. Tudi, H. D. Ruan, L. Wang, J. Lyu, R. Sadler, D. Connell, C. Chu and D. T. Phung, *Int. J. Environ. Res. Public Health*, 2021, **18**, 1112.
254 M. Li, Y. Dong, Q. Wang, Z. Li and Q. Wu, *Food Chem.*, 2025, **492**, 145451.
255 A. T. Cardoso and F. M. Lanças, *Microchem. J.*, 2025, **215**, 114270.
256 K. A. Conrad, H. Kim, M. Qasim, A. Djehal, A. D. Hernday, L. Désaubry and J. M. Rauceo, *Pathogens*, 2023, **12**, 126.
257 X. Feng, Z. Liu, S. V. Duy, L. Parent, B. Barbeau and S. Sauvé, *Water Res.*, 2025, **277**, 123339.
258 R. Hou, G. Fu, S. Ma, S. Tang, F. Guo, Y. Wang, S. Huang, D. Cheng, Z. Zhang and C. Zhao, *Chem. Eng. J.*, 2025, **515**, 163805.
259 X. Chen, Y. Li, H. Guo, J. Zhang and J. Cao, *Chem. Eng. Sci.*, 2025, **314**, 121762.
260 F. A. Drummond, A. L. Averill and B. D. Eitzer, *Insects*, 2024, **15**, 567.
261 A. López, E. Fuentes-Ferragud, A. Muñoz, E. Borràs, T. Vera and C. Coscollà, *Environ. Pollut.*, 2025, **383**, 126770.
262 H. Zhang, S. Yang, X. Zhang, Y. Pei, M. Chen, H. Chen and J. Zhang, *Environ. Technol. Innovation*, 2025, **39**, 104221.
263 Y. Hao, Y. Li, J. Wang, S. Pang and S. Li, *Foods*, 2024, **13**, 3247.
264 S. Lamnoi, T. Boonupara, S. Sumitsawan, P. Vongruang, T. Prapamontol, P. Udomkun and P. Kajitvichyanukul, *Toxics*, 2024, **12**, 86.
265 P. N. Smith, K. L. Armbrust, R. A. Brain, W. Chen, N. Galic, L. Ghebremichael, J. M. Giddings, M. L. Hanson, J. Maul, G. V. D. Kraak and K. R. Solomon, *J. Toxicol. Environ. Health, Part B*, 2021, **24**, 223–306.
266 C. M. Rocha, A. M. Lastre-Acosta, M. P. S. Parizi and A. C. S. C. Teixeira, *Environ. Sci. Pollut. Res.*, 2022, **29**, 42290–42304.
267 R. Chen, P. Nie, L. Wang, G. Wang, C. Zhang, X. Zhao and X. Xue, *Front. Plant Sci.*, 2025, **16**, 1527183.
268 R. Streletskii, A. Astaykina, V. Cheptsov, A. Belov and V. Gorbatov, *Agriculture*, 2023, **13**, 1330.
269 A. K. Tamta and R. P. Srivastava, *J. Entomol. Res.*, 2023, **47**, 489–495.
270 D. Fernández-Calviño, J. Rousk, E. Bååth, U. E. Bollmann, K. Bester and K. K. Brandt, *Soil Biol. Biochem.*, 2021, **154**, 108130.
271 S. M. S. Khademi, V. Ilbeigi, Y. Valadbeigi, M. Tabrizchi and U. Telgheder, *Int. J. Environ. Sci. Technol.*, 2024, **21**, 6925–6934.
272 S. M. S. Khademi, A. Salemi, M. Jochmann, S. Joksimoski and U. Telgheder, *Microchem. J.*, 2021, **164**, 106006.
273 Q. Wu, F. Li, X. Zhu, Y. Ahn and Y. Zhu, *Environ. Sci. Pollut. Res.*, 2022, **29**, 67765–67775.
274 C. L. Brueck, X. Xin, S. N. Lupolt, B. F. Kim, R. E. Santo, Q. Lyu, A. J. Williams, K. E. Nachman and C. Prasse, *Environ. Sci. Technol.*, 2024, **58**, 3690–3701.
275 T. Sultana, J. Tasnim, M. W. H. Talukder, M. L. Mia, S. N. Suchana, F. Akter, M. Abu Saleh, M. F. Afrin and M. Uzzaman, *Inf. Med. Unlocked*, 2023, **42**, 101378.
276 M. Qu, H. Merzendorfer, B. Moussian and Q. Yang, *Front. Agric. Sci. Eng.*, 2022, **9**, 82–97.
277 E. G. Frank, *Science*, 2024, **385**, eadg0344.
278 M. F. Araújo, E. M. S. Castanheira and S. F. Sousa, *Molecules*, 2023, **28**, 3641.
279 J. K. Pandey, G. Dubey and R. Gopal, *J. Fluoresc.*, 2022, **32**, 2159–2172.
280 J. F. L. Leal, J. Borella, A. d. S. Souza, A. C. Langaro, R. d. M. Carneiro, G. d. S. da Silva, F. F. d. O. Junior, F. R. de Souza, A. F. L. Machado and C. F. de Pinho, *Acta Physiol. Plant.*, 2023, **45**, 94.
281 I. Y. Vitkalova, A. P. Gureev, E. A. Shaforostova, O. N. Boyko, A. U. Igamberdiev and V. N. Popov, *Pestic. Biochem. Physiol.*, 2021, **172**, 104764.
282 Z. Wang, Q. Jiang, Q. Zhu, C. Ji, J. Li, M. Yin, J. Shen and S. Yan, *J. Agric. Food Chem.*, 2024, **72**, 22562–22573.
283 E. Asimakis, A. A. Shehata, W. Eisenreich, F. Acheuk, S. Lasram, S. Basiouni, M. Emekci, S. Ntougias, G. Taner, H. May-Simera, M. Yilmaz and G. Tsiamis, *Microorganisms*, 2022, **10**, 307.
284 N. F. Abd Rani, K. A. Kamil, F. Aris, N. M. Yunus and N. A. Zakaria, *Biocatal. Biotransform.*, 2022, **40**, 233–247.
285 S. Rostami, S. Jafari, Z. Moeini, M. Jaskulak, L. Keshtgar, A. Badeenezhad, A. Azhdarpoor, M. Rostami, K. Zorena and M. Dehghani, *Environ. Technol. Innovation*, 2021, **24**, 102019.
286 M. M. G. Brambila, H. H. L. Santiesteban, G. M. T. Aguilar, J. A. C. Luna, J. C. G. Martínez and R. R. Chilpa, *Int. J. Chem. React. Eng.*, 2025, **22**, 1265–1288.
287 Y. Liang, L. Ding, Q. Song, B. Zhao, S. Wang and S. Liu, *Environ. Pollut. Bioavailability*, 2022, **34**, 549–563.
288 D. Wang, Q. Ma, H. Lin, J. Zhou, S. Yuan, B. Ma, Y. Bai and J. Qu, *Heliyon*, 2023, **9**, e15092.
289 A. Kumar and N. Singh, *Environ. Monit. Assess.*, 2016, **188**, 142.
290 X. Li, J. Wang, X. Wang, Y. Ou, H. Liu, L. Yan and M. Shang, *Chem. Eng. J.*, 2025, **519**, 165124.
291 S. Demeshko, G. Leibeling, S. Dechert and F. Meyer, *Dalton Trans.*, 2004, 3782–3787.
292 A. Barakat, A. El-Faham, M. Haukka, A. M. Al-Majid and S. M. Soliman, *Appl. Organomet. Chem.*, 2021, **35**, e6317.
293 Y. Cui, J. Zhang, H. He and G. Qian, *Chem. Soc. Rev.*, 2018, **47**, 5740–5785.
294 S. Keller, A. Prescimone, E. C. Constable and C. E. Housecroft, *Polyhedron*, 2016, **116**, 3–11.

Open Access Article. Published on 21 Oktober 2025. Downloaded on 9/06/2026 1:40:11 PG.
This article is licensed under a Creative Commons Attribution-NonCommercial 3.0 Unported Licence.

295 J.-C. Berthet, J.-M. Onno, F. Gupta, C. Rivière, P. Thuéry, M. Nierlich, C. Madic and M. Ephritikhine, *Polyhedron*, 2012, **45**, 107–125.
296 H. Hadadzadeh, M. Maghami, J. Simpson, A. D. Khalaji and K. Abdi, *J. Chem. Crystallogr.*, 2012, **42**, 656–667.
297 F. Gallou, P. GUO, J. Zhou and M. Parmentier, *US Pat.*, US11235316B2, 2022.
298 M. S. Congreve, S. P. Andrews, J. S. Mason, C. M. Richardson and G. A. Brown, *US Pat.*, US12054472B2, 2024.
299 M.-P. Collin, D. Brohm, M. Héroult, M. Lobell, W. Hübsch, K. Lustig, S. Grunewald, U. Bömer, V. Vöhringer and N. Lindner, *US Pat.*, US9598416B2, 2017.
300 D. Tadesse and J. Yu, *US Pat.*, US9120786B2, 2015.
301 C. Yang, L. Meng, Y. Chen, X. Wang, C. Tan, J. Li, J. Ding and Y. Chen, *US Pat.*, US9724352B2, 2017.
302 R. Shibin, B. Haiyang, H. Daiyu and H. Deman, *CN Pat.*, CN109251285B, 2021.
303 A. V. Purandare, B. E. Fink, A. V. Gavai, W. L. Johnson, A. C. Hart, L. He, T. N. Huynh, J. Inghrim, H. Mastalerz, X. Sang, C. M. Tarby, H. Wan, W. Vaccaro, G. Zhang, Y. Zhao and K. Zimmermann, *US Pat.*, US9556178B2, 2017.
304 B. L. Hodous, J. L. Kim, K. J. Wilson, D. Wilson and Y. Zhang, *US Pat.*, US11827642B2, 2023.
305 Z. Zhaochao, T. Dandan and L. Chong, *CN Pat.*, CN109449304B, 2021.
306 A. A. IvashchenkoA. V. IvashchenkoO. D. Mitkin, RU2720305C1, 2020.
307 T. Shishido, T. Noshi, A. Yamamoto and M. Kitano, *US Pat.*, US11040048B2, 2021.
308 N. Nishimura, Y. Koide and M. Ozawa, *US Pat.*, US9469729B2, 2016.

© 2025 The Author(s). Published by the Royal Society of Chemistry